(2)

AD

US ARMY
LABORATORY COMMAND
MATERIALS TECHNOLOGY LABORATORY

MTL TR 89-13

DIAMONDLIKE CARBON COATINGS FOR OPTICAL SYSTEMS

February 1989

R. WU, D. INGRAM, A. McCORMICK, A. RAI, P. PRONKO,
J. WOOLLAM, B. DE, and N. IANNO
Universal Energy Systems, Inc.
4401 Dayton-Xenia Road
Dayton, OH 45432

FINAL REPORT

Contract DAAL04-86-C-0030

Prepared for

U.S. ARMY MATERIALS TECHNOLOGY LABORATORY
Watertown, Massachusetts 02172-0001

The findings in this report are not to be construed as an official Department of the Army position, unless so designated by other authorized documents.

Mention of any trade names or manufacturers in this report shall not be construed as advertising nor as an official indorsement or approval of such products or companies by the United States Government.

DISPOSITION INSTRUCTIONS

Destroy this report when it is no longer needed.
Do not return it to the originator.

UNCLASSIFIED

SECURITY CLASSIFICATION OF THIS PAGE (When Data Entered)

REPORT DOCUMENTATION PAGE		READ INSTRUCTIONS BEFORE COMPLETING FORM
1. REPORT NUMBER MTL TR 89-13	2. GOVT ACCESSION NO.	3. RECIPIENT'S CATALOG NUMBER
4. TITLE (and Subtitle) DIAMONDLIKE CARBON COATINGS FOR OPTICAL SYSTEMS		5. TYPE OF REPORT & PERIOD COVERED Final Report - Sept. 1986 to Sept. 1988 6. PERFORMING ORG. REPORT NUMBER
7. AUTHOR(s) R. Wu, D. Ingram, A. McCormick, A. Rai, P. Pronko, J. Woollam, B. De, and N. Ianno		8. CONTRACT OR GRANT NUMBER(s) Contract DAAL04-86-C-0030
9. PERFORMING ORGANIZATION NAME AND ADDRESS Universal Energy Systems, Inc. 4401 Dayton-Xenia Road Dayton, OH 45432		10. PROGRAM ELEMENT, PROJECT, TASK AREA & WORK UNIT NUMBERS
11. CONTROLLING OFFICE NAME AND ADDRESS U.S. Army Materials Technology Laboratory ATTN: SLCMT-PR Watertown, MA 02172-0001		12. REPORT DATE February 1989 13. NUMBER OF PAGES
14. MONITORING AGENCY NAME & ADDRESS(if different from Controlling Office)		15. SECURITY CLASS. (of this report) Unclassified 15a. DECLASSIFICATION/DOWNGRADING SCHEDULE

16. DISTRIBUTION STATEMENT (of this Report)

Approved for public release; distribution unlimited.

17. DISTRIBUTION STATEMENT (of the abstract entered in Block 20, if different from Report)

18. SUPPLEMENTARY NOTES

19. KEY WORDS (Continue on reverse side if necessary and identify by block number)

Diamondlike carbon	Thin films	Coatings
Protective coatings	Ellipsometry	Carbon
Antireflection coatings	Ion beam deposition	
Optical coatings	RF discharge deposition	

20. ABSTRACT (Continue on reverse side if necessary and identify by block number)

(SEE REVERSE)

DD FORM 1 JAN 73 1473 EDITION OF 1 NOV 65 IS OBSOLETE

UNCLASSIFIED

SECURITY CLASSIFICATION OF THIS PAGE (When Data Entered)

Block No. 20

ABSTRACT

Diamondlike carbon (DLC) coatings have been deposited on seven infrared transmitting substrates utilizing three different techniques: ion-beam deposition, rf-plasma discharge, and hollow cathode discharge methods. Optimum deposition parameters for each technique have been established as a function of substrate material. Extensive characterization of the DLC films was also performed. Rutherford backscattering and proton recoil detection techniques were used to analyze carbon and hydrogen content and impurities. These films contain typically 70% C and 30% H. Transmission electron microscopy was used to analyze the crystallinity, void structure, surface microstructure, and thickness of the films which were found to be amorphous and dense. Optical properties such as refractive index, extinction coefficient, and optical band gap of the films were determined by variable angle spectroscopic ellipsometry (VASE) over the spectral range from 300 nm to 10.6 μm. Optical properties were found to be related to the preparation procedure used. Antireflection thicknesses of the DLC films for use at specific wavelengths were deposited on all but the ZnS substrates, and even for this case it is now known how to deposit thick DLC. Environmental testing was performed using various acids and solvents. The thermal stability, moisture penetration, rain erosion, and sand ballistic impact effects on these DLC films were extensively investigated. The effect of high energy ion radiation on DLC films was studied. Details of preparation methods and characterization of DLC films are presented.

FINAL REPORT

DIAMONDLIKE CARBON COATINGS FOR OPTICAL SYSTEMS

CONTRACT NO. DAAL04-86-C-0030

OCTOBER 1988

PREPARED FOR

U.S. ARMY MATERIALS TECHNOLOGY LABORATORY
SLCMT-ISC
WATERTOWN, MA 02172-0001

PREPARED BY

UNIVERSAL ENERGY SYSTEMS, INC.
4401 DAYTON-XENIA ROAD
DAYTON, OH 45432
(513) 426-6900

FOREWORD

This research project entitled "Diamondlike Carbon Coatings for Optical Systems" was fully supported by U.S. Army Materials Technology Laboratory under the Phae II SBIR program with Universal Energy Systems, Inc. (UES), Dayton, Ohio (Contract DAAL04-88-C-0030). The two major subcontractors of this project were: (1) University of Nebraska, Department of Electrical Engineering, Lincoln, NE; and (b) J. A. Woollam Company, Lincoln, NE.

The ion beam deposition technqiue was developed at UES, and the rf-plasma discharge and hollow-cathode discharge techniques were developed at the University of Nebraska. The varible angle of incidence spectroscopic ellipsometry was designed and contracted by J. A. Woollam Company.

As a result of the work done during this program, eight manuscripts have been submitted and published in refereed journals, and eight presentations were given at professional meetings. A total of 210 DLC coatings on seven substrates of lexan, silicon, fused silica, KG-3 glass, BK-7 glass, ZnS and heavy metal fluoride (HMF) using three different deposition techniques were delivered to the Army Materials Technology Laboratory for further testing. A variable angle of incidence spectroscopic ellipsometer (VASE), which represents the state of the art in advanced optical technology, was completed and delivered to the Army Materials Technology Laboratory.

Dr. Richard L.C. Wu, Senior Scientist at UES, was the Program Manager.

ABSTRACT

Diamondlike carbon (DLC) coatings have been deposited on seven infrared transmitting substrates utilizing three different techniques: ion-beam deposition, rf-plasma discharge, and hollow cathode discharge methods. Optimum deposition parameters for each technique have been established as a function of substrate material. Extensive characterization of the DLC films was also performed. Rutherford backscattering and proton recoil detection techniques were used to analyze carbon and hydrogen content and impurities. These films contain typically 70% C and 30% H. Transmission electron microscopy was used to analyze the crystallinity, void structure, surface microstructure, and thickness of the films which were found to be amorphous and dense. Optical properties such as refractive index, extinction coefficient, and optical band gap of the films were determined by variable angle spectroscopic ellipsometry (VASE) over the spectral range from 300 nm to 10.6 μm. Optical properties were found to be related to the preparation procedure used. Antireflection thicknesses of the DLC films for use at specific wavelengths were deposited on all but the ZnS substrates, and even for this case it is now known how to deposite thick DLC. Environmental testing was performed using various acids and solvents. The thermal stability, moisture penetration, rain erosion, and sand ballistic impact effects on these DLC films were extensively investigated. The effect of high energy ion radiation on DLC films was studied. Details of preparation methods and characterization of DLC films are presented.

TABLE OF CONTENTS

TABLE OF CONTENTS (cont'd)

LIST OF ILLUSTRATIONS

LIST OF ILLUSTRATIONS (cont'd)

LIST OF TABLES

LIST OF TABLES (cont'd)

LIST OF TABLES (cont'd)

1.0 INTRODUCTION

Diamondlike carbon (DLC) is an amorphous form of carbon, typically containing on the order of 30% hydrogen. It is transparent in the longer wavelength part of the visible spectrum, but the optical band gap can vary over a wide range. Values of the optical gap of above 3 eV have been reported [1-4], making the latter films transparent beyond about 400 nm, but values in the range of tenths of electron volts can also be prepared. The optical band gap correlates with hydrogen content. The hydrogen content determines most of the physical properties of DLC. Thus optical band gap is a good property to use as a "monitor."

An unusual and highly desirable property of DLC films is that they can be extremely hard and resistant to chemical attack. DLC film can be deposited by ion-beam sputtering, rf-plasma and hollow-cathode discharge techniques. The essential ingredient for forming hard carbon films is the simultaneous impact of energetic atomic or ionic species at the surface during deposition.

Numerous works on diamondlike carbon film were published in the literature. Several comprehensive reviews were reported by Angus, Koidl and Domitz [1], Robertson [5] and Tsai and Bogy [6].

The objectives of this program were:

(a) Demonstrate DLC film adhesion to silicon, heavy metal flouride, lexan, fused silica, zinc sulfide, BK-7, and KG-3 glass. Demonstrate continued adhesion and lack of degradation of films after exposure to standard tests for optical coatings including military specification MIL-C-48497. This includes exposure to acids as well as organic solvents and to extremes of temperature and humidity.

(b) Compare film properties under (1) Ion assisted deposition, and (2) hollow cathode discharge techniques and (3) parallel plate rf-plasma deposition.

(c) Determine (qualitatively, at least, and semiquantitatively, if possible) the effect of ballistic impact damage to films, especially from high velocity sand and high velocity water jets.

(d) Determine the effects of deposition parameters on film properties.

(e) Determine fundamental properties that keep the film atoms bonded together, bonded to substrates, and make the material hard and chemically resistant. Determine the role of hydrogen in this process.

(f) Assemble, test, and deliver to the Army a spectroscopic ellipsometer capable of determining optical properties of materials over a wide range of wavelengths (350-840 nm).

Extensive film depositions were carried out using three different techniques. The optimum deposition parameters were established. The deposited DLC film samples were then subjected to various environmentally damaging conditions such as soaking in organic solvents, strong acids, and exposure to extremes of temperature and rubbing. Rain erosion testing was done using several DLC films on ZnS substrates. In addition, a series of grain sizes of sand were projected at the surface of DLC coated and uncoated samples. Finally, several samples were subjected to damaging high energy ion beams of fluorine and gold at a series of fluences.

Optical measurements were made to characterize the samples for use on infrared substrates. These properties were a function of preparation conditions, such as plasma pressure and power. Samples deposited on quartz were used to measure optical band gap using Tauc plots, and variable angle spectroscopic ellipsometry (VASE) was used to determine the index of refraction and extinction coefficient. VASE was also used to determine the ability of the film to protect the substrate from moisture.

The results show that DLC films can be prepared (with some control of properties) on all substrates used. Certain substrates worked better than others. However, sticking was sometimes a problem for thick films. In other cases, optical quarter wave thicknesses of DLC could be deposited. Samples generally held up under the extreme environmental conditions imposed experimentally. Especially encouraging was the discovery that moisture penetration of DLC was extremely small. The lack of grain boundaries in amorphous films is a contributing factor to this desirable property.

The remainder of this report is devoted to giving further detail to the results summarized above.

2.0 DESCRIPTION OF DEPOSITION TECHNIQUES

2.1 DEPOSITION APPARATUS

2.1.1 Ion-Beam Deposition

The schematic diagram of the system used to ion beam deposit diamondlike carbon (DLC) films is shown in Figure 1. It consists of four sections: (a) the ion source, (b) the gas inlet system, (c) the vacuum system, and (d) the target fixture.

(a) The Ion Source Assembly. The ion source is a 2.5 cm (D) Kaufman source made by Ion-Tech Inc. A systematic circuit diagram of the source is shown in Figure 2. The ion beam is produced by a plasma discharge. A typical ion current is 10 mA. The ion kinetic energy used in the deposition can be varied from 100 to 1500 eV. The beam profiles of the ion source have been extensively characterized under various conditions such as ion energy, and external magnetic and electrostatic field [7]. Due to the current source design limitation, no effect was found in the ion beam profile. This ion source produced a narrow peaked beam profile.

(b) The Gas Inlet System. The sample inlet system permits introduction of two pre-mixed gases into the ion source. The flow rate of each gas can be controlled by an MKS flow controller. The two gases used in this work were methane (99.99%, Matheson) and hydrogen (99.99%, Matheson).

(c) The Vacuum System. The reaction chamber is a glass bell jar 45 cm in diameter and 75 cm in height. The system is pumped by a 15.24 cm diffusion pump and backed by a 500 ℓ/min mechanical pump. A liquid nitrogen trap was used to improve vacuum quality. The background pressure was typically 10^{-6} torr. The operating pressure was on the order of 10^{-5} ~ 10^{-4} torr.

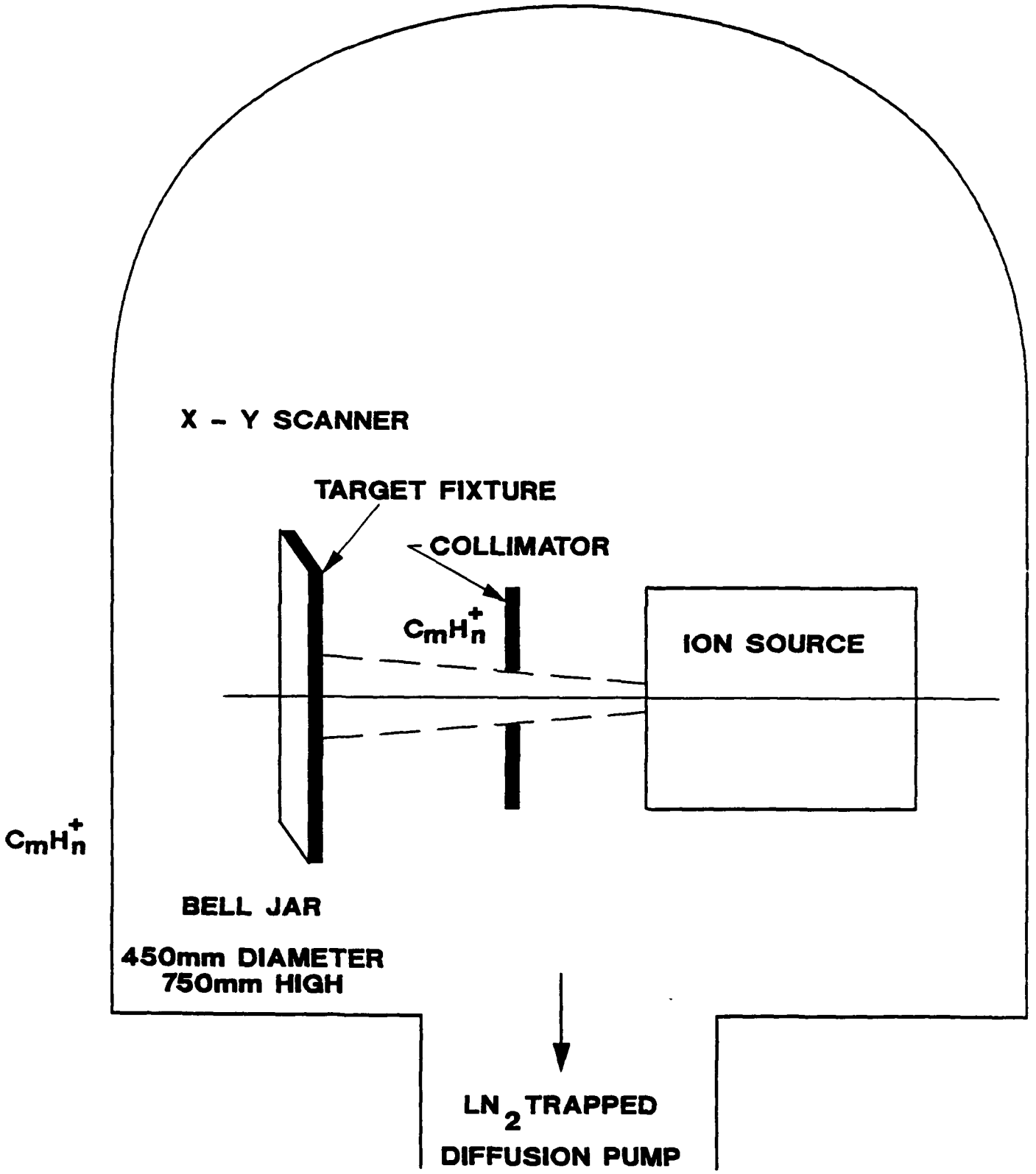

Figure 1 Schematic drawing showing the relationship of the ion source to the target fixture inside the bell jar

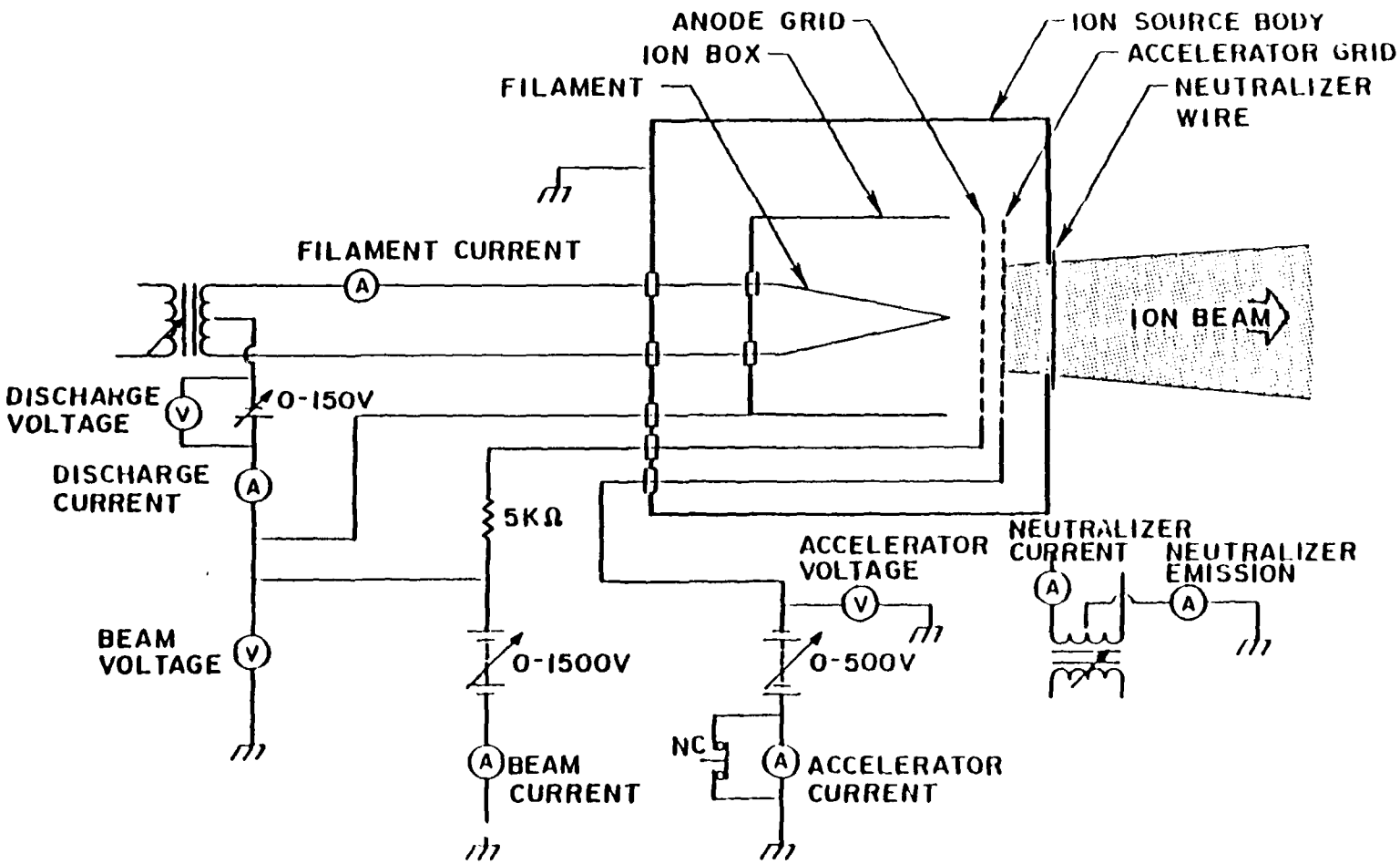

Figure 2 Circuit diagram of the ion source

(d) The Target Fixture. The target fixture was mounted about 8 cm from the ion source. Using the present ion source, the directly deposited films were found to be nonuniform when depositions were made on them as a stationary target. In order to obtain a uniform and large area film, a special design of target fixture was constructed. Figure 3 shows the conceptual drawing of this X-Y scanner. The target plate was able to move approximately ±175. mm in two orthogonal directions in a plane perpendicular to the beam. The X-Y motion of the target plate was accomplished by stepping motors which were controlled by SLO-SYN indexers (430-PI, The Superior Electric Co.). The indexers were interfaced to a host IBM XT-compatible computer via an RS-232 port. This allowed the user to change parameters, i.e., feed-rate and travel distance, in the indexers. The feed-rate of the indexer could be varied from 6 cm/sec to 0.04 cm/sec for the Y-direction and from 1.6 cm/sec to 0.04 cm/sec for the X-direction. Extensive tests have been performed to determine the optimum scan rates. First, the test was carried out by mounting a plotter on the scanner to trace the beam pattern of the paper at various X-Y scanning rates. Second, direct ion-beam depositions of DLC films on various silicon substrates were performed. The carbon content of the deposited film was then analyzed for uniformity using RBS across a 5.5x5.5 cm^2 area. The optimum conditions were determined to be 0.04 cm/sec for the X-direction and 1.6 cm/sec for the Y-direction. This set of scan rates was used on all substrates.

2.1.2 RF-Plasma Configuration I

A rf sputtering system was purchased from Cooke Corporation, consisting of a cryopumped stainless steel bell jar chamber. Inside the chamber were two parallel plate electrodes which were driven by a 13.56 MHz, 0 to 500 watt rf generator and load matching network.

In Configuration I, one electrode was grounded, and the other driven by the rf generator. The driven electrode was much smaller in area than the grounded electrode, as sketched in Figure 4. This geometry created an intense plasma above the driven electrode which was

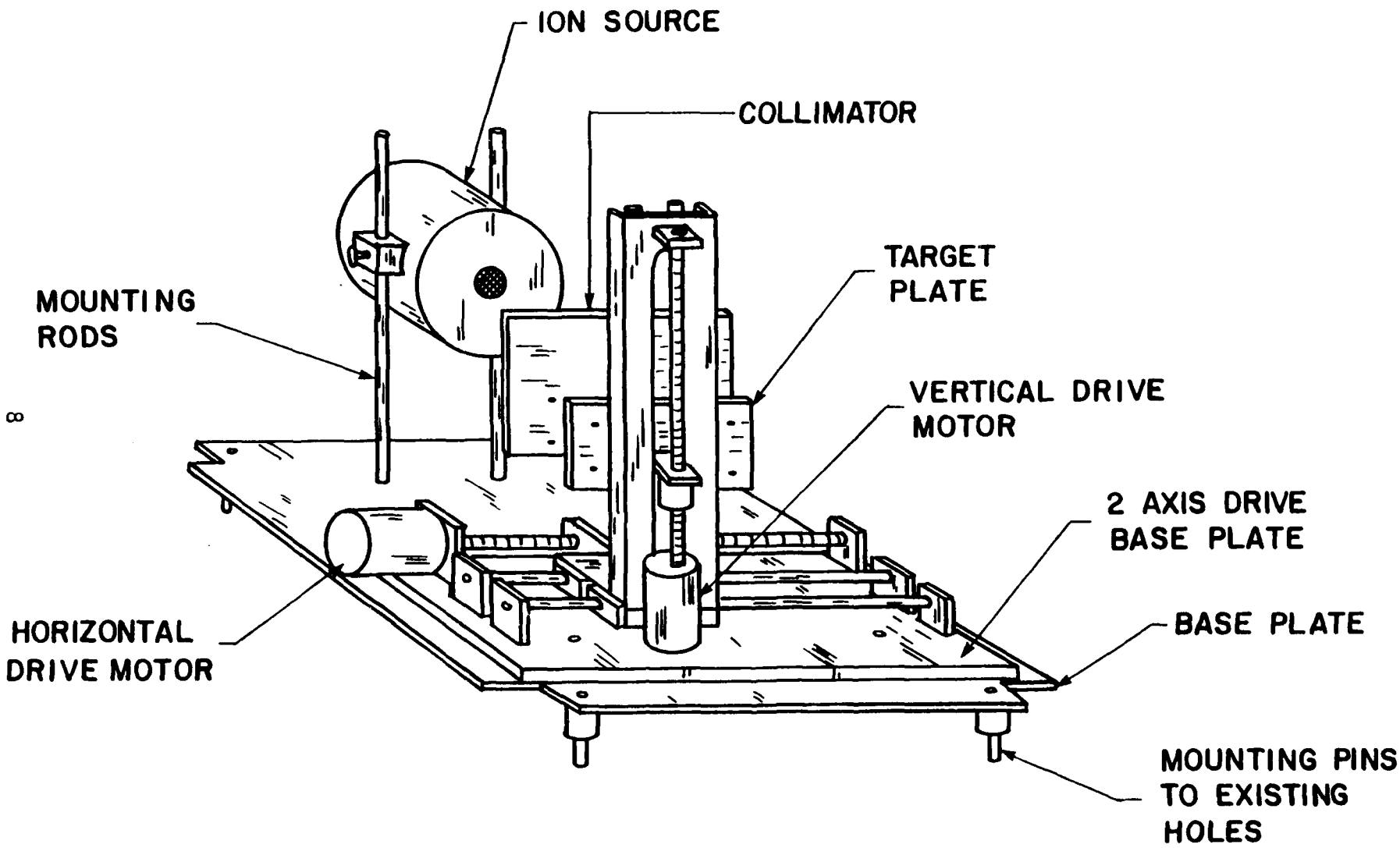

Figure 3 Schematic layout of the target scanner

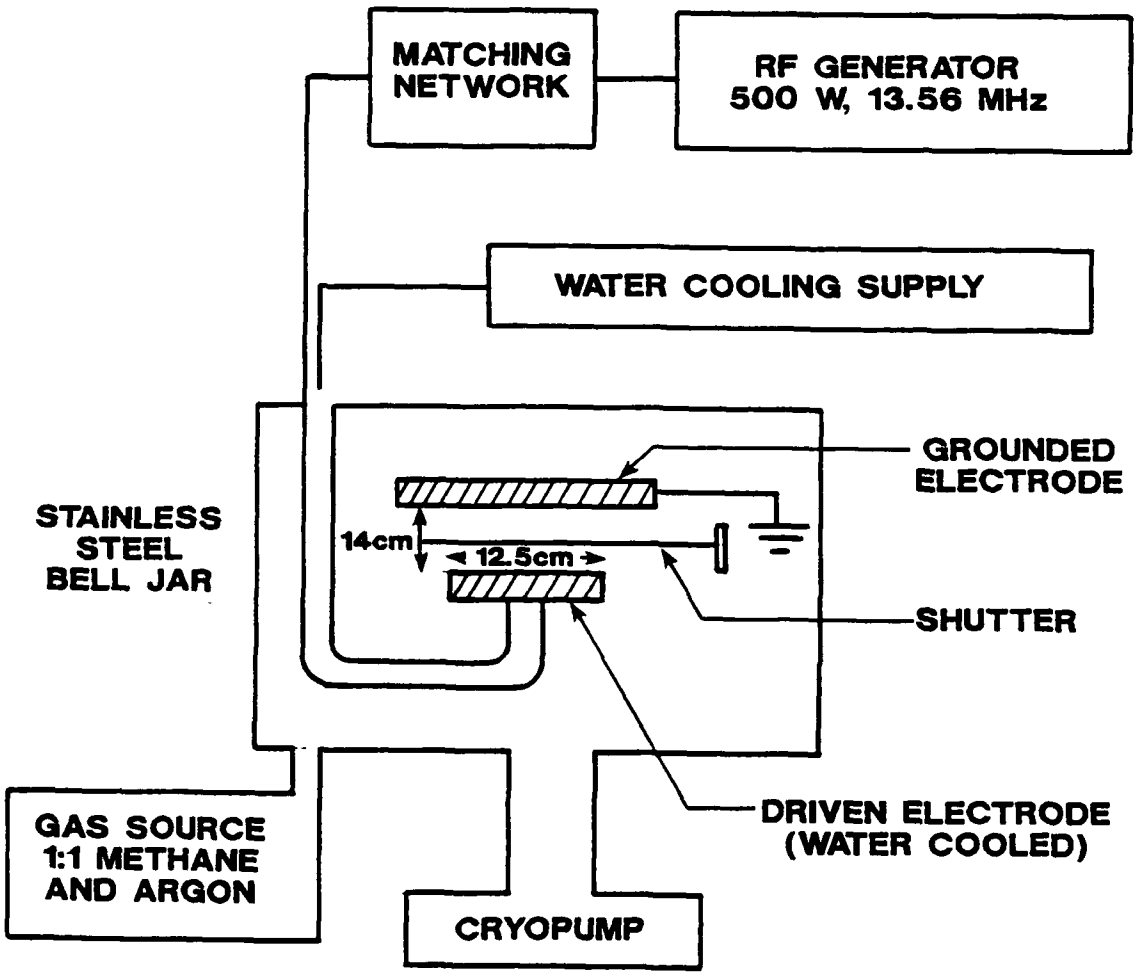

Figure 4 Configuration I schematic design

accompanied by a large self-induced DC bias. Also, a rather diffuse plasma existed at the ground plane with virtually no DC bias. In our work, we placed the substrate on the driven electrode to take advantage of the intense plasma and the high deposition rate. During depositions at low power, the self-induced dc bias was moderate and did not appear to alter the film characteristics. However, significant high energy ion bombardment of the depositing film occurred. We feel the main effect of the ion bombardment was to heat the depositing film and drive out the hydrogen, leaving a low band gap material. This conclusion was based on the results obtained when a deposit was made at 500 watts rf power, 140 μm total pressure for 30 minutes, and another deposit was made under the same conditions except the discharge was run for 2 minutes and turned off 3 minutes until a total time of 30 minutes deposition was achieved. The former deposit exhibited a band gap of approximately 0.2 eV. The band gap of the latter film was comparable to that observed in films deposited at low powers. In view of this, we modified the Cooke system such that the areas of the driven electrode and ground plane were approximately equal (Configuration II). This eliminated the self-induced bias and the accompanying heating effect. This modified system allowed a more accurate exploration of the effect of various plasma parameters on the film properties (see Section 2.2).

2.1.3 RF-Plasma Configuration II

The reason behind the design for this configuration as presented in Section 2.1.2 was to eliminate high energy ion impact and loss of hydrogen during deposition. This configuration has a hollow 30 cm diameter stainless cathode on the bottom (Figure 5), 28 cm diameter stainless steel upper electrode with an appropriate ground shield.

The center of the lower grounded electrode was connected to the gas inlet pipe by means of a small plastic tube. A small metal screen was placed over the center of the hole in the lower plate to prevent the gas discharge from igniting in the gas outlet opening. This electrode was also water cooled by a 28-cm diameter stainless steel plate with copper cooling coils soldered to it.

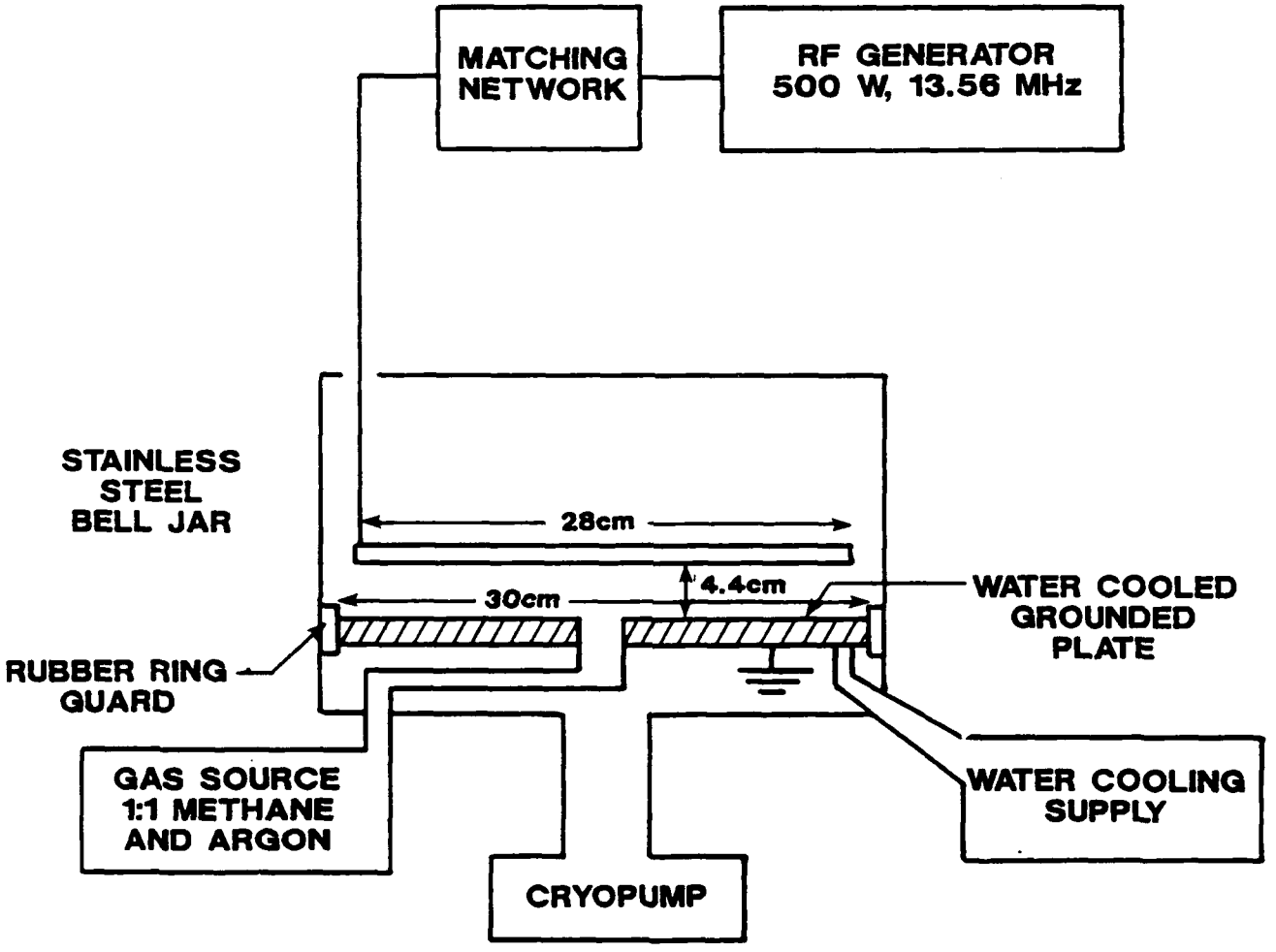

Figure 5 Configuration II schematic design

This Configuration II design reduced the self-induced DC bias, by forcing the area of the driven electrode to be approximately equal to the area of the ground plane. This reduced the high energy ion bombardment of the depositing film and the subsequent heating effects. This design provided a uniform gas flow over the lower electrode for a wide range of input gas flow rates and pumping speeds, creating a large area of uniform deposition for samples placed on this electrode. A rubber ring guard was placed around the outside of the lower electrode to prevent the discharge from igniting around the edges. The frequency was either 30 kHz or 13.56 MHz.

2.2 OPTIMIZATION OF EXPERIMENTAL PARAMETERS

The physical properties of these DLC films on various substrates were found to be strongly dependent upon the deposition parameters. Optimum deposition parameters, for each technique, were established and are described below.

2.2.1 Ion-Beam Deposition

(a) Effect of Excess Hydrogen in the Ion Source. An attempt was made to optimize the hydrogen content of DLC film by varying the hydrogen-to-methane ratio inside the ion source. A series of experiments were performed on silicon substrates. The hydrogen concentration was varied from 0% to 98%. The deposition conditions were as follows: beam voltage - 1000 V; accelerator voltage - 100 V; discharge voltage increased from 58 V to 98 V with increasing hydrogen content in order to maintain the source discharge; filament current typically 6 A; neutralizer current typically 6 A with 3 mA emission; gas flow increased from 1.5 to 10 SCCM with increasing hydrogen content.

The deposited film composition was determined by Rutherford backscattering (RBS) analysis for carbon content and proton recoil detection (PRD) for the hydrogen content. The results are shown in Table 1. It can be seen that the hydrogen content in the deposited film was found to increase from 34% to 40% as compared to using a pure methane

TABLE 1. Effect of Hydrogen in the Source Gas on the Carbon, Hydrogen Contents of Direct Ion Beam Deposited Diamondlike Carbon Films

Sample No.	% Hydrogen in the Source	% Hydrogen in the Film (±5%)	% Carbon in the Film (±5%)
DLC - C	0	30	70
DLC 140	2	40	60
DLC 141	5	36	64
DLC 142	10	38	62
DLC 143	20	35	65
DLC 144	50	40	60
DLC 145	80	41	59
DLC 146	90	NO FILM	NO FILM
DLC 147	90	NO FILM	NO FILM
DLC 148	98	NO FILM	NO FILM
DLC 149	95	39	61

ion source, which resulted in 30% hydrogen. In the present ion-beam deposition technique, the increase of hydrogen ions in the ion beam was found to increase the hydrogen content in the deposited films. From reports in the literature, for a more dense and much harder DLC film, it is better to use pure CH_4 as the gaseous source, which results in a lower percentage hydrogen [3].

(b) Effect of Ion-Impact Energy. The effect of ion-impact energy on the film quality (uniformity, pinhole, adhesion, and optical properties), on the deposition rate, and on the damage to the substrate was investigated. Two impact ion-energies of [illegible] 1000 eV were used to deposit diamondlike carbon on silicon substrates. A pure CH_4 gas was used in these experiments. The gas flow rate was 3 SCCM and the chamber pressure was 9.0×10^{-5} torr. Both films appeared to be uniform and golden in color. The film growth rate, hydrogen content and carbon content were analyzed. The results are shown in Table 2. Within the uncertanties of the RBS, PRD and Dektak film thickness analyses, the deposition rate and the hydrogen concentration in the film were found to be the same. The cross-sectional transmission electron micrograph of the DLC film at 1000 eV showed no damage on the surface of the silicon substrate. At high energy ion impact, the ion current seemed more intense and the films stuck well to the substrate.

TABLE 2. Effect of Ion Impact Energy on the Direct Ion Beam Deposited Diamondlike Carbon Films

Sample No.	Ion Impact Energy (eV)	% Hydrogen in the Film (±5%)	% Carbon in the Film (±5%)	Film Growth Rate A/min ± 5 A/min
871-365	1000	33.0	67.0	23
871-366	500	37.5	63.5	25

(c) Effect of Methane Pressure in the Ion Source. The increase of methane molecules resulted in ion-molecule reactions inside the ion source; higher molecular weights of hydrocarbon ions were produced. The present experiments were carried out at three different pressures: 2.6×10^{-4} torr, 9×10^{-5} torr and 6×10^{-5} torr brought about by controlling the CH_4 flow rate 7.32, 3.00 and 1.32 SCCM. An ion-impact energy of 1000 eV and silicon substrates were used. Uniform golden color films were observed for deposition pressures of 2.6×10^{-4} torr and 9×10^{-5} torr. However, the darker films were obtained using a pressure of 6×10^{-5} torr. The carbon and hydrogen content of the films were analyzed, and results are shown in Table 3.

TABLE 3. Effect of Methane Pressure on the Direct Ion Beam Deposited Diamondlike Carbon Films

Sample No.	CH_4 Source Pressure (torr)	Flow Rate (SCCM)	% Hydrogen in the Film (±5%)	% Carbon in the Film (±5%)
871-367	6×10^{-5}	1.32	38.4	61.6
871-365	9×10^{-5}	3.0	33	67
871-368	2.6×10^{-4}	7.32	33.4	66.7

It can be seen that at the lowest pressure, the hydrogen content in the film was slightly increased. Therefore, if harder films have less hydrogen, it is better to use higher methane pressures.

(d) Effect of Substrate Material. The effect of substrate material (silicon, fused silica, lexan, KG-3, BK-7 glass, ZnS and HMF) on DLC film growth rate and film quality was investigated using the same experimental

conditions: pure CH_4 at flow rates of 3.0 SCCM, 1 KeV ion energy, source pressure of 9×10^{-5} Torr, deposition times from 65 to 450 minutes. All films on the above listed substrates were found to be uniform. The film thicknesses were measured using a Dektak instrument. Table 4 gives the average growth rate of DLC on various substrates over an area of 306 cm^2. The last column lists the deposition rate of DLC on each substrate (having an area of 4.9 cm^2). These were direct ion beam depositions, with the present 2.5 cm diameter ion source.

TABLE 4. Diamondlike Carbon Film Growth Rate on Various Substrates

Substrate	Deposition Rate (Å/min)	Direct ion beam Deposition Rate (Å/sec)
Lexan	11	11.5
BK-7	8	8.3
KG-3	8	8.3
Silicon	6	6.3
Fused Silica, Glass	5.5	5.7
ZnS, ZnSe	6.5	6.8
HMF	6.5	6.8

(e) Effect of Substrate Surface Cleaning Procedures. The effect of cleaning the substrate surface prior to ion deposition of the DLC films was studied extensively. Bonding of the DLC film on various substrates was found to be strongly dependent upon the surface cleaning procedures. The initial cleaning procedures included: (1) washing with 1,1,1 Trichlorethane, (2) washing with acetone, (3) washing with methanol and finally (4) blow drying by dry nitrogen. All samples were cleaned by these four procedures, except the lexan substrate which used only procedures (3) and (4). It was found that DLC films adhered to BK-7, KG-3, ZnS, silicon and lexan substrates quite well, and passed the initial "Scotch" tape tests. However, the DLC film on fused silica and heavy metal fluoride glass failed the "Scotch" tape tests. Thus an attempt was made to investigate the surface cleaning procedures for HMF glass and fused silica. The substrates of HMF (Sample No. 871-357) and fused silica (Sample No. 871-166) were cleaned by procedures (1), (2), (3), and (4), and cleaned again by 1000 eV Ar^+ ion beam for 20 minutes

prior to DLC deposition. The DLC films on both substrates again failed the "Scotch" tape test. Another cleaning procedure was tried to clean the surface by washing with methanol and drying using a heat gun or dry nitrogen. The DLC films on both substrates were found to stick well to these substrates. The new cleaning procedure was thus adapted for cleaning of HMF and fused silica substrates.

(f) Effect of Substrate Temperature. In the present direct ion-beam deposition technique, the temperature of the substrate was constantly monitored by a temperature tape and was found to be less than 60°C. Since the current project was focused on optical materials that are temperature sensitive, no attempt was made to heat the substrate.

2.2.2 RF Plasma Discharge Configuration I

In this section, we describe how best to deposit DLC on the seven substrates; we also relate some early difficulties and how they were overcome.

The DLC deposition (plasma process) was extremely successful on glass slides (Thickness = 1 μm) and Si-wafers. Sometimes there were problems with pinholes. At high power (especially 250 and 500 watts), the film quality became significantly degraded, in terms of the uniformity of the film thickness and the ability to adhere to glass. The thickest films spalled off the edges of the glass slides if the power was too high. As measured from UV-VIS absorption measurements on samples deposited on glass slides, the optical energy gap was about 0.2 eV for the 500-watt sample. Substrate heating was suspected to occur at high rf powers. To test for this postulate, sample K3 was prepared on glass, at 500-watt power, 140 μm pressure, and deposited for 10 minutes (1 minute times 10 with 5 minutes cooling interrupt periods in between); the resulting sample had an optical gap of 1.1 eV, the same value that occurred when low powers were used. This supported the hypothesis that heating caused the drop in optical gap.

Depositions were then tried on other substrates: KG-3 glass, BK-7 glass, fused silica, lexan, and ZnS. The method of preparation and resultant film qualities are described below.

(a) KG-3 Glass (Sample No. KG3-1). The power was 25 watts and the pressure 140 μm. The sample was deposited for 45 minutes. The film quality was extremely bad. The film was partially spalling off from different places, especially from the edges. The conclusion was that the substrate, because of being thick, was getting extremely hot.

(b) KG-3 glass (Sample No. KG3-2). Power was 125 watts, 140 μm pressure, deposited for 30 minutes (5 minutes each x 6 depositions with 5 minutes interrupt time in between). This film looked better than KG3-1; however, there were still many pinholes, and there was slight spalling off the edges at long times after removal from the deposition system.

(c) BK-7 glass (Sample No. BK7-1). Power was 25 watts, 140 μm pressure, and deposition time 30 minutes (5 minutes each x 6 times with 5-minute intervals between deposition as a cooldown period); there were many pinholes and the film was partially removed (spalled) especially around the center part.

The cause of the pinholes was suspected to be the low power that caused the carbon species to be less mobile. So the power was increased to 125 watts.

(d) BK7 glass (Sample No. BK7-2). 125 watts, 140 μm, time of deposition 30 minutes (5 minutes each x 6 times with 5-minute intervals). There were many large pinholes, however, the film was now sticking well to the glass.

(e) Fused Silica (Sample No. FS-1). 125 watts, 140 μm, time of deposition 30 minutes (5 minutes each x 6 times with 5-minute intervals). There were a few pinholes; otherwise, the film quality was very good.

(f) Lexan (Sample No. LX-1). 125 watts and 140 μm, deposition time 50 minutes (5 minutes each x 5 times plus 15 minutes with 5-minute intervals between). The sample was full of pinholes and fractures of interesting criss crossing patterns.

There was a mistake made near the end of this deposition; instead of 5 minutes deposition, there was one of 15 minutes duration; this may have heated the substrate and caused fractures. Therefore, growth on this same substrate was repeated under the same conditions.

(g) Lexan (Sample No. LX-2). 125 watts, 140 μm, deposition time 30 minutes (5 minutes each x 6 deposition with 6-minute intervals in between). There were pinholes and fractures with the same interesting grid patterns. But the number of fractures generated was drastically smaller than encountered in Sample No. LX-1.

Up to this time, all samples were deposited for 30 minutes (2 minutes x 15 times with a 3-minute cooldown time in between), unless otherwise specified.

(h) ZnS (Sample No. ZS-1). 125 watts, 140 μm. Almost all of the film spalled off the surface by itself. Additional cleaning with a methane soaked paper took off the rest of the sample. This same substrate was later used for depositing Samples No. ZS-2 and No. ZS-3.

(i) KG-3 Glass (Sample No. KG3-3). 125 watts, 140 μm, deposition time 6 minutes (2 minutes each x 3 times with a 3-minute cooldown time in between). The spalling tendency was lower than for the previous case (h). As time went on, the film extensively spalled off the substrate by itself. Ultimately, as before, a little scrubbing with Kim-wipe paper soaked in methanol removed remainder of the sample.

For the depositions described above, all glass samples were cleaned by washing with:

(1) 1,1,1,-Trichloroethane
(2) acetone

(3) methanol

(4) deionized water

and ultimately drying with dry nitrogen. All lexan samples were cleaned by washing with:

(1) methanol

(2) deionized water, and finally drying with dry nitrogen

(j) KG-3 glass (Sample No. KG3-4). 125 watts, 140 μm. There were still some pinholes. The film quality was almost the same as for Sample No. KG3-3.

(k) BK-7 glass (Sample No. BK7-3). 125 watts, 140 μm. There were significantly fewer pinholes in this sample than for BK7-2. Also, BK7-3 was slightly darker than BK7-2; which might be due to the greater sample thickness of Sample No. BK7-3.

(l) Lexan (Sample No. LX-3). 125 watts, 140 μm, 24 minutes (2 minutes each x 12 times with a 3-minute interval in between) of deposition time. The film quality was similar to LX-2 (many fractures and pinholes).

We noticed that the pinholes were caused by segregated granular carbon deposits. The pinholes were exposed after the film was blown with dry nitrogen. These granular carbon deposits were probably formed before reaching the substrate, and were likely caused by the excessive amount of carbon atoms in the gas phase (in the plasma). Thus, the next logical step was to reduce the carbon atom density within the plasma. That could be achieved in two ways:

(1) By reducing the pressure

(2) By reducing the power

We took the second alternative. Thus, the following batches of samples were made at 25 watts power and 140 μ pressure. The results were highly successful.

(m) BK-7 glass (Sample No. BK7-4). Very few pinholes were found in the sample. Also, it was brownish and lighter than BK7-3. The sample thickness was nonuniform away from the center because the lateral size of the plasma was smaller than before.

(n) Lexan (Sample No. LX-4). Time of deposition 6 minutes (2 minutes each x 3 with a 3-minute interval in between). The sample was good.

(o) ZnS (Sample No. ZS-3). Time of deposition 1 minute. The sample stuck to the surface very well: no pinholes.

(p) Lexan (Sample No. LX-5). Deposition time 10 minutes (2 minutes x 5 times with a 3-minute interval). This was also a very good film with no pinholes.

2.2.3 Plasma Discharge Configuration II

Table 5 shows the sample number, deposition time, optical energy gap, rf power, gas pressure and voltage bias for a series of samples deposited at the University of Nebraska for purposes of carrying out experiments before making the final set of samples for the Army. Details of how the optical gap was determined are given below.

A 1:1 mixture of methane and argon and a 13.6-MHz RF power source, capable of delivering up to 500 watts, were used for the generation of the plasma. The plate areas were made almost equal in order to deliver the power with a minimum DC bias voltage between the plates. The maximum DC bias voltage observed was 550 volts. The lower plate was grounded and the upper plate was driven by an RF power supply. A cryopump was used to pump down the chamber. This pump needed frequent regeneration. The usual regeneration took about three hours, using the "quick" regeneration system from Cryo-Torr that was installed on the cryopump. A flow of heated dry nitrogen was used for this purpose. The usual deposition time between two successive regenerations was about 15 minutes. The process responsible for this poor cryopump performance is not clear. For longer

TABLE 5. Experimental Samples Made Using Configuration II

SAMPLE NO.	DEPOSITION TIME (MIN)	ENERGY GAP (eV) (TAUC PLOT)	POWER (W)	PRESSURE (MICRON)	J/T BIAS
W4B	30	1.02-1.62	25	5	875/0
W1Z	30	0.92-1.06	25	20	380/0
W20	30	0.8-1.16	26	20	400/0
W38	30	1.13-1.2	25	20	60/0
W1T	30	1.7	25	20	480/0
W4E	30	1.14	25	80	375/0
W21	30	1.2	25	140	375/0
W3C	19	1.2-1.26	25	140	60/0
W4A	30	1.1	50	5	625/0
W2E	27	1.1	50	20	625/0
W1X	30	1.12	50	20	625/0
W30	30	0.98-1.18	50	20	100/0
W5A	30	1.0-1.14	50	80	500/0
W2J	30	1.16-1.1	50	140	490/0
W2H	30	1.08	100	20	670/0
W2Q	30	0.86	125	20	1000/0
W1W	30	1.2	125	20	880/0
W58	30	1.00	125	80	750/0
W2K	18	1.1	125	140	680/0
W2L	30	0.78-1.04	125	290	625/0
W4C	30	0.8-1.5	250	5	1250/0
W1U	30	0.96	250	20	1300/0
W5C	20	0.76-0.9	250	80	1000/0
W2N	30	0.6-0.72	250	140	1000/0
W2R	5	0.88	250	140	900/0
W2M	27	0.65-0.8	250	230	875/0
W4D	30	0.8-1.3	500	5	1750/0
W1V	30	0.96-3.62	500	20	1650/0
W50	30	0.42	500	80	1350/0
W2P	30	0.17	500	140	1250/0

TABLE 5. Experimental Samples Made Using Configuration II (cont'd)

SAMPLE NO.	DEPOSITION TIME (MIN)	ENERGY GAP (eV) (TAUC PLOT)	POWER (W)	PRESSURE (MICRON)	J/T BIAS
W4B	30	1.02-1.62	25	5	875/0
W4A	30	1.1	50	5	625/0
W4C	30	0.8-1.5	250	5	1250/0
W4D	30	0.8-1.3	500	5	1750/0
W1Z	30	0.92-1.06	25	20	380/0
W3B	30	1.13-1.2	25	20	60/0
W1T	30	1.7	25	20	480/0
W2D	30	0.8-1.16	25	20	400/0
W2E	27	1.1	50	20	625/0
W3D	30	0.98-1.18	50	20	100/0
W1X	30	1.12	50	20	625/0
W2H	30	1.08	100	20	670/0
W2Q	30	0.86	125	20	1000/0
W1W	30	1.2	125	20	880/0
W1U	30	0.96	250	20	1300/0
W1V	30	0.96-3.62	500	20	1650/0
W4E	30	1.14	25	80	375/0
W5A	30	1.0-1.14	50	80	500/0
W5B	30	1.00	125	80	750/0
E5C	20	0.76-0.9	250	80	1000/0
W5D	30	0.42	500	80	1350/0
W3C	19	1.2-1.26	25	140	60/0
W2I	30	1.2	25	140	375/0
W2J	30	1.16-1.1	50	140	490/0
W2K	18	1.1	125	140	680/0
W2R	5	0.88	250	140	900/0
W2N	30	0.6-0.72	250	140	1000/0
W2P	30	0.17	500	140	1250/0
W2M	27	0.65-0.8	250	230	875/0
W2L	30	0.78-1.04	125	290	625/0

deposition times (more than about 5 minutes), we had to turn off the RF power to let the pump cool down and to return the base pressure to its normal value (which was about 25 μm).

The substrates used for final depositions for the 70 Army deliverable samples were: Si, KG3 glass, BK7 glass, fused silica, lexan, heavy metal fluoride (HMF) glass, and ZnS. Before the actual final depositions started, we ran into a series of difficulties as explained in the next few paragraphs.

Before the actual depositions started, the lower plate area was made large enough that it nearly touched the wall of the chamber. This was done to prevent the plasma from spilling down to the bottom of the chamber (around the edge of the lower ground plate). As a consequence, the delivered power was confined to the smaller volume occupied by the plasma. This enlarged plate area caused some difficulty in starting the discharge, and we used a tesla-coil to initiate this process. Starting the discharge was made more difficult due to the fact that the plasma volume was above the quartz viewing window of the chamber and was completely surrounded by the metallic wall of the chamber.

To measure the rate of deposition, we mounted a quartz glass slide on the lower ground plate of the chamber. The deposition was made at a 12.5 sccm flow rate of both methane and argon with a base pressure of 80 μm and a delivered RF power to the plasma of 200 watts (the corresponding DC bias voltage between the plates was 375 volts). To make a step in the DLC film for thickness measurements, a small piece of Si was placed on the glass slide with the polished face of the Si chip making contact with the glass slide. The deposition was made for a period of 15 minutes and the results of profilometric measurements are shown in Figure 6. From this measurement, the estimated rate of deposition was about 170Å per minute.

When the system shown in Figure 5 was first designed and operated, the rubber guard ring was not present, and the plasma was very unsteady and sometimes passed beyond the lower ground plate to the bottom of the chamber. Also, sometimes it became incredibly hard to start the plasma;

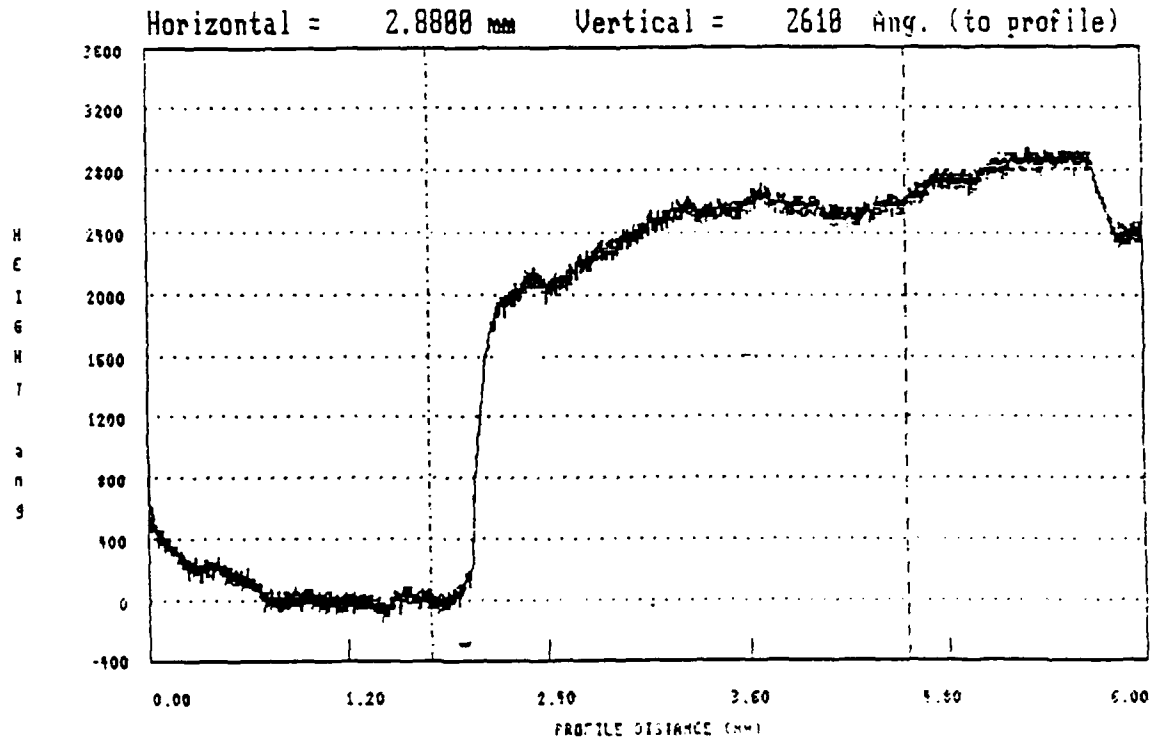

Figure 6 Profilometric measurement of DLC film on quartz glass

even after using the tesla coil and adjusting the matching network of the RF power supply we could not start the plasma, (at the 80 μm base pressure and the flow rate of 12.5 sccm for both methane and argon). Figure 7 shows more details of the Figure 5 design which permitted easier igniting of the plasma due to a better gas flow geometry. We made 16 small holes in the plate and closed the gap between the lower ground plate and the chamber using a vacuum compatible rubber strip as shown in Figure 7. The gas thus entered the plasma region through the center and flowed radially outward. We planned to use the external DC INPUT to start the plasma (instead of the tesla coil), but found that after modifying the system, the gas plasma was generated rather easily by increasing the gas pressure to 100 μm. Sometimes, use of a tesla coil in combination with some adjustment of the matching network of the RF power supply was helpful in starting the gas discharge. The plasma was found to be confined within the volume above the lower ground plate.

To find the homogeneity of the film over the surface of the chamber and the rate of DLC film deposition, we mounted five pieces of Si test strips on the ground plate as shown in Figure 8. We also placed three Si chips on the strips, numbered 1, 3 and 4 to make the steps of DLC film for the thickness measurements. The depositions were made at 13 sccm flow rates of both methane and argon and at the base pressure of 100 μm; the power was 200 watts and the time of deposition was 15 minutes. The result of a profilometric measurement is shown in Figure 9. We basically have the same rate of deposition as for the glass slide mentioned previously. Also, the film was uniform within a certain range of radii from the center of the ground plate, as shown by the color of the film. We were then prepared for the final deposition of the films for the Army deliverables.

Except for Si, Lexan, HMF glass, and ZnS, all the substrates were first ultrasonically cleaned using 1,1,1-Trichloroethane; then washed with acetone, methanol, and deionized water successively and finally dried by blowing dry nitrogen. Lexan was ultrasonically cleaned using methanol, washed with deionized water and finally dried using dry nitrogen. HMF surface was found to be deteriorated by the use of any of the organic solvents mentioned previously. An example of the surface

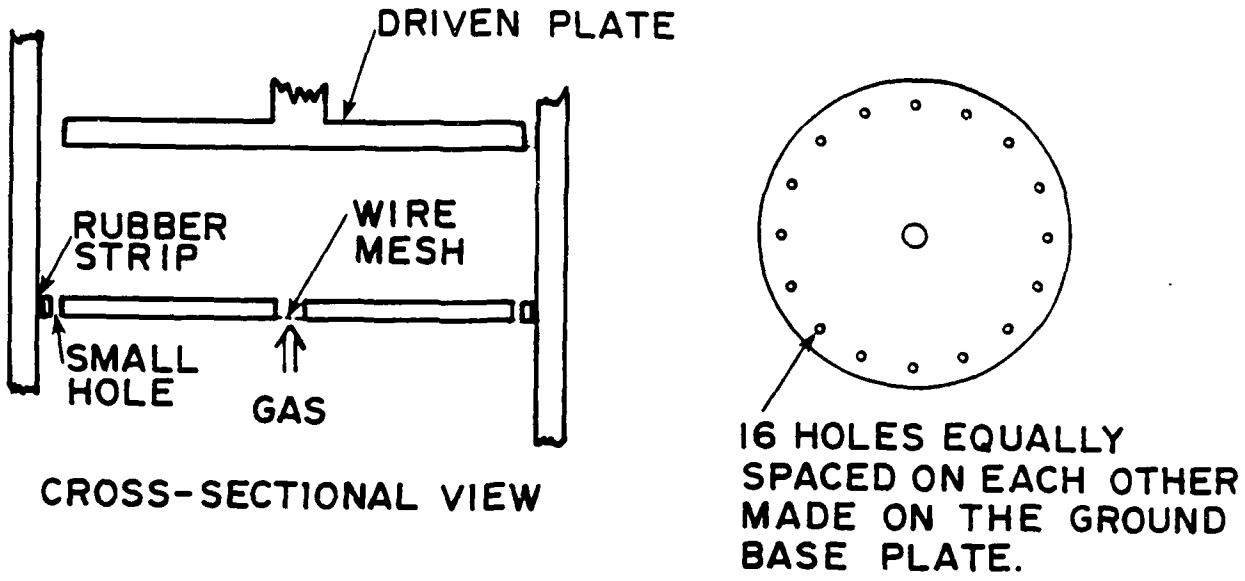

Figure 7 Cross-sectional view of the plasma discharge Configuration II

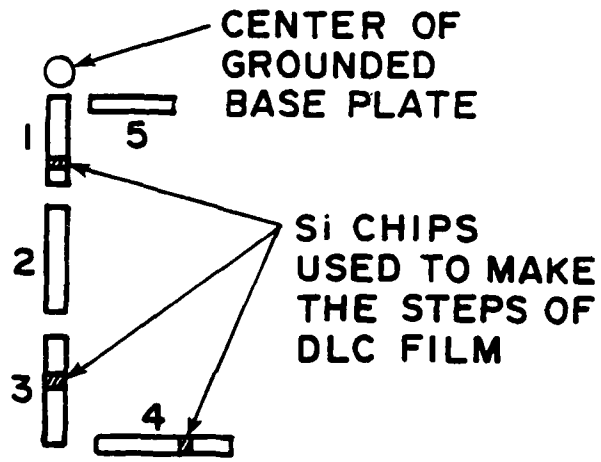

Figure 8 Test strips inside the discharge chamber for homogeneity studies in the discharge region

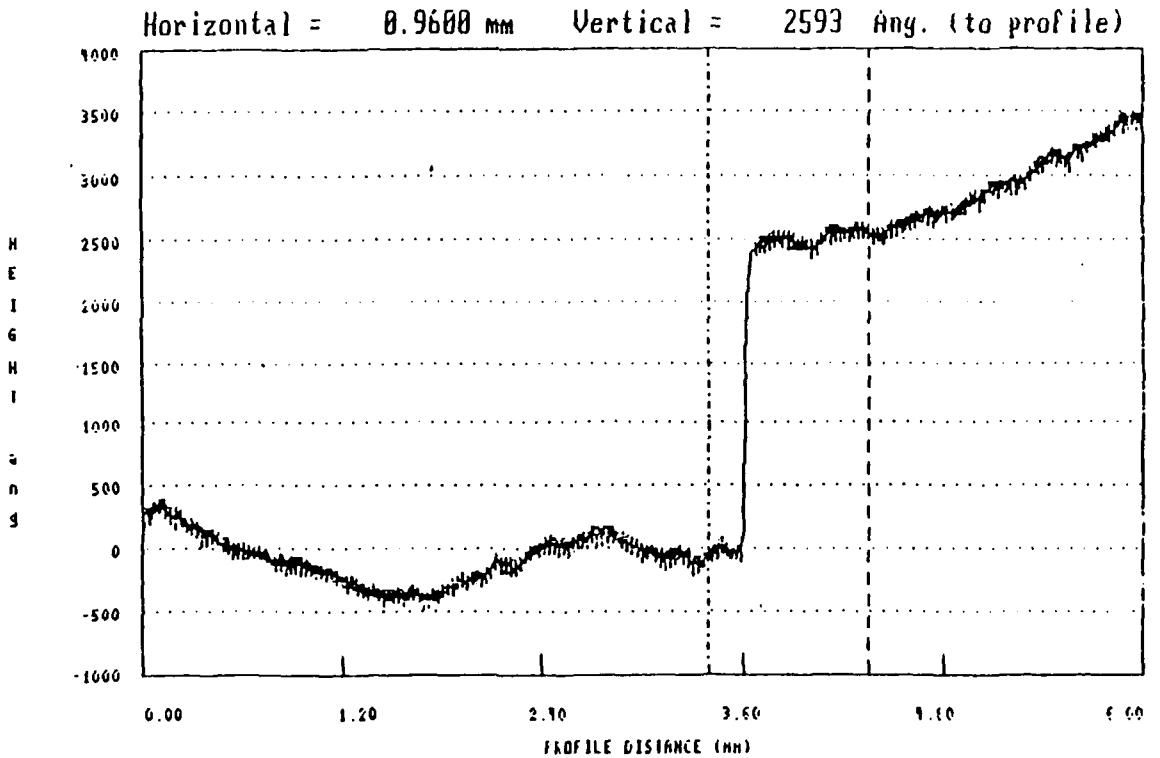

Figure 9 Profilometric measurement of DLC film on glass slide

morphology as a result of the cleaning can be found in the sample named DLC/HMF #1.) Therefore, we visually looked for the clean surface of HMF, dried it by blowing dry nitrogen, and mounted it on the ground base plate so that the clean surface was up. The Si surface was clean; therefore we used only dry nitrogen to clean the surface. For ZnS, we followed the same procedure.

All the depositions for the final deliverable samples were made under the following conditions unless specifically mentioned otherwise:

- o flow rate for methane and argon: 13 sccm each,
- o base pressure: 100 μm,
- o power: 200 watts, and
- o DC bias between the two plates: 300 volts.

The following gives the list of the substrates names, the sample names and the times of deposition:

I -- Si wafer, DLC/SI #1...DLC/SI#10, 19 minutes of deposition.

II -- BK7 glass, DLC/BK7#1...DLC/BK7 #10, 10 minutes of deposition.

III -- KG3 glass, DLC/KG#1...DLC/KG2#10,5 minutes of deposition.

IV -- fused silica glass, DLC/FS #1...DLC/FS #10, 12.5 minutes of deposition.

V -- lexan, DLC/LX #1...DLC/LX #4, 14 minutes and 46 seconds of deposition.

VI -- lexan, DLC/LX #7...DLC/LX #12, 14 minutes and 10 seconds of deposition.

VII -- HMF glass, DLC/HMF #1, DLC/HMF#2, 7 minutes and 46 seconds of deposition.

VIII -- HMF glass, DLC/HMF #3...DLC/HMF #10, 7 minutes of deposition.

IX -- ZnS glass, DLC/ZnS #1...DLC/ZnS #5, 100 microns of base pressure, 16 sccm methane and argon flow rate, 2 minutes of deposition.

X -- ZnS glass, DLC/ZnS #6...DLC/ZnS #10, 2 minutes of deposition.

From the depositions using Configuration I, we found that DLC films on ZnS substrates tended to spall very easily if the film was thicker than a few hundred angstrom units. Because of that, we deposited for 2 minutes (only) on the ZnS substrate, resulting in an estimated film thickness of about 300Å. Recently, the work of Banks and coworkers at NASA Lewis with DLC deposition on ZnS and ZnSe has come to our attention. These people showed that DLC will adhere to ZnS and ZnSe if a thin (300Å) Ge film is deposited between the semiconductor and the DLC layer [8].

Figures 10 and 11 show a strong dependence of deposition rate on substrate temperature and gas flow rate, and the lack of dependence on rf power. The configuration for these depositions was II, as depicted in Figures 5 and 7.

TABLE 6. Deposition conditions and optical bandgap:DLC using Configuration II

Sample Name	Pressure (μ)m	Power (W)	DC Self-Bias (V)	Band Gap (eV)
B6	50	50	190	2.6
B5	50	150	500	2.1
B4	50	300	500	2.1
B2&B3	50	500	600	2.1
B7	100	50	190	2.6
B8	100	150	290	2.5
B9	100	300	500	2.3

2.3 SUMMARY OF SAMPLES DELIVERED TO THE ARMY

2.3.1 Ion-Beam Deposition

Tables 7 through 13 give the detailed experimental conditions for producing 10 DLC films each on seven substrates, which were delivered to the Army Material Technology Laboratory on May 20, 1988.

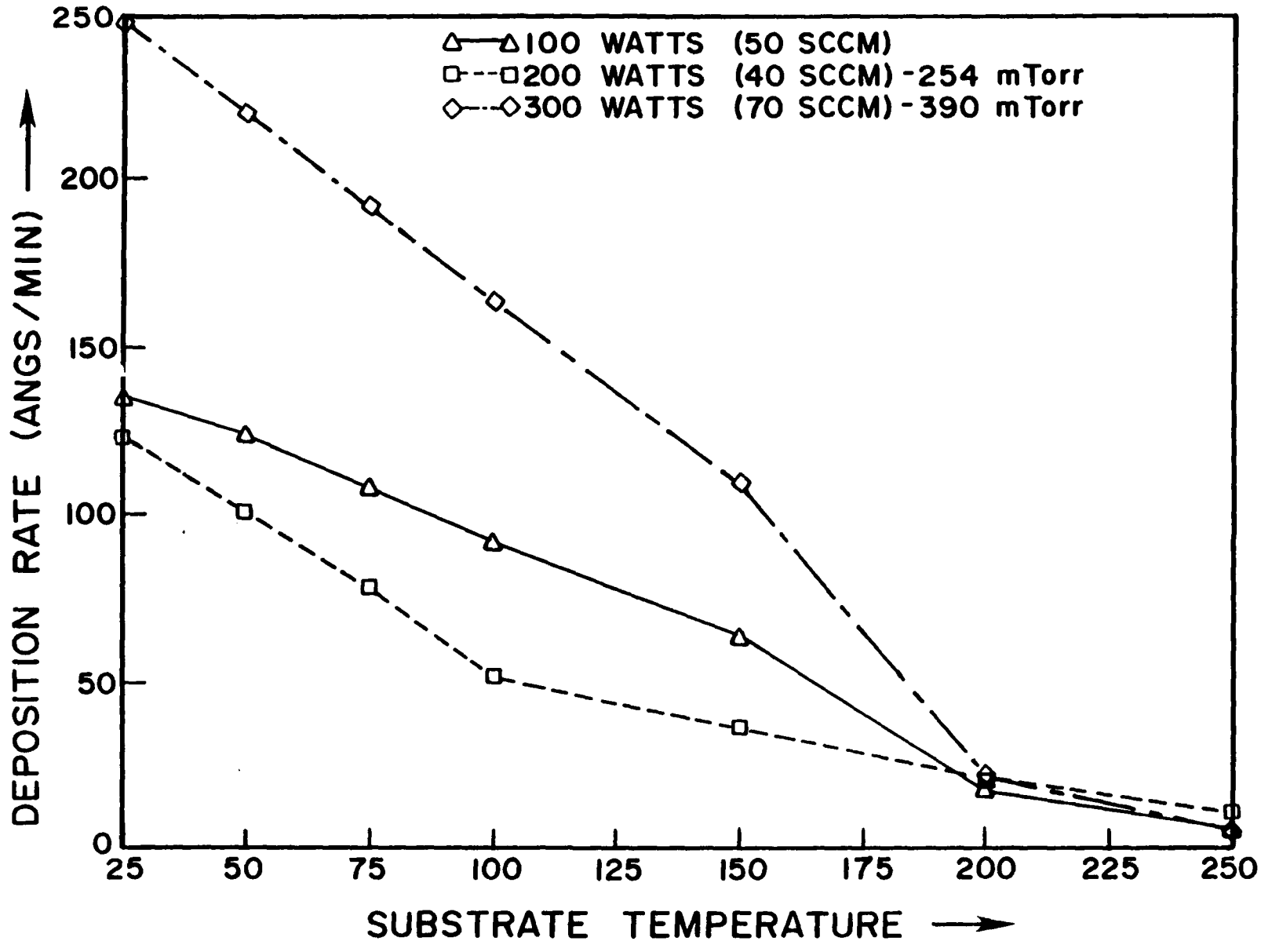

Figure 10 Deposition rate for Configuration II (30 kHz) deposited DLC films: dependence on power and substrate temperature

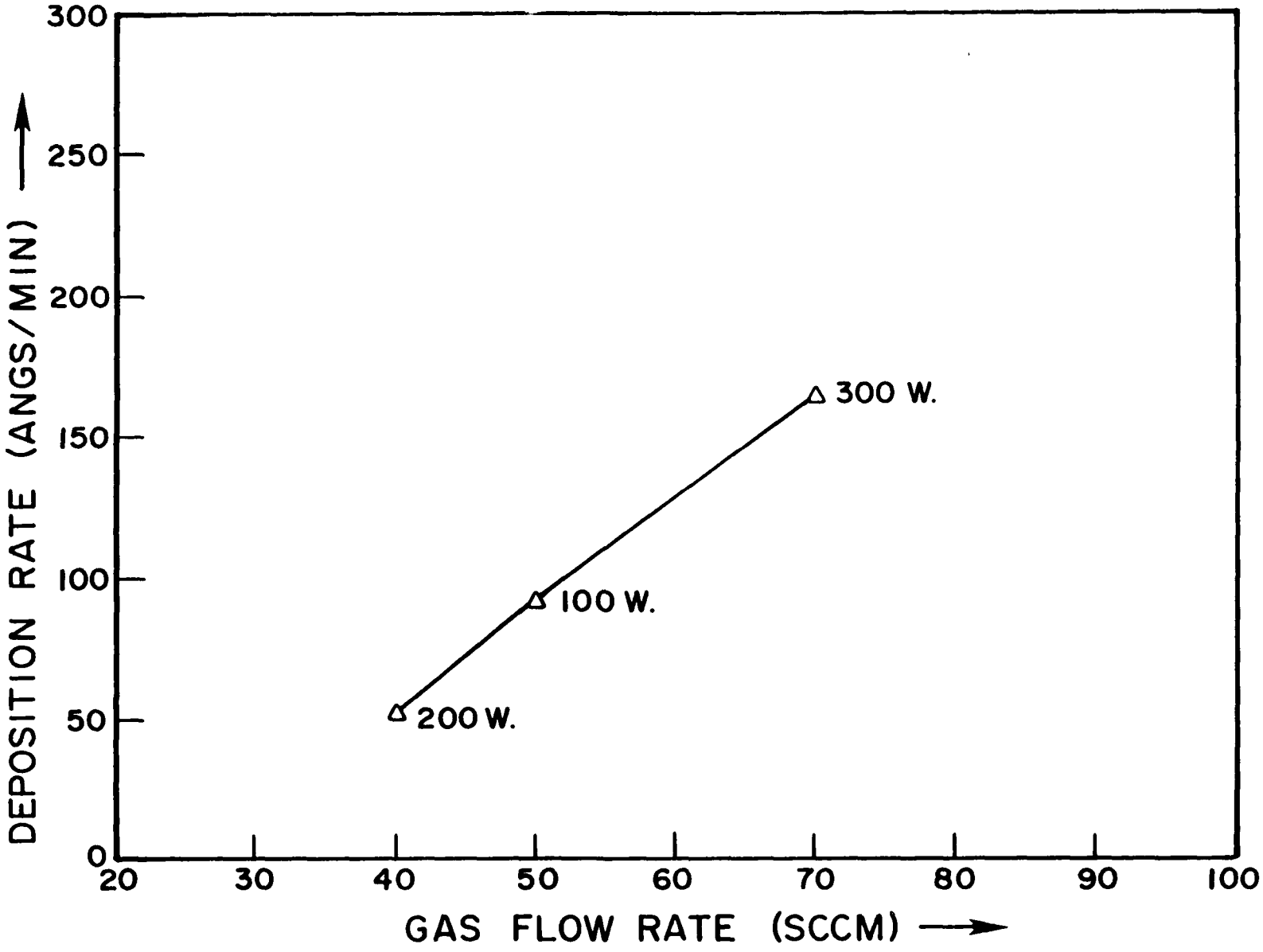

Figure 11 Deposition rate for Configuration II (30 kHz) DLC films: dependence on gas flow

TABLE 7. Ion Beam Diamondlike Carbon: ZnS

SUBSTRATE : ZnS

Gas : 99.99% Methane Gas rate : 3.25 SCCM

sample # / film (Å) / date	dep. time (min)	chamber press. (Torr)	beam voltage (volts)	beam current (mA)	accel. voltage (volts)	discharge voltage (volts)	cathode current (amps)	cleaning proc. (see *)
871-208 / 900 / 29 FEB 88	240	1.0E-4	1000	12	100	70	6.0	a
Comments	Excellent film (some scratches on substrate)(brown color;masked)							
871-209 / 900 / 29 FEB 88	240	1.0E-4	1000	12	100	70	6.0	a
Comments	Excellent film (some scratches on substrate) (brown color)							
871-210 / 900 / 29 FEB 88	240	1.0E-4	1000	12	100	70	6.0	a
Comments	Excellent film (some scratches on substrate) (brown color)							
871-211 / 900 / 29 FEB 88	240	1.0E-4	1000	12	100	70	6.0	a
Comments	Excellent film (some scratches on substrate) (brown color)							
871-214 / 3413 / 24 MAR 88	450	1.6E-4	1000	10	100	69	5.8	c
Comments	Film blistered on edges after approx. 2 wks.(dark brown color)							
871-216 / 2911 / 25 MAR 88	600	9.2E-5	1000	11	100	70	6.1	c
Comments	Film blistered on one side after approx. 2 wks)(brown color)							
871-222 / 4513 / 1 APR 88	600	9.6E-5	1000	10.5	100	70	6.1	c
Comments	film blistered after approx. 2 weeks (dark brown color;masked)							
871-217 / 2056 / 8 APR 88	300	6.2E-5	1000	11	100	70	6.2	e
Comments	Excellent film (one scratch on substrate)(brown color;masked)							
871-110 / 2056 / 8 APR 88	300	6.2E-5	1000	11	100	70	6.2	e
Comments	Excellent film (brown color) (masked) (thick substrate)							
CVD-#6 / 2056 / 8 APR 88	300	6.2E-5	1000	11	100	70	6.2	e
Comments	Excellent film (brown color)							

* a = 1,1,1 Trichloroethane, Acetone, Methanol, nitgrogen dried
b = 1,1,1 Trichloroethane , Methanol, nitrogen dried
c = Methanol, heat dried
d = Soaked in hexane, lightly swabbed, nitrogen dried
e = Ethanol, lightly swabbed, heat dried

TABLE 8. Ion Beam Diamondlike Carbon: Silicon

SUBSTRATE : SILICON

Gas : 99.99% Methane Gas rate : 3.25 SCCM

sample # / film (A) / date	dep. time (min)	chamber press. (Torr)	beam voltage (volts)	beam current (mA)	accel. voltage (volts)	discharge voltage (volts)	cathode current (amps)	cleaning proc. (see *)
871-369 / 1400 / 23 FEB 88	240	1.7E-4	1000	9.5	100	70	6.2	a
Comments	Excellent film (gold color) (masked region + partial masking)							
871-370 / 1400 / 23 FEB 88	240	1.7E-4	1000	9.5	100	70	6.2	a
Comments	Excellent film (gold color) (small masked region)							
871-371 / 1400 / 23 FEB 88	240	1.7E-4	1000	9.5	100	70	6.2	a
Comments	Excellent film (gold color)							
871-372 / 1400 / 23 FEB 88	240	1.7E-4	1000	9.5	100	70	6.2	a
Comments	Excellent film (gold color)							
871-373 / 4746 / 1 APR 88	600	9.6E-5	1000	10.5	100	70	6.1	c
Comments	Excellent film (greenish dark silver color) (masked)							
871-374 / 4746 / 1 APR 88	600	9.6E-5	1000	10.5	100	70	6.1	c
Comments	Excellent film (greenish dark silver color)							
871-375 / 5334 / 4 APR 88	600	8.0E-5	1000	11	100	70	6.1	c
Comments	Excellent film (greenish color) (masked)							
871-376 / 5334 / 4 APR 88	600	8.0E-5	1000	11	100	70	6.1	c
Comments	Excellent film (greenish color, fringed on two edges)							
871-377 / 5334 / 4 APR 88	600	8.0E-5	1000	11	100	70	6.1	c
Comments	Excellent film (greenish color, fringed in two areas)							
871-378 / 5334 / 4 APR 88	600	8.0E-5	1000	11	100	70	6.1	c
Comments	Excellent film (greenish color, fringed on one edge)							

* a = 1,1,1 Trichloroethane, Acetone, Methanol, nitrogen dried
  b = 1,1,1 Trichloroethane, Methanol, nitrogen dried
  c = Methanol, heat dried
  d = Soaked in hexane, lightly swabbed, nitrogen dried
  e = Ethanol, lightly swabbed, heat dried

TABLE 9. Ion Beam Diamondlike Carbon: Lexan

SUBSTRATE : LEXAN

Gas : 99.99% Methane Gas rate : 3.25 SCCM

sample # / film (Å) / date	dep. time (min)	chamber press. (Torr)	beam voltage (volts)	beam current (mA)	accel. voltage (volts)	discharge voltage (volts)	cathode current (amps)	cleaning proc. (see *)
871-042 / 2455 / 19 FEB 88	120	1.2E-4	1000	10	100	72	6.0	b
Comments	Excellent film (gold color) (masked)							
871-043 / 2455 / 19 FEB 88	120	1.2E-4	1000	10	100	72	6.0	b
Comments	Excellent film (one scratch across surface) (gold color)							
871-044 / 2455 / 19 FEB 88	120	1.2E-4	1000	10	100	72	6.0	b
Comments	Excellent film (gold color)							
871-045 / 2455 / 19 FEB 88	120	1.2E-4	1000	10	100	72	6.0	b
Comments	Excellent film (gold color)							
871-046 / 2300 / 19 FEB 88	120	7.0E-5	1000	11	100	70	5.9	b
Comments	Excellent film (gold color)							
871-047 / 2300 / 19 FEB 88	120	7.0E-5	1000	11	100	70	5.9	b
Comments	Excellent film (one scratch about 8mm long) (gold color)							
871-048 / 2300 / 19 FEB 88	120	7.0E-5	1000	11	100	70	5.9	b
Comments	Excellent film (gold color)							
871-049 / 2300 / 19 FEB 88	120	7.0E-5	1000	11	100	70	5.9	b
Comments	Excellent film (one pinhole from substrate) (gold color)							
871-050 / 1800 / 22 FEB 88	120	9.6E-5	1000	10	100	70	5.9	b
Comments	Excellent film (gold color)							
871-051 / 1800 / 22 FEB 88	120	9.6E-5	1000	10	100	70	5.9	b
Comments	Excellent film (gold color)							

* a = 1,1,1 Trichloroethane, Acetone, Methanol, nitgrogen dried
b = 1,1,1 Trichloroethane , Methanol, nitrogen dried
c = Methanol, heat dried
d = Soaked in hexane, lightly swabbed, nitrogen dried
e = Ethanol, lightly swabbed, heat dried

TABLE 10. Ion Beam Diamondlike Carbon: KG-3

SUBSTRATE : KG-3

Gas : 99.99% Methane Gas rate : 3.25 SCCM

sample # / film (A) / date	dep. time (min)	chamber press. (Torr)	beam voltage (volts)	beam current (mA)	accel. voltage (volts)	discharge voltage (volts)	cathode current (amps)	cleaning proc. (see *)
871-071 / 982 / 16 MAR 88	150	1.6E-4	1000	10	100	69	6.0	a
Comments	Excellent film (gold color) (masked)							
871-072 / 982 / 16 MAR 88	150	1.6E-4	1000	10	100	69	6.0	a
Comments	Some pinholes in one corner (gold color film)							
871-073 / 982 / 16 MAR 88	150	1.6E-4	1000	10	100	69	6.0	a
Comments	Some staining and holes in one corner (gold color film)							
871-074 / 982 / 16 MAR 88	150	1.6E-4	1000	10	100	69	6.0	c
Comments	Some staining and clouding of film in one corner (gold color)							
871-075 / 1435 / 23 MAR 88	150	1.6E-4	1000	10	100	69	6.0	c
Comments	Excellent film (gold color)							
871-076 / 1435 / 23 MAR 88	150	1.6E-4	1000	10	100	69	6.0	c
Comments	Excellent film (gold color)							
871-077 / 1435 / 23 MAR 88	150	1.6E-4	1000	10	100	69	6.0	c
Comments	Excellent film (gold color)							
871-079 / 220 / 24 MAR 88	150	8.0E-5	1000	10.5	100	70	6.0	c
Comments	Excellent film (gold tint)							
871-080 / 220 / 24 MAR 88	150	8.0E-5	1000	10.5	100	70	6.0	c
Comments	Excellent film (gold tint)							
871-081 / 220# / 24 MAR 88	150	8.0E-5	1000	10.5	100	70	6.0	c
Comments	Excellent film (gold tint)							

* a = 1,1,1 Trichloroethane, Acetone, Methanol, nitgrogen dried
  b = 1,1,1 Trichloroethane , Methanol, nitrogen dried
  c = Methanol, heat dried
  d = Soaked in hexane, lightly swabbed, nitrogen dried
  e = Ethanol, lightly swabbed, heat dried

TABLE 11. Ion Beam Diamondlike Carbon: HMF

SUBSTRATE : HMF

Gas : 99.99% Methane Gas rate : 3.25 SCCM

sample # / film (A) / date	dep. time (min)	chamber press. (Torr)	beam voltage (volts)	beam current (mA)	accel. voltage (volts)	discharge voltage (volts)	cathode current (amps)	cleaning proc. (see *)
871-368 / 1750 / 6 APR 88	240	7.0E-5	1000	10	100	70	6.2	e
Comments	Excellent film (some holes) (brown color) (masked)							
871-369 / 1750 / 6 APR 88	240	7.0E-5	1000	10	100	70	6.2	e
Comments	Uniform film (some defects) (brown color)							
871-370 / 1750 / 6 APR 88	240	7.0E-5	1000	10	100	70	6.2	e
Comments	Excellent film (brown color)							
871-371 / 1750 / 6 APR 88	240	7.0E-5	1000	10	100	70	6.2	e
Comments	Excellent film (brown color)							
871-372 / 1750 / 6 APR 88	240	7.0E-5	1000	10	100	70	6.2	e
Comments	Excellent film (brown color)							
871-373 / 1750 / 6 APR 88	240	7.0E-5	1000	10	100	70	6.2	e
Comments	Excellent film (small chip in substrate) (brown color)							
871-361 / 900 / 7 APR 88	150	6.6E-5	1000	11	100	70	5.9	e
Comments	Uniform film (substrate scratched) (brown tint)							
871-365 / 900 / 7 APR 88	150	6.6E-5	1000	11	100	70	5.9	e
Comments	Film thinned in area approx. 4 mm in dia. (brown tint)							
871-366 / 900 / 7 APR 88	150	6.6E-5	1000	11	100	70	5.9	e
Comments	Uniform film (substrate scratched) (brown tint)							
871-367 / 900 / 7 APR 88	150	6.6E-5	1000	11	100	70	5.9	e
Comments	Uniform film (defect in substrate) (brown tint)							

* a = 1,1,1 Trichloroethane, Acetone, Methanol, nitgrogen dried
b = 1,1,1 Trichloroethane , Methanol, nitrogen dried
c = Methanol, heat dried
d = Soaked in hexane, lightly swabbed, nitrogen dried
e = Ethanol, lightly swabbed, heat dried

TABLE 12. Ion Beam Diamondlike Carbon: BK-7

SUBSTRATE : BK-7

Gas : 99.99% Methane Gas rate : 3.25 SCCM

sample # / film (Å) / date	dep. time (min)	chamber press. (Torr)	beam voltage (volts)	beam current (mA)	accel. voltage (volts)	discharge voltage (volts)	cathode current (amps)	cleaning proc. (see *)
871-122 / 276 / 07 MAR 88	100	1.2E-4	1000	10	100	70	6.0	c
Comments	Excellent film (brown tint)							
871-123 / 276 / 07 MAR 88	100	1.2E-4	1000	10	100	70	6.0	c
Comments	Excellent film (brown tint) (masked)							
871-124 / 276 / 07 MAR 88	100	1.2E-4	1000	10	100	70	6.0	c
Comments	Excellent film (brown tint)							
871-125 / 276 / 07 MAR 88	100	1.2E-4	1000	10	100	70	6.0	c
Comments	Excellent film (brown tint)							
871-126 / 274 / 11 MAR 88	100	8.4E-5	1000	9.5	100	70	5.9	c
Comments	Some pinholes in film							
871-127 / 274 / 11 MAR 88	100	8.4E-5	1000	9.5	100	70	5.9	c
Comments	Several pinholes and some staining							
871-128 / 645 / 23 MAR 88	100	9.0E-5	1000	9.5	100	69	6.0	c
Comments	Excellent film (gold color)							
871-129 / 645 / 23 MAR 88	100	9.0E-5	1000	9.5	100	69	6.0	c
Comments	Excellent film (gold color)							
871-130 / 645 / 23 MAR 88	100	9.0E-5	1000	9.5	100	69	6.0	c
Comments	Excellent film (gold color)							
871-131 / 645 / 23 MAR 88	100	9.0E-5	1000	9.5	100	69	6.0	c
Comments	Excellent film (gold color)							

* a = 1,1,1 Trichloroethane, Acetone, Methanol, nitgrogen dried
  b = 1,1,1 Trichloroethane , Methanol, nitrogen dried
  c = Methanol, heat dried
  d = Soaked in hexane, lightly swabbed, nitrogen dried
  e = Ethanol, lightly swabbed, heat dried

TABLE 13. Ion Beam Diamondlike Carbon: Fused Silica

SUBSTRATE : FUSED SILICA

Gas : 99.99% Methane Gas rate : 3.25 SCCM

sample # / film (Å) / date	dep. time (min)	chamber press. (Torr)	beam voltage (volts)	beam current (mA)	accel. voltage (volts)	discharge voltage (volts)	cathode current (amps)	cleaning proc. (see *)
871-168 / 987 / 21 MAR 88	185	1.6E-4	1000	10	100	69	6.0	c
Comments	Excellent film (gold color) (masked)							
871-169 / 987 / 21 MAR 88	185	1.6E-4	1000	10	100	69	6.0	c
Comments	Excellent film (gold color)							
871-170 / 987 / 21 MAR 88	185	1.6E-4	1000	10	100	69	6.0	c
Comments	Excellent film (gold color)							
871-171 / 1011 / 22 MAR 88	185	9.8E-5	1000	10	100	70	5.9	c
Comments	Excellent film (one defect approx. 1mm in dia:gold color;masked)							
871-172 / 1011 / 22 MAR 88	185	9.8E-5	1000	10	100	70	5.9	c
Comments	Excellent film (small fine scratch in center) (gold color)							
871-173 / 1011 / 22 MAR 88	185	9.8E-5	1000	10	100	70	5.9	c
Comments	Excellent film (one defect approx. 1mm in dia.) (gold color)							
871-174 / 1011 / 22 MAR 88	185	9.8E-5	1000	10	100	70	5.9	c
Comments	Excellent film (gold color)							
871-175 / 801 / 23 MAR 88	185	9.4E-5	1000	10	100	70	5.8	c
Comments	Excellent film (gold color)							
871-176 / 801 / 23 MAR 88	185	9.4E-5	1000	10	100	70	5.8	c
Comments	Excellent film (gold color)							
871-177 / 801 / 23 MAR 88	185	9.4E-5	1000	10	100	70	5.8	c
Comments	Excellent film (gold color)							

* a = 1,1,1 Trichloroethane, Acetone, Methanol, nitgrogen dried
b = 1,1,1 Trichloroethane , Methanol, nitrogen dried
c = Methanol, heat dried
d = Soaked in hexane, lightly swabbed, nitrogen dried
e = Ethanol, lightly swabbed, heat dried

2.3.2 RF-Plasma Discharge Configuration I

The following is a summary of the laboratory notes for the first set of 70 DLC depositions on the seven different substrates (five samples per substrate) constituting the set of deliverable samples sent to the Army in December 1987. These samples were prepared using Configuration I at the University of Nebraska. The chamber pressure during deposition was always at 140 μm with the Ar and CH_4 flow rates set accordingly.

Silicon substrate (5 samples);

RF power = 125 W
Target Bias = 620 V (approximately)
Deposition cycle = 2 minutes ON / 3 minutes OFF

Sample No.	Nominal Thickness (angstroms)	Comments
Si-A5	13500	Small particles on surface. Probably due to carbon flaking from chamber during extremely long deposition (56 minutes).
Si-A6	800	Good film, color violet
Si-A7	1250	Good film, light green
Si-A8	1750	Some pinholes, violet
Si-A9	2250	Good film, dark green

BK7 Substrate (5 samples):

RF power = 25 W
Target Bias = 275 V (approximately)
Deposition cycle = 2 minutes ON / 3 minutes OFF

Sample No.	Nominal Thickness (angstroms)	Comments
BK7-A1	688	Some pinholes
BK7-A2	688	Good film
BK7-A3	688	Some scratches at edges
BK7-A4	688	Good film
BK7-A5	688	Good film

Lexan Substrate (5 samples):

RF power = 25 W
Target Bias = 275 V (approximately)
Deposition cycle = 2 minutes ON / 3 minutes OFF

Sample No.	Nominal Thickness (angstroms)	Comments
LEX-A1	688	Good film
LEX-A2	688	Good film, some abrasions on substrate
LEX-A3	688	Good film, some abrasions on substrate
LEX-A4	688	Good film, some abrasions on substrate
LEX-A5	688	Good film, some abrasions on substrate

ZnS Substrate (5 samples):

RF power = 25 W
Target Bias = 285 V (approximately)
Deposition cycle = 2 minutes ON / 3 minutes OFF

Sample No.	Nominal Thickness (angstroms)	Comments
ZnS-A1	300	Substrate scratched, film good
ZnS-A2	300	Substrate scratched, film good
ZnS-A3	300	Film good
ZnS-A4	300	Film good
ZnS-A5	300	Film good

NOTE: Small piece of tape in corner of sample indicates deposition side.

Fused Silica Substrate (5 samples):

RF power = 25 W
Target Bias = 625 V (approximately)
Deposition cycle = 2 minutes ON / 3 minutes OFF

Sample No.	Nominal Thickness (angstroms)	Comments
FS-A1	688	Good films
FS-A2	688	Good films
FS-A3	688	Good films
FS-A4	688	Good films
FS-A5	688	Good films

KG3 Substrates (5 samples):

RF power = 125 W
Target Bias = 625 V (approximately)
Deposition cycle = 2 minutes ON / 3 minutes OFF

Sample No.	Nominal Thickness (angstroms)	Comments
KG3-A1	1472	Some spalling at edges
KG3-A2	1472	Some spalling at edges
KG3-A3	1472	Some spalling at edges
KG3-A4	1472	Some spalling at edges
KG3-A5	1472	Some spalling at edges

HMF Substrates (5 samples):

RF power = 25 W
Target Bias = 290 V (approximately)
Deposition cycle = 2 minutes ON / 3 minutes OFF, except for HMF-A6

Sample No.	Nominal Thickness (angstroms)	Comments
HMF-A1	688	Soaked 45 minutes in Tri-clor, then ultrasonic cleaning 5 minutes, then washed with acetone, methanol, and DI water. Dried with Dry-N_2. Substrate fogging occurred (due to etching?). Some scratches due to use of tweezers. Good film adhesion.
HMF-A2	688	To avoid fogging of surface, ultrasonic cleaning in methanol only, rinse DI water, dried with dry-N_2. No fogging, but still film did spall off around edges.

HMF-A3 was an attempt at depositions with no cleaning at all (front side of sample), or 5-minute sputter-cleaning in Ar at 50 W power (back side of same sample).

HMF-A3	688	No cleaning at all. Spalling-off at edges.
HMF-A3.1	688	Spalled-off at center.
HMF-A4	688	Same procedure as HMF-A1, except no 45-minute soaking. Less surface fogging, but less adhesion (there was spalling at substrate edges.
HMF-A5	688	Ultrasonic cleaning with "Micro" laboratory glassware cleaner, rinsed with DI water, then short Tri-clor, acetone and methanol baths. Rinsed again with DI water, then dried with dry-N_2. No fogging visible, but still spalls off at edges.
HMF-A6	688	Same procedure as HMF-A4. However, the deposition-cycle consisted of 1-minute of deposition/3-minutes of cooling, in an attempt to allow the sample to cool further. Some spalling-off at edges.

We tried to determine if the adhesion problem for HMF was due to the substrate expansion-coefficient (Sample No. HMF-A6) or to improper cleaning procedures (all other samples).

2.3.3 RF-Plasma Discharge Configuration II

A second set of 70 samples of diamondlike carbon (DLC) was deposited on 7 different substrates at the University of Nebraska. These 70 samples were sent to the Army on May 31, 1988 to satisfy the 140 deliverable samples part of the contract.

All the depositions were made under the following conditions unless specifically mentioned otherwise:

- o flow rate for methane and argon: 13 sccm each,
- o base pressure: 100 μm,
- o power: 200 watts, and
- o DC bias between the two plates: 300 volts.

The following gives the list of the substrates names, the sample names and the times of deposition:

I -- Si wafer, DLC/SI #1...DLC/SI#10, 19 minutes of deposition.

II -- BK7 glass, DLC/BK7#1...DLC/BK7 #10, 10 minutes of deposition.

III -- KG3 glass, DLC/KG#1...DLC/KG2#10,5 minutes of deposition.

IV -- fused silica glass, DLC/FS #1...DLC/FS #10, 12.5 minutes of deposition.

V -- lexan, DLC/LX #1...DLC/LX #4, 14 minutes and 46 seconds of deposition.

VI -- lexan, DLC/LX #7...DLC/LX #12, 14 minutes and 10 seconds of deposition.

VII -- HMF glass, DLC/HMF #1, DLC/HMF#2, 7 minutes and 46 seconds of deposition.

VIII -- HMF glass, DLC/HMF #3...DLC/HMF #10, 7 minutes of deposition.

IX -- ZnS glass, DLC/ZnS #1...DLC/ZnS #5, 100 microns of base pressure, 16 sccm methane and argon flow rate, 2 minutes of deposition.

X -- ZnS glass, DLC/ZnS #6...DLC/ZnS #10, 2 minutes of deposition.

3.0 CHARACTERIZATION OF DEPOSITED DLC FILMS

3.1 ELEMENTAL ANALYSIS

Elemental analysis of the films was done by a combination of Rutherford backscattering (RBS) and proton recoil detection (PRD) analysis. RBS was used to determine how much carbon was in the films, whether any other impurities were in the films, how uniform the films were, and if there were any pinholes involving more than 1% of the surface. PRD was used to determine the hydrogen content of the films. The uncertainty in the analysis was ±5 at.%. The detector limit was on the order of < 1 at.%.

3.1.1 Ion-Beam Deposition

Table 14 gives the carbon and hydrogen content of DLC films on silicon substrates. The films typically contained 30% hydrogen and 70% carbon, respectively. No other impurities (e.g., oxygen) were detected in the film.

TABLE 14. Hydrogen and Carbon Contents of DLC Films Produced by the Ion-Beam Technique

Sample No.	% C (atom) (±5%)	% H (atom) (±5%)
023/4	70.6	29.3
024	70.8	29.1
023/2	69.9	30.0
016/1	71.4	28.1
017	69.7	30.3
026	69.01	31.0
021	69.3	30.8
016/4	69.2	30.8
365	67.0	33.0
368	66.7	33.3

3.1.2 RF-Discharge Configuration I

The carbon and hydrogen contents of these films under various discharge conditions are shown in Table 15. All the films typically contain 68% carbon and 32% hydrogen.

TABLE 15. Carbon and Hydrogen Content of Diamondlike Samples Produced by RF Discharge

Sample No.	Power (W)	Pressure (μm)	Energy Gap (eV)	J/T BIAS	C (%)	H (%)
B1	25	80	1.24	375/0	68.2	31.9
C1	50	80	1.15	500/0	68.0	32.0
D1	125	80	0.95	760/0	68.0	32.0
E1	250	80	0.7	1062/0	69.4	30.6
F1	500	80	0.24	1350/0	58.9	41.1
F2	500	80	0.66	1500/0	67.5	32.5
G1	25	140	1.19	375/0	68.0	32.0
H1	50	140	1.19	510/0	71.0	29.0
I1	125	140	0.96-1.10	750/0	66.8	33.2
J1	250	140	0.62	1062/0	68.8	31.2
J2	250	140	0..85-0.93	825/0	69.8	30.2
K1	500	140	0.6	1300/0	45.8	54.2

3.2 MORPHOLOGY OF DIAMONDLIKE CARBON FILM

Cross-sectional transmission electron microscopy (TEM) analysis was performed on DLC films deposited on silicon substrates using ion-beam deposition techniques. The purpose of this study was to characterize the morphology of the film, the uniformity, the pinhole site, if any, and the film-substrate interface.

Figure 12 shows the cross-sectional TEM of a DLC film (Sample No. 871-368). The film thickness was found to be 2150Å. The film appeared to be very uniform and no pinholes were observed. Using selected area diffraction analysis (SAD), the DLC film was found to be amorphous as shown in Figure 13. From the present study, it was concluded that DLC films produced by the ion-assisted deposition technique are amorphous, uniform and have no pinholes, and thus are high quality DLC films. In the Phase I final report we made the same conclusion regarding plasma deposited DLC films.

Figure 12 The cross-sectional TEM micrograph of DLC deposited on silicon substrate under high pressure condition

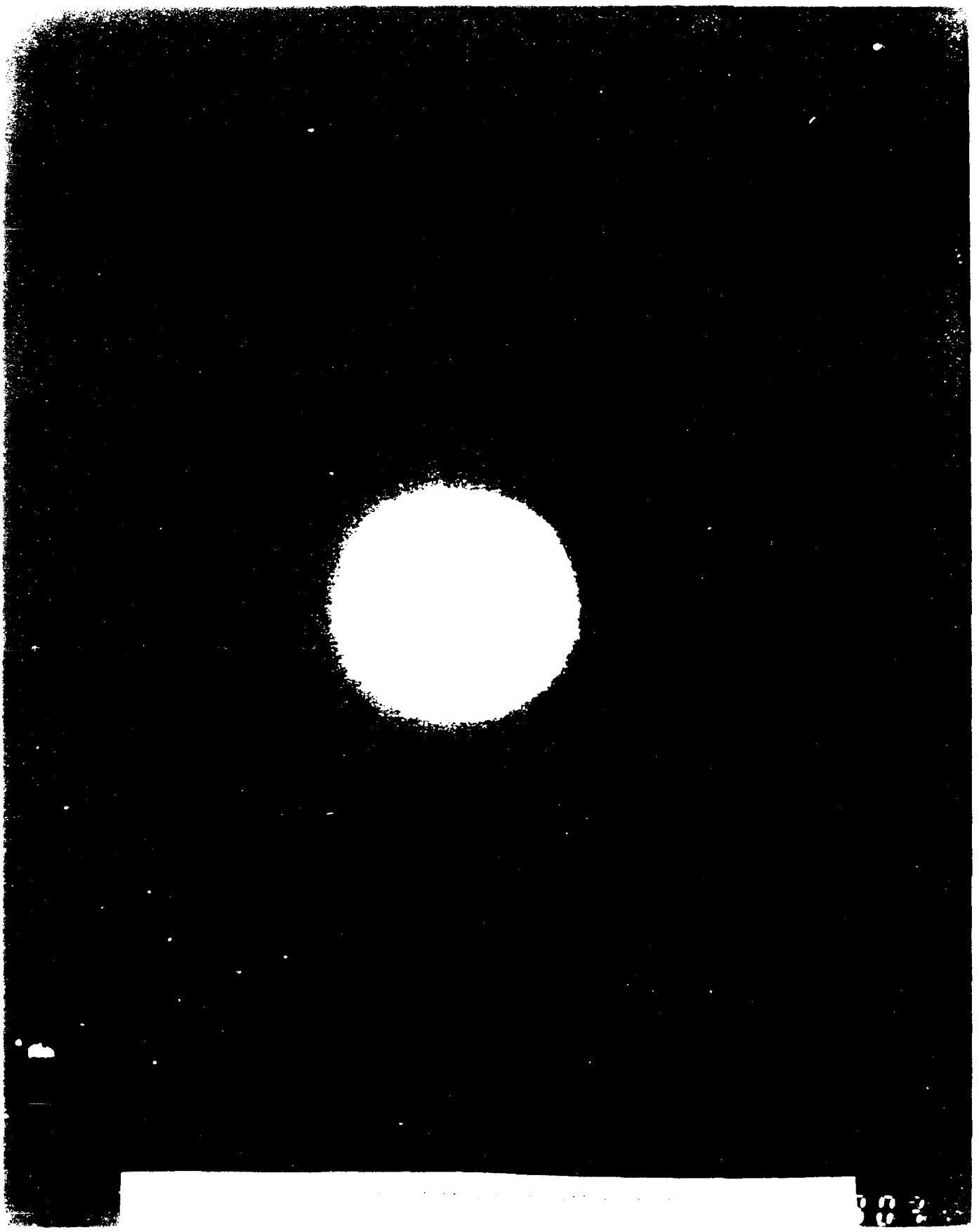

3.3 OPTICAL PROPERTIES MEASUREMENTS

Optical properties are central to the Army interest in DLC films since these films are proposed to be used for infrared optics. The optical properties are also important for scientific characterization.

Optical properties were measured using three systems.

- o Ultraviolet-Visible (UV-Vis) Dual Beam Spectometer for quickly measuring relative optical absorption (University of Nebraska)
- o Optical Measurements 300 to 850 nm by variable angle spectroscopic ellipsometry (VASE) (University of Nebraska)
- o Infrared Optical Measurements (University of Dayton Research Institute and University of Nebraska)

3.3.1 Ultraviolet-Visible (UV-Vis) Dual Beam Spectrometer

For these measurements, samples were deposited on quartz and absorption measured as a function of wavelength. The latter data were then digitized and run through a computer program to calculate the optical band gap, assuming a Tauc behavior:

$$\alpha = \frac{(h\upsilon - E_g^o)^n}{h\upsilon}$$

where α is the absorption coefficient, υ is the frequency ($h\upsilon$ is the photon energy), E_g^o is the optical gap, and n is a constant usually near 2 [9]. Plots of $(\alpha h\upsilon)^{1/2}$ vs $h\upsilon$ yields straight lines with intercept = E_g^o. Tauc plots are valid over the higher ranges of absorption in amorphous semiconductors. In the lowest range, an Urbach edge is sometimes found. Figure 14 shows a Tauc plot with a probable Urbach edge, for a scientific sample from the Configuration II system. Figure 15 shows a similar plot with the Tauc region extending over a wider range. Hundreds of such plots were analyzed at the University of Nebraska during this program.

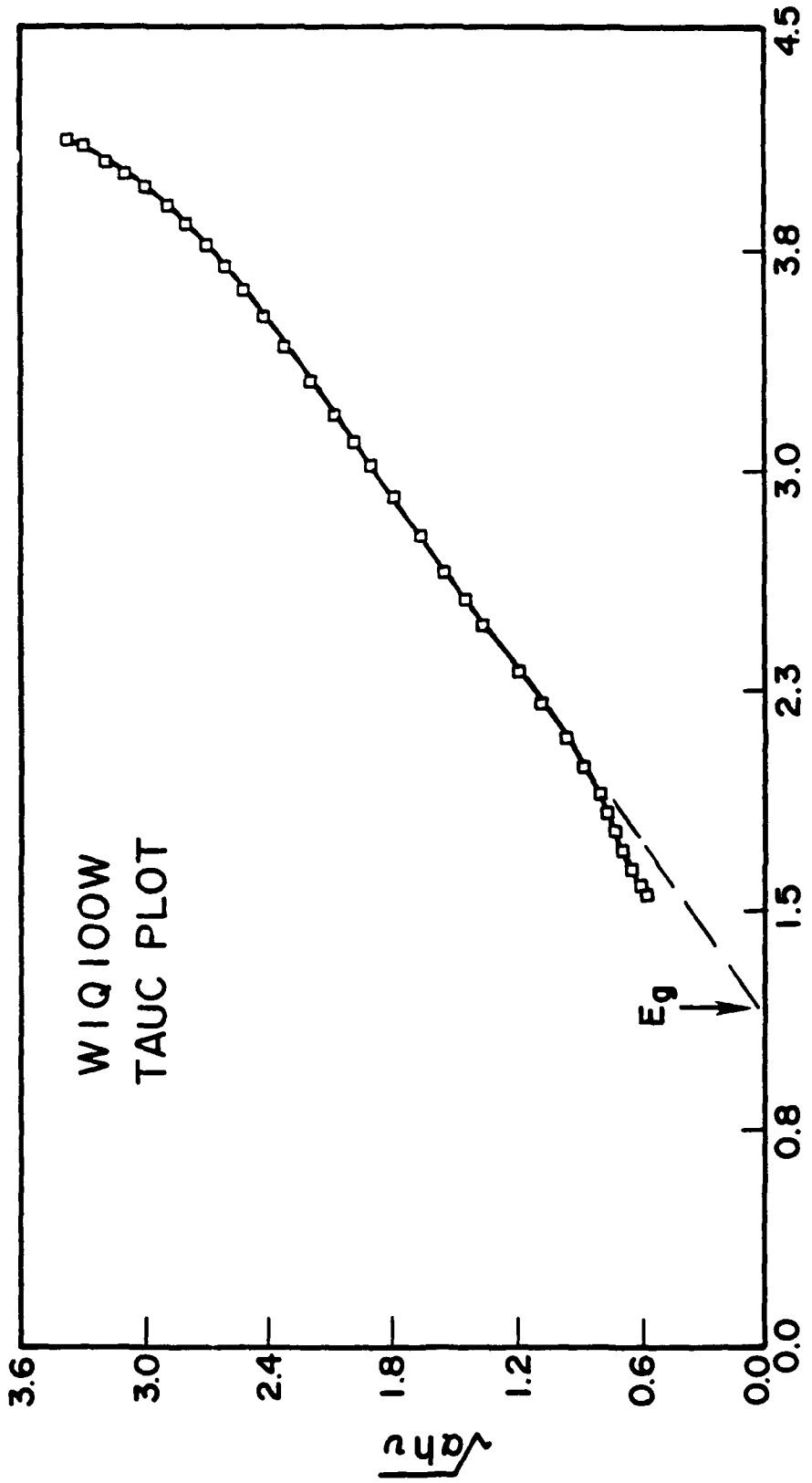

Figure 14 Tauc plot for Configuration II (13.56 MHz) DLC

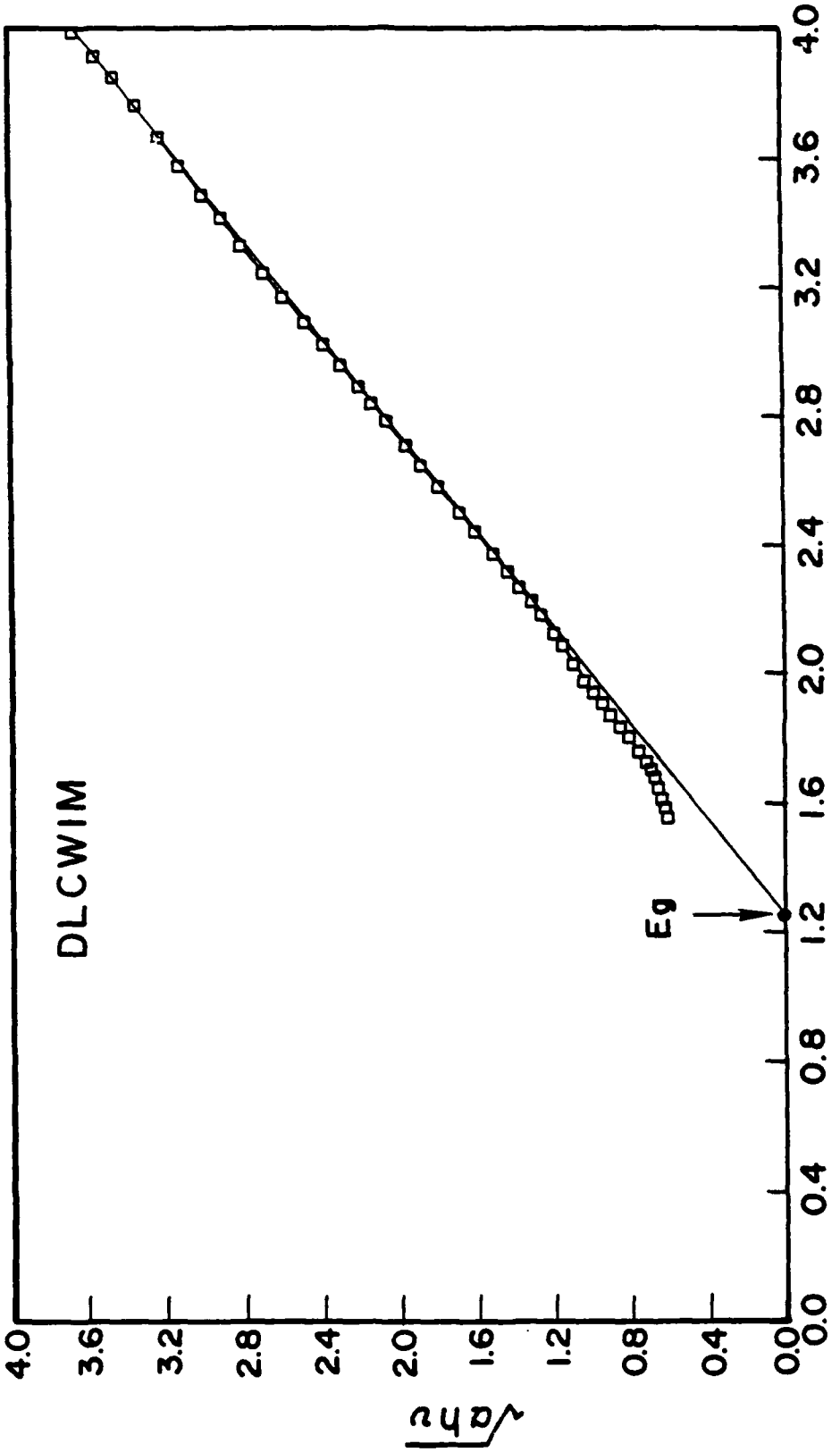

Figure 15 Tauc plot for Configuration II (13.56 MHz) DLC

Figure 16 shows optical gap plotted vs methane gas pressure for five different power levels for samples from Configuration II. Note that there seems to be little systematic dependence on pressure except for the samples deposited at 500 watts.

Figure 17 shows optical gap plotted vs rf power for various gas pressures. There is an obvious dependence on power, especially for the highest pressures. This graph shows that the optical properties can be controlled by controlling power levels for given gas pressures.

Figures 18 and 19 show absorbance vs wavelength, and Tauc plots respectively for a sample chosen from the second set of 70 delivered to the Army (Configuration II).

3.3.2 Optical Measurements 300 to 850 nm by variable angle spectroscopic ellipsometry

The University of Nebraska ellipsometry laboratory is internationally famous, and has been in existence for 30 years. There are three automated variable angle spectroscopic ellipsometers (VASE), and a research team of approximately 15 faculty, post doctoral fellows, and graduate students. Sophisticated computer programs have been developed over the past 15 years, and these are extremely powerful for materials analysis involving ellipsometric and other optical measurements.

Ellipsometric experiments are generally used to determine the index of refraction (n), extinction coefficient (k), film thickness (t), alloy ratios (x) in A_xB_{1-x} (where A and B represent two elements), and surface and interface roughness.

This program involved ellipsometry in two different ways. First, the contract called for measurement of the n and k of DLC over a wide range of wavelengths. Second, an operating VASE was a deliverable of the contract. A detailed description of how to make VASE measurements is not appropriate in this report. In a later section, we describe the VASE being delivered to the Army, and further details on ellipsometry can be obtained from the literature cited in that section.

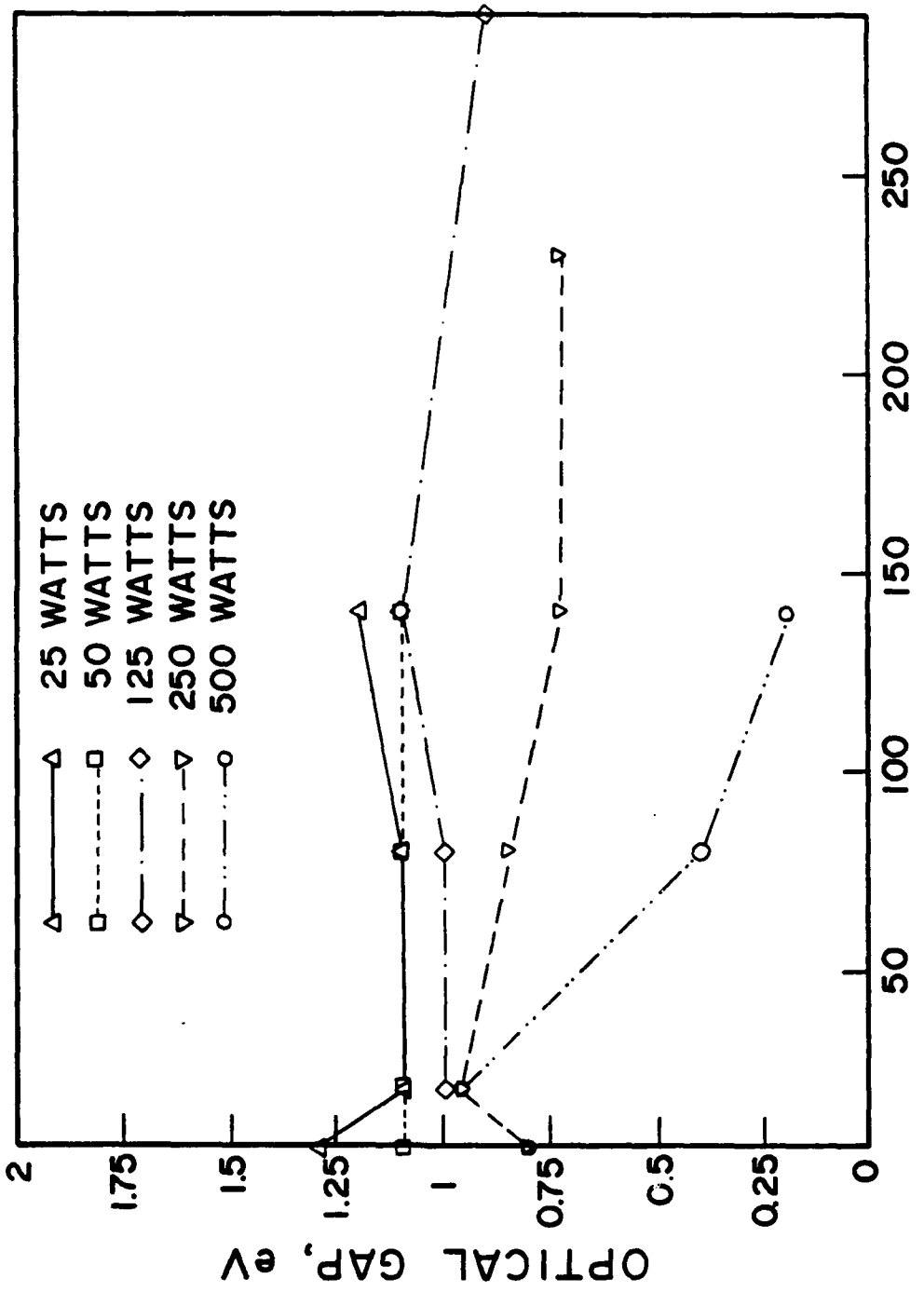

Figure 16 Optical gap for Configuration II (13.56 MHz) DLC

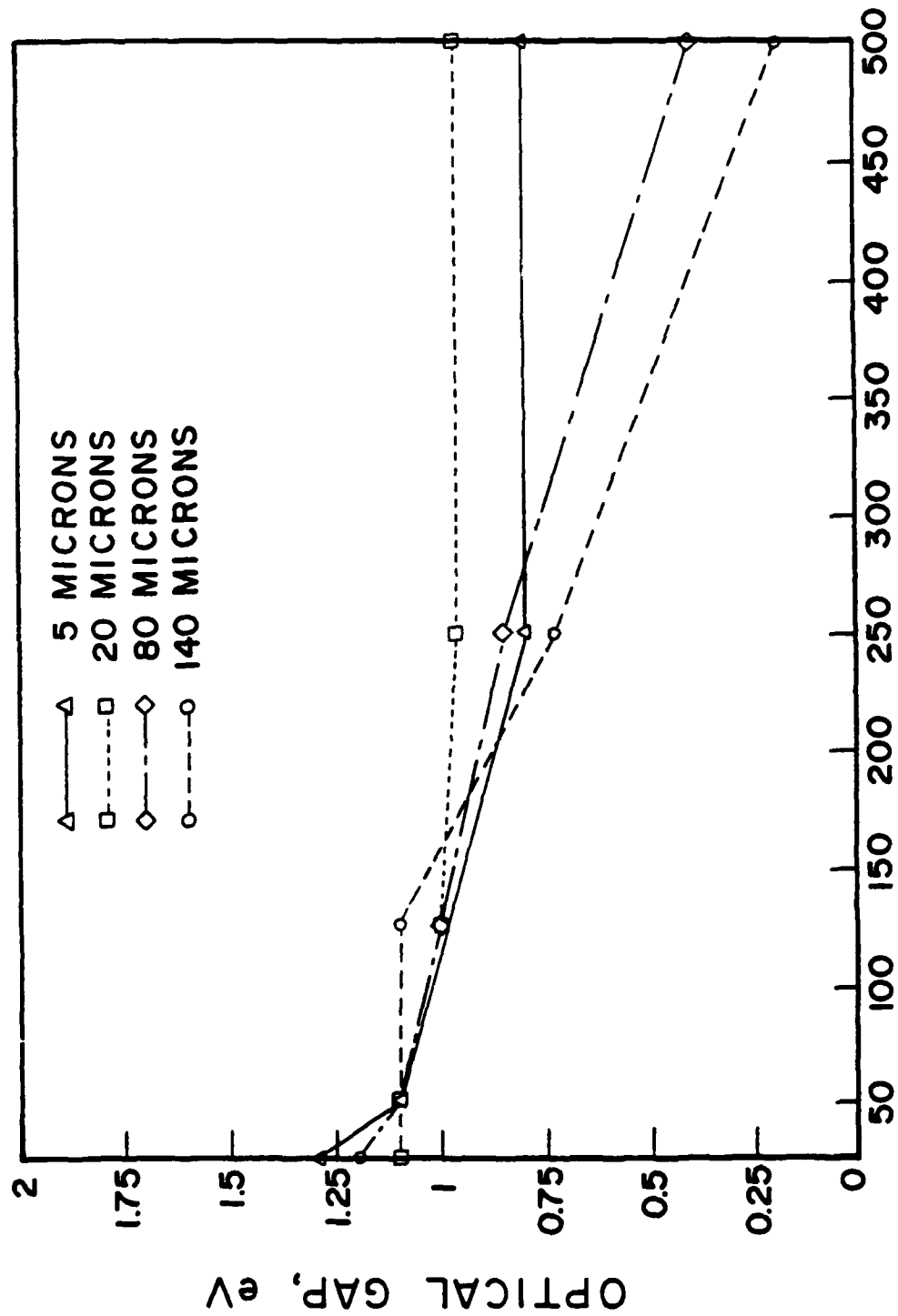

Figure 17 Optical gap for Configuration II (13.56 MHz) DLC

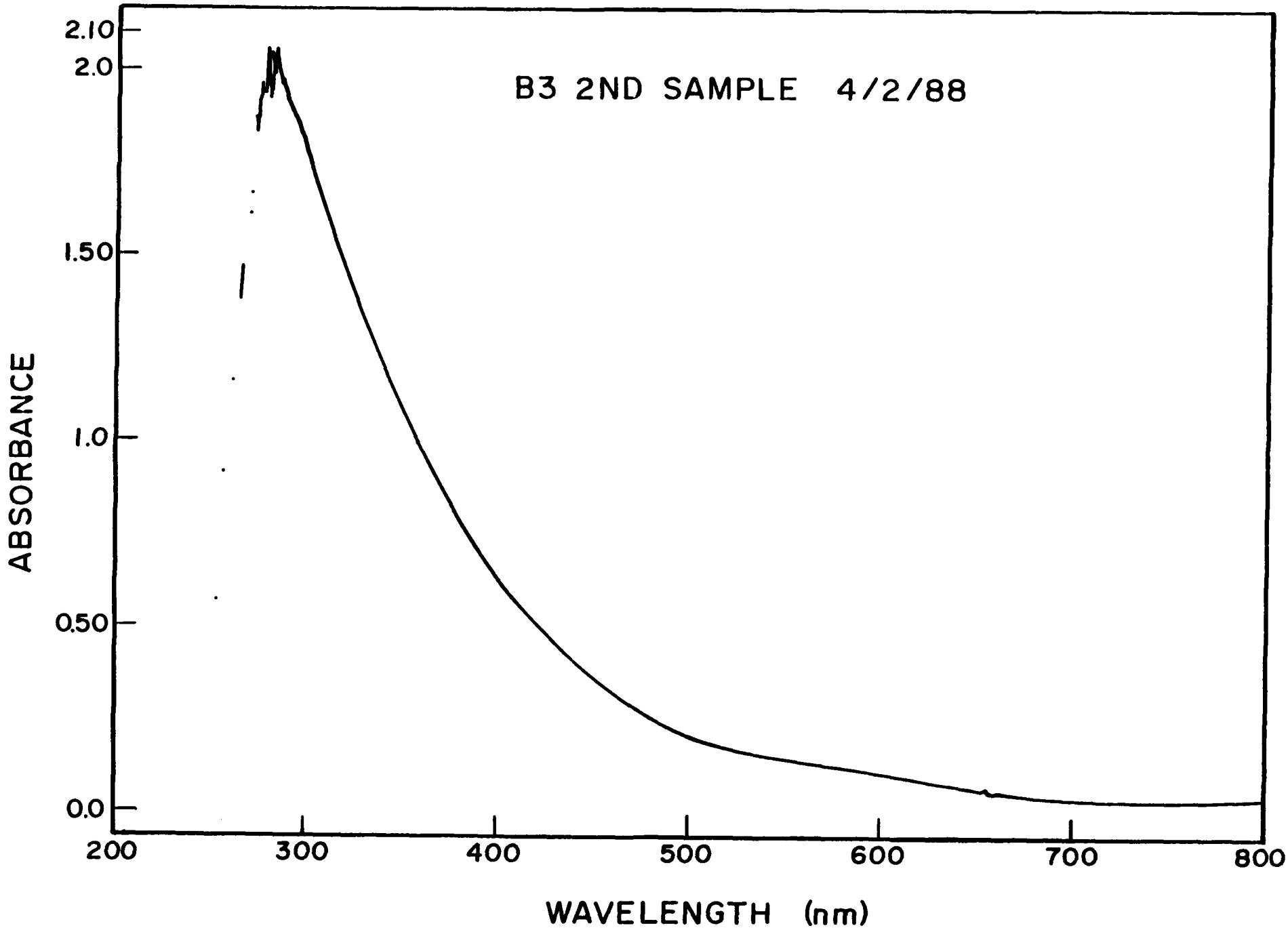

Figure 18 Optical absorbance for Configuration II (13.56 MHz) DLC

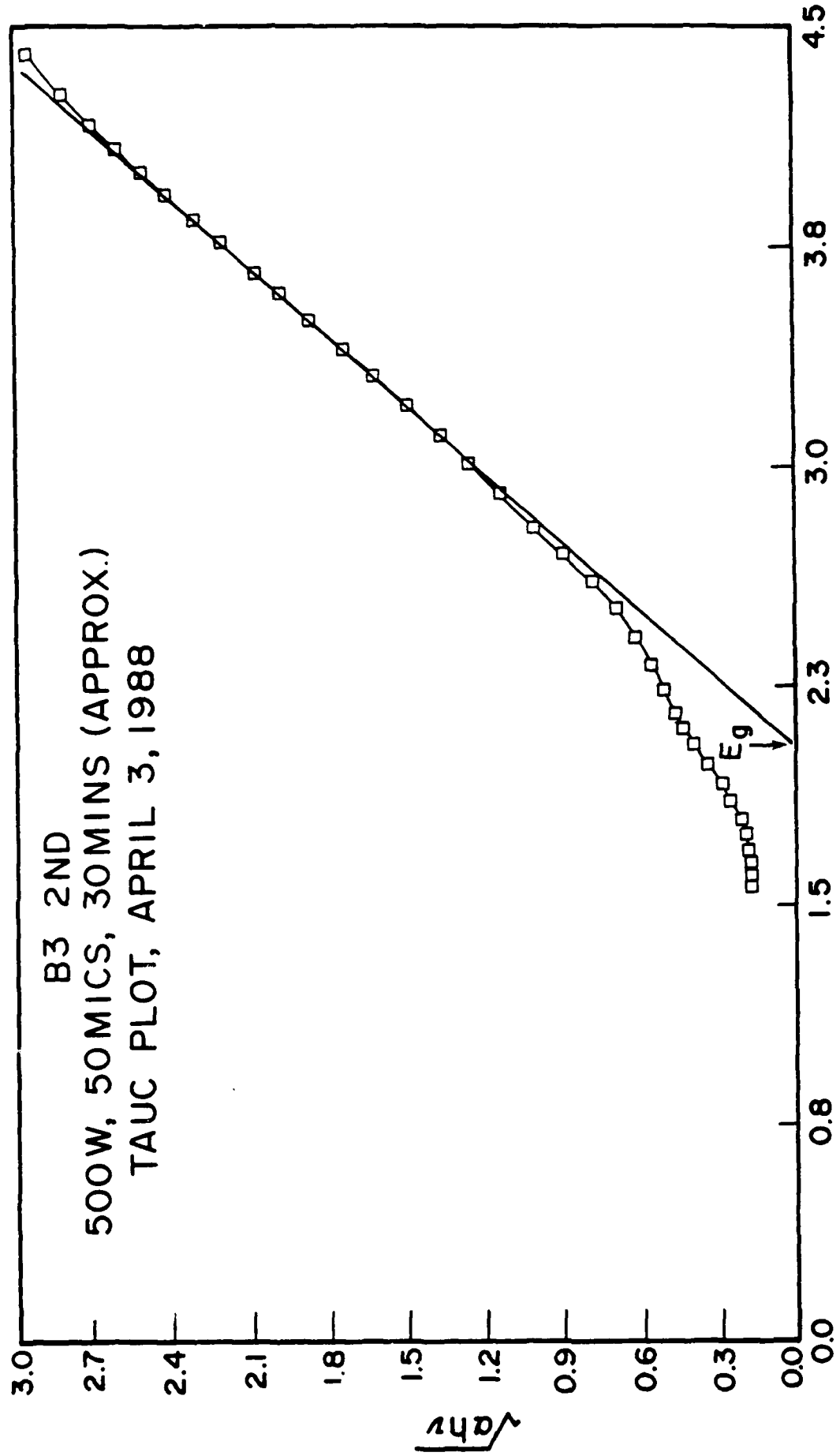

Figure 19 Tauc plot for Configuration II (13.56 MHz) DLC

For the 300 to 850 nm range, all VASE optical data were taken on DLC on silicon substrates. Example results for index n and extinction coefficient k are shown in Figures 20 and 21. The DLC film was 125Å thick on a silicon substrate. Note that the index of refraction is near 2 and dropping slowly for longer wavelengths.

Figure 22 shows the index of refraction vs wavelength for unimplanted and fluorine implanted ion beam deposited DLC on silicon. Note that the index is near 2 and, like previous samples, falls slowly at longer wavelengths.

Eight refereed journal articles were written based on work sponsored entirely or in part by this contract as shown in Appendix A.

3.3.3 Infrared Optical Measurements

Measurements of the index of refraction were made in the mid-infrared 4 μm and at the CO_2 laser wavelength of 10 μm. Measurements were made by null ellipsometry using a Nernst glower light source, wire grid polarizers, and InSb (mid-IR) or HgCdTe (10 μm) detectors. The measurements were made over four "zones" and then averaged. (For a description of null-ellipsometry measurements, see Azzam and Bashara's book Ellipsometry and Polarized Light, North Holland, 1977). Angles of incidence from 25 to 65 degrees were used, with intervals of 10 degrees generally, and 5 degrees in regions near the pseudo Brewster angle. Two substrates were used: silicon and heavy metal fluoride. Figure 23a shows the fits of the ellipsometric (psi and delta) data for experiment and theory for the HMF substrate at 4 μm. Figure 23b shows the reflectance vs wavelength measured in conventional reflectometers. From the positions of maxima and minima, the optical thickness was determined, and used to aid in interpreting the ellipsometric data.

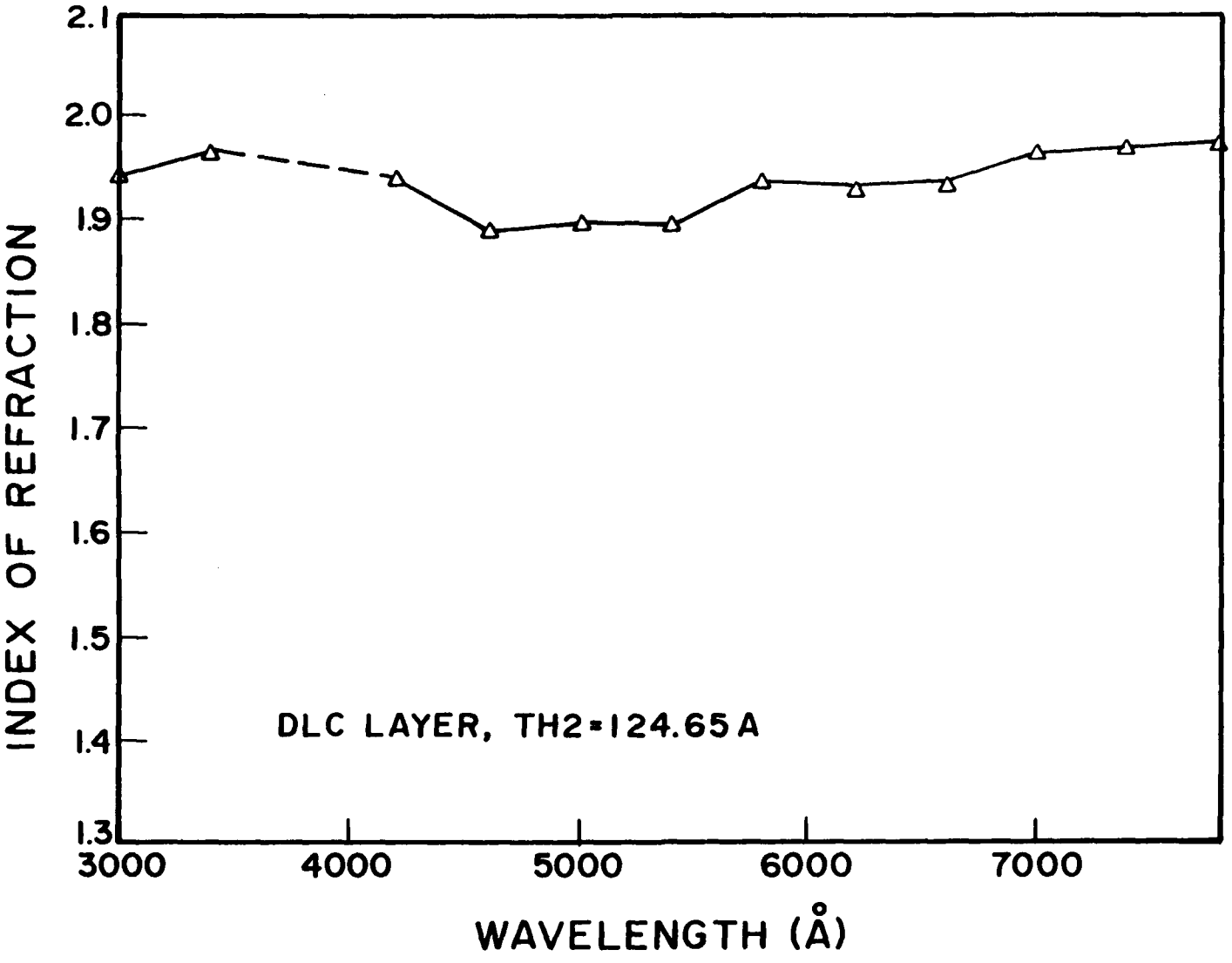

Figure 20 Index of refraction for Configuration II (13.56 MHz) DLC

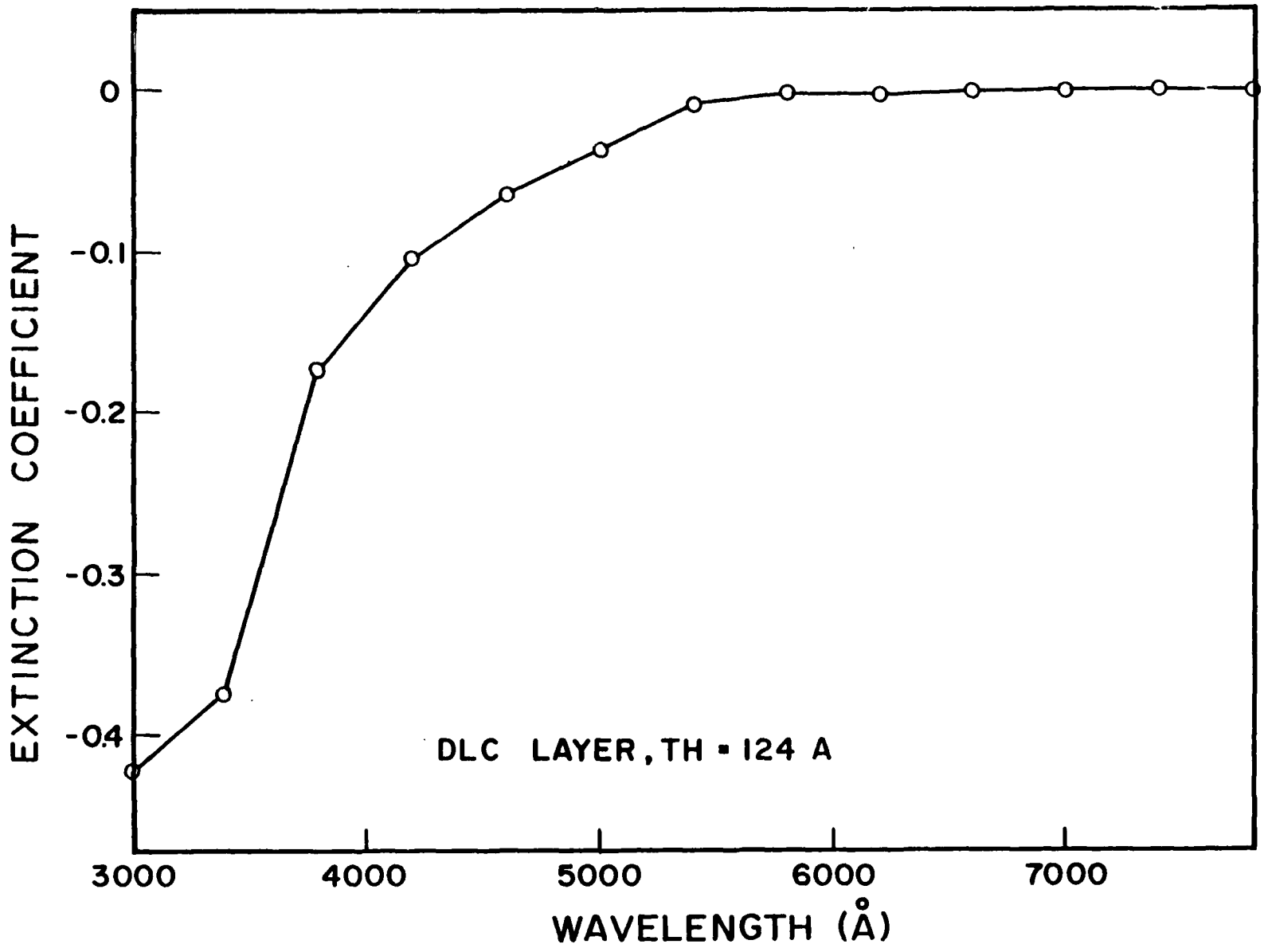

Figure 21 Extinction coefficient for Configuration II (13.56 MHz) DLC

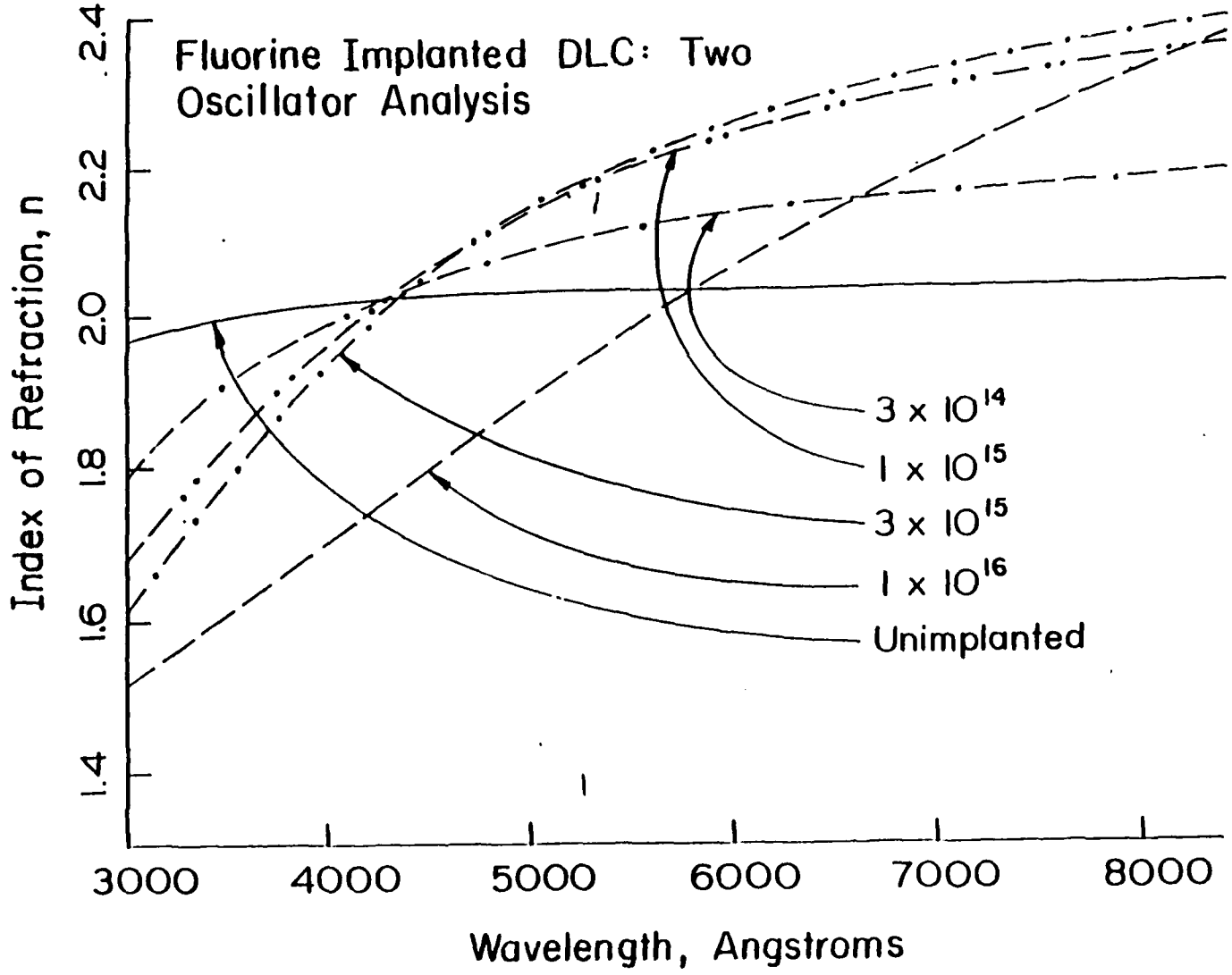

Figure 22 Index of refraction for ion beam deposited samples after F implantation at the fluences indicated

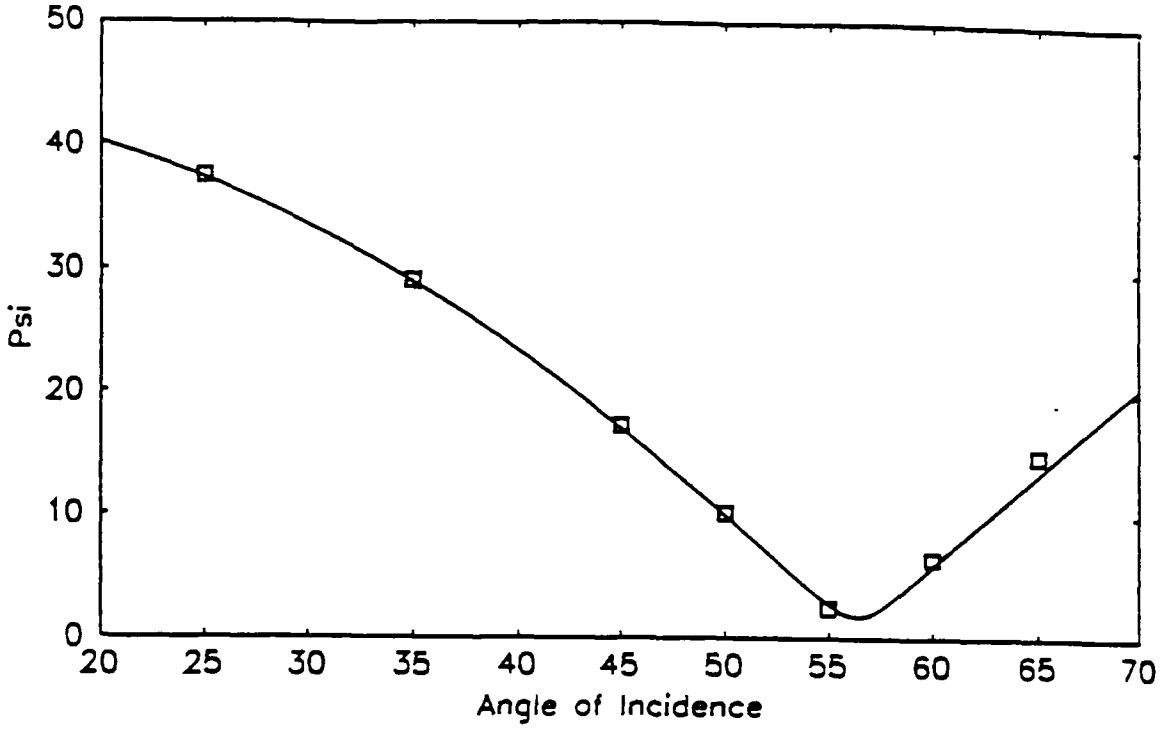

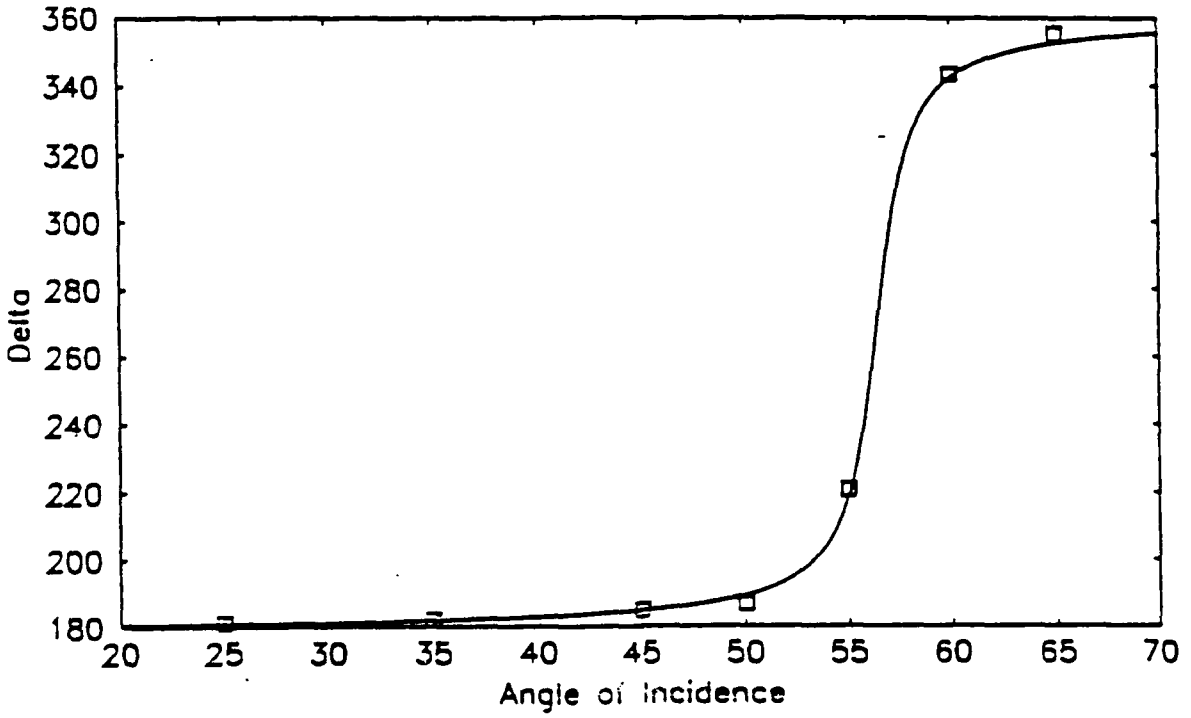

Figure 23a Experimental data for ψ and Δ as a function of angle of incidence for the heavy-metal glass substrate at a wavelength of 4 μm. The curves are based on the theoretical model described in the text

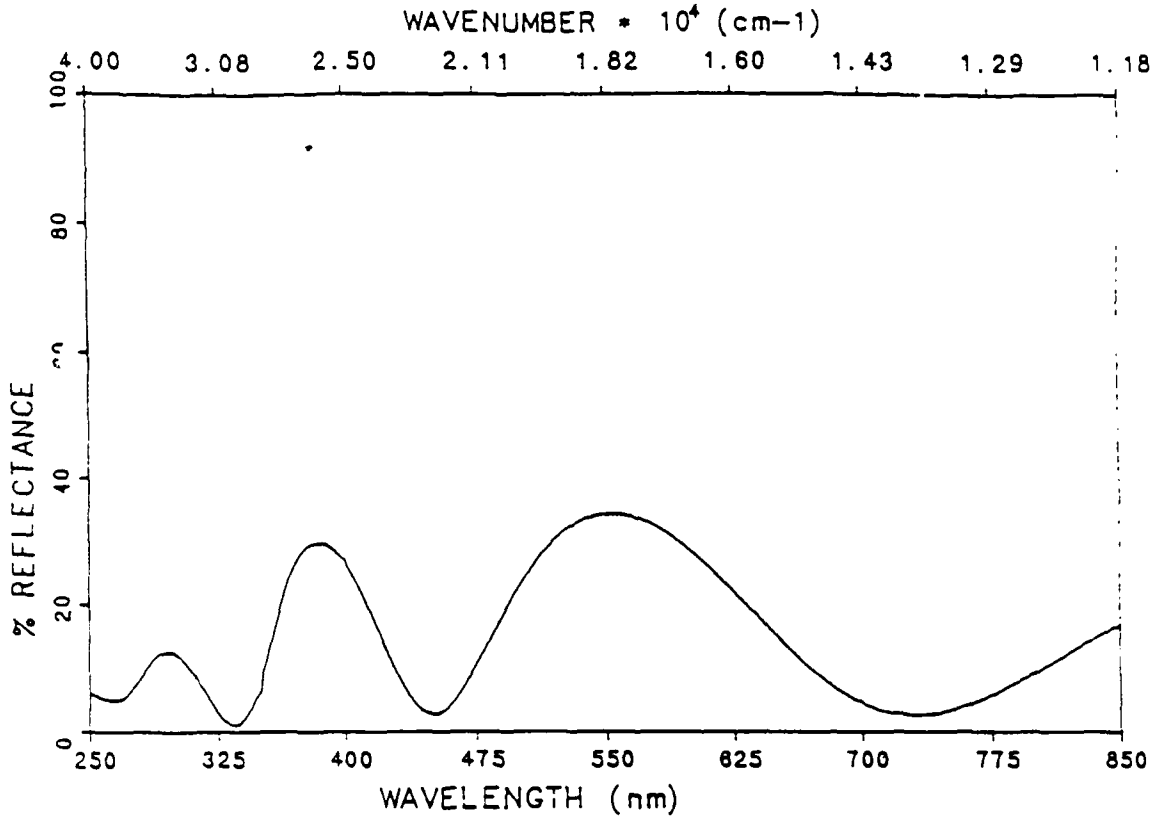

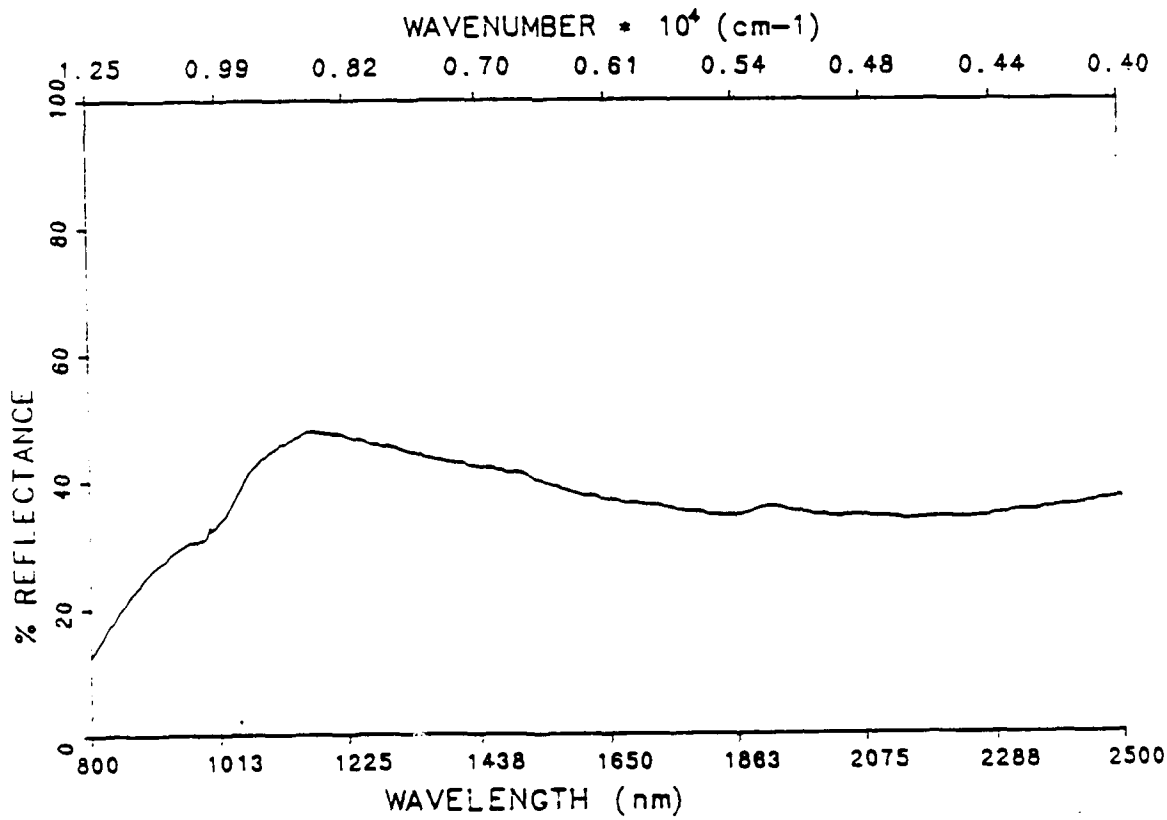

Figure 23b Experimental data for reflectance as a function of wavelength for the silicon sample, with light incident on the green (coated) surface

The results for the index of refraction and extinction coefficient are as follows:

4 microns	$n = 1.67 \pm 0.03$ HMF substrate
	$n = 1.62 \pm 0.05$ Si substrate
	$k \leq 0.01$ (the limits of sensitivity)
10 microns	$n = 1.75 \pm 0.15$
	$k \leq 0.01$ (the limits of sensitivity)

These IR measurements were taken at the University of Dayton Research Institute by John Loomis and Gordon Little and interpreted by John Loomis and John Woollam. A detailed report is available on request. These data are consistent with optical data determined in the 300-850 nm range by VASE.

3.4 ENVIRONMENTAL EFFECT ON DIAMONDLIKE FILMS

3.4.1 Mechanical, Chemical and Thermal Tests of Diamondlike Carbon on Various Substrates

The environmental tests of DLC on substrates of BK-7 glass, KG-3 glass, ZnS, silicon, lexan, heavy metal fluoride (HMF) and fused silica were carried out extensively. The procedures were described in detail in the fourth quarterly report [10] according to the military specification MIL-C-48497A. A new sample was used in each test, and the Scotch adhesion test was performed before and after the organic solvent, mineral acid attack, humidity and temperature cycling tests. The film was examined by optical microscope before and after testing. Details of the results are given as follows.

3.4.1.1 Ion-Beam Deposition

The environmental test results are tabulated in Tables 16-43. The DLC film produced under the optimum conditions adhered very well on the substrates of lexan, fused silica, KG-3, BX-7 glass, ZnS, and silicon.

TABLE 16. Organic Solvent, Scotch Tape/Adhesion and Rubber Wear/Adhesion Tests on Ion-Assisted Deposited Diamondlike Carbon on Various Substrates

Substrate	Scotch Tape	1,1,1 Tri-Chloroethane	Acetone	Methanol	Scotch Tape	Rubber Wear Test
BK-7	NE	NE	NE	NE	NF	NE
KG-3	NE	NE	NE	NE	NE	NE
ZnS	NE	NE	NE	NE	NE	NE
Silicon	NE	NE	NE	NE	NE	NE
Lexan	NE	C	C	NE	NE	PS
HMF	NE	NE	NE	NE	NE	S
Fused Silica	NE	NE	NE	NE	NE	NE

NE: No Effect
PR: Partial Removal
TR: Total Removal
S : Scratched
PS: Partial Scratched
B: Blistered
PH: Pinholes
C : Cracked

TABLE 17. Mineral Acid Attack, Scotch Tape/Adhesion Tests on Ion-Assisted Deposited Diamondlike Carbon on Various Substrates

Substrate	Sulfuric Acid	Nitric Acid	Hydrochloric Acid	Hydrofluoric Acid	Scotch Tape
BK-7	NE	NE	B	B	NE
KG-3	NE	NE	NE	TR	NE
ZnS	NE	B	B	NE	PR
Silicon	NE	NE	NE	NE	NE
Lexan	B	C	NE	PH	NE
HMF	NE	TR	B		
Fused Silica	NE	NE	NE	NE	NE

TABLE 18. Humidity Test for Three Hours Over Boiling Water on Ion-Assisted Deposited DLC on Various Substrates

Substrate	After 3 hrs Exposure	Scotch Tape
BK-7	NE	NE
KG-3	NE	NE
ZnS	NE	NE
Silicon	NE	NE
Lexan	NE	NE
HMF	NE	PR
Fused Silica	NE	NE

TABLE 19. Low Temperature Test in Liquid Nitrogen and Subsequent in High Temperature for Two Hours and Followed Scotch Tape Adhesion Tests on Ion-Assisted Deposited Diamondlike Carbon on Various Substrates

Substrate	After 2 hrs in Ln2	Room Temperature	After 2 hrs at 98°C	Scotch Tape
BK-7	NE	NE	NE	NE
KG-3	NE	NE	NE	NE
ZnS	NE	NE	NE	NE
Silicon	NE	NE	NE	NE
Lexan	NE	NE	NE	NE
HMF	NE	NE	B	NE
Fused Silica	NE	NE	NE	NE

3.4.1.2 RF-Plasma Discharge Configuration I

KEY

NE NO EFFECT
PR PARTIAL REMOVAL
TR TOTAL REMOVAL
S SCRATCHED

TABLE 20. Organic Solvent Tests on 100W rf Deposited DLC on Si

Deposition Temperature	Trichloro-Ethylene	Acetone	Ethyl Alcohol
RT	NE	NE	NE
50C	NE	NE	NE
100C	NE	NE	NE
150C	NE	NE	NE
200C	NE	NE	NE
250C	NE	NE	NE

TABLE 21. Rubber Wear/Adhesion Tests After Organic Solvent Tests

Deposition Temperature	Trichloro-Ethylene	Acetone	Ethyl Alcohol
RT	NE	NE	NE
50C	NE	NE	NE
100C	NE	NE	NE
150C	NE	NE	NE
200C	NE	NE	NE
250C	NE	NE	NE

TABLE 22. "Scotch" Tape Adhesion Tests After Organic Solvent Tests

Deposition Temperature	Trichloro-Ethylene	Acetone	Ethyl Alcohol
RT	NE	NE	NE
50C	NE	NE	NE
100C	NE	NE	NE
150C	NE	NE	NE
200C	NE	NE	NE
250C	NE	NE	NE

TABLE 23. Mineral Acid Attack Tests on 100W rf Deposited DLC on Si

Deposition Temperature	Sulfuric Acid	Nitric Acid	Hydrochloric Acid	Hydrofluoric Acid
RT	NE	NE	NE	NE
50C	NE	NE	NE	NE
100C	NE	NE	NE	NE
150C	NE	NE	NE	NE
200C	NE	NE	NE	NE
250C	NE	NE	NE	NE

TABLE 24. Rubber Wear/Adhesion Tests After Mineral Acid Tests

Deposition Temperature	Sulfuric Acid	Nitric Acid	Hydrochloric Acid	Hydrofluoric Acid
RT	NE	NE	NE	NE
50C	NE	NE	NE	NE
100C	NE	NE	NE	NE
150C	NE	NE	NE	NE
200C	NE	NE	NE	NE
250C	NE	NE	NE	NE

TABLE 25. "Scotch" Tape Adhesion Tests After Mineral Acid Tests

Deposition Temperature	Sulfuric Acid	Nitric Acid	Hydrochloric Acid	Hydrofluoric Acid
RT	NE	NE	NE	NE
50C	NE	NE	NE	NE
100C	NE	NE	NE	NE
150C	NE	NE	NE	NE
200C	NE	NE	NE	NE
250C	NE	NE	NE	NE

TABLE 26. Humidity Test for 3 Hours Over Boiling Water on 100W rf Deposited DLC on Si and Subsequent Rubber Wear/Adhesion and "Scotch" Tape Adhesion Tests

Deposition Temperature	After 3 hrs Exposure	Rubber Test	Tape Test
RT	NE	NE	NE
50C	NE	NE	NE
100C	NE	NE	NE
150C	NE	NE	NE
200C	NE	NE	NE
250C	NE	NE	NE

TABLE 27. Low Temperature Test for 15 min in Liquid Nitrogen on 100 W rf Deposited DLC on Si and Subsequent Rubber Wear/Adhesion and "Scotch" Tape Adhesion Tests.

Deposition Temperature	After 15 min Exposure	Rubber Test	Tape Test
RT	NE	NE	NE
50C	NE	NE	NE
100C	NE	NE	NE
150C	NE	NE	NE
200C	NE	NE	NE
250C	NE	NE	NE

TABLE 28. Organic Solvent Tests on 200W rf Deposited DLC on Si

Deposition Temperature	Trichloro-Ethylene	Acetone	Ethyl Alcohol
RT	NE	NE	NE
75C	NE	NE	NE
100C	NE	NE	NE
150C	NE	NE	NE
200C	NE	NE	NE
250C	NE	NE	NE

TABLE 29. Rubber Wear/Adhesion Tests After Organic Solvent Tests

Deposition Temperature	Trichloro-Ethylene	Acetone	Ethyl Alcohol
RT	PR	PR	PR
75C	NE	NE	NE
100C	NE	NE	NE
150C	NE	NE	NE
200C	NE	NE	NE
250C	NE	NE	NE

TABLE 30. "Scotch" Tape Adhesion Tests After Organic Solvent Tests

Deposition Temperature	Trichloro-Ethylene	Acetone	Ethyl Alcohol
RT	NE	NE	NE
75C	NE	NE	NE
100C	NE	NE	NE
150C	NE	NE	NE
200C	NE	NE	NE
250C	NE	NE	NE

TABLE 31. Mineral Acid Attack Tests on 200W rf Deposited DLC on Si

Deposition Temperature	Sulfuric Acid	Nitric Acid	Hydrochloric Acid	Hydrofluoric Acid
RT	NE	NE	NE	NE
75C	NE	NE	NE	NE
100C	NE	NE	NE	NE
150C	NE	NE	NE	NE
200C	NE	NE	NE	NE
250C	NE	NE	NE	NE

TABLE 32. Rubber Wear/Adhesion Tests After Mineral Acid Tests

Deposition Temperature	Sulfuric Acid	Nitric Acid	Hydrochloric Acid	Hydrofluoric Acid
RT	PR	PR	PR	PR
75C	NE	NE	NE	NE
100C	NE	NE	NE	NE
150C	NE	NE	NE	NE
200C	NE	NE	NE	NE
250C	NE	NE	NE	NE

TABLE 33. "Scotch" Tape Adhesion Tests After Mineral Acid Tests

Deposition Temperature	Sulfuric Acid	Nitric Acid	Hydrochloric Acid	Hydrofluoric Acid
RT	NE	NE	NE	NE
75C	NE	NE	NE	NE
100C	NE	NE	NE	NE
150C	NE	NE	NE	NE
200C	NE	NE	NE	NE
250C	NE	NE	NE	NE

TABLE 34. Humidity Test for 3 Hours Over Boiling Water on 200W rf Deposited DLC on Si and Subsequent Rubber Wear/Adhesion and "Scotch" Tape Adhesion Tests

Deposition Temperature	After 3 hrs Exposure	Rubber Test	Tape Test
RT	NE	PR	NE
75C	NE	NE	NE
100C	NE	NE	NE
150C	NE	NE	NE
200C	NE	NE	NE
250C	NE	NE	NE

TABLE 35. Low Temperature Test for 15 min in Liquid Nitrogen on 200 W rf Deposited DLC on Si and Subsequent Rubber Wear/Adhesion and "Scotch" Tape Adhesion Tests

deposition temperature	after 15 min exposure	rubber test	tape test
RT	NE	PR	NE
75C	NE	NE	NE
100C	NE	NE	NE
150C	NE	NE	NE
200C	NE	NE	NE
250C	NE	NE	NE

TABLE 36. Organic Solvent Tests on 300 W rf Deposited DLC on Si

deposition temperature	trichloro-ethylene	acetone	ethyl alcohol
RT	NE	NE	NE
100C	NE	NE	NE
150C	NE	NE	NE
200C	NE	NE	NE
250C	NE	NE	NE

TABLE 37. Rubber Wear/Adhesion Tests After Organic Solvent Tests

Deposition Temperature	Trichloro-Ethylene	Acetone	Ethyl Alcohol
RT	PR/S	PR/S	PR/S
100C	NE	NE	NE
150C	NE	NE	NE
200C	NE	NE	NE
250C	NE	NE	NE

TABLE 38. "Scotch" Tape Adhesion Tests After Organic Solvent Tests

Deposition Temperature	Trichloro-Ethylene	Acetone	Ethyl Alcohol
RT	NE	NE	NE
100C	NE	NE	NE
150C	NE	NE	NE
200C	NE	NE	NE
250C	NE	NE	NE

TABLE 39. Mineral Acid Attack Tests on 300 W rf Deposited DLC on Si

Deposition Temperature	Sulfuric Acid	Nitric Acid	Hydrochloric Acid	Hydrofluoric Acid
RT	NE	NE	NE	NE
100C	NE	NE	NE	NE
150C	NE	NE	NE	NE
200C	NE	NE	NE	NE
250C	NE	NE	NE	NE

TABLE 40. Rubber Wear/Adhesion Tests After Mineral Acid Tests

Deposition Temperature	Sulfuric Acid	Nitric Acid	Hydrochloric Acid	Hydrofluoric Acid
RT	PR	PR	PR	PR
100C	NE	NE	NE	NE
150C	NE	NE	NE	NE
200C	NE	NE	NE	NE
250C	NE	NE	NE	NE

TABLE 41. "Scotch" Tape Adhesion Tests After Mineral Acid Tests

Deposition Temperature	Sulfuric Acid	Nitric Acid	Hydrochloric Acid	Hydrofluoric Acid
RT	NE	NE	NE	NE
100C	NE	NE	NE	NE
150C	NE	NE	NE	NE
200C	NE	NE	NE	NE
250C	NE	NE	NE	NE

TABLE 42. Humidity Test for 3 Hours Over Boiling Water on 300 W rf Deposited DLC on Si and Subsequent Rubber Wear/Adhesion and "Scotch" Tape Adhesion Tests

Deposition Temperature	After 3 hrs Exposure	Rubber Test	Tape Test
RT	NE	PR	NE
100C	NE	NE	NE
150C	NE	NE	NE
200C	NE	NE	NE
250C	NE	NE	NE

TABLE 43. Low Temperature Test for 15 min in Liquid Nitrogen on 300 W rf Deposited DLC on Si and Subsequent Rubber Wear/Adhesion and "Scotch" Tape Adhesion Tests.

Deposition Temperature	After 15 min Exposure	Rubber Test	Tape Test
RT	NE	PR	NE
100C	NE	NE	NE
150C	NE	NE	NE
200C	NE	NE	NE
250C	NE	NE	NE

3.4.2 Moisture Penetration Studies

Extensive experiments using variable angle spectroscopic ellipsometry (VASE) were done to determine how well DLC protects against moisture penetration. In optical thin films, moisture is probably the most important degradation source. DLC is amorphous and so there are no grain boundaries through which moisture would rapidly penetrate.

The results of our work show that DLC is impressively effective in preventing moisture penetration. An article was published in Thin Solid Films as a result of a paper given at the International Conference on Metallurgical Coatings held in April 1988 (see Appendix). We have published a more extensive article in the Journal of Applied Physics for the reader interested in more details.

3.4.3 Radiation Resistance

High energy ion irradiation of DLC films were made to determine the durability of these coatings in a very adverse environment where high energy particles are present. The DLC film was produced by ion-beam deposition on a silicon substrate. The irradiation of the films was performed with 1 MeV gold and 6.4 MeV fluorine ions from a 1.7-MV General Ionex 4117A Tandetron. The effect of carbon and hydrogen content, resistivity and optical properties of the DLC film were studied as a function of ion fluence. The fluence ranged from 2×10^{14} cm^{-2} to 10^{16} cm^{-2}. Both RBS and PRD techniques were used to determine the carbon and hydrogen and any impurities. Optical analysis was performed by variable angle spectroscopic ellipsometry (VASE) assuming the Lorentz Oscillator Model. The resistivity was measured by a Keithley 610C electrometer according to the method by et al. [11].

(a) Effect of Carbon and Hydrogen Content. Tables 44 through 47 give the carbon and hydrogen content of the DLC films unirradated and irradiated with 6.4 MeV fluorine ions and with 1 MeV gold ions. The carbon content of the film did not change with ion fluence. However, the hydrogen content was found to decrease with increasing ion fluence as shown in Figure 24. The fluorine ion was more effective than the gold ion in removing hydrogen from the DLC film [12].

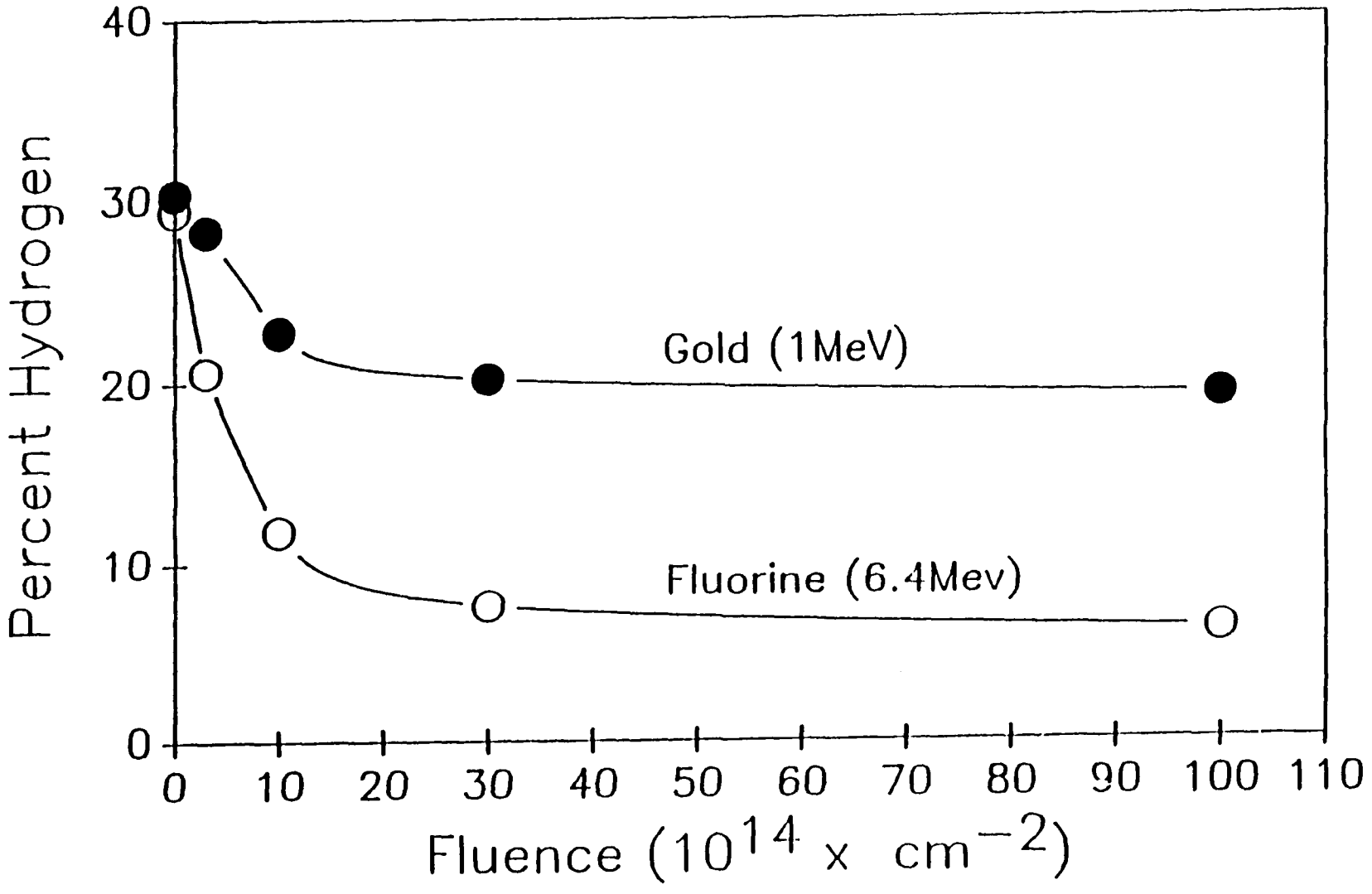

Figure 24 Atomic percent hydrogen as a function of ion fluence

TABLE 44. Hydrogen and Carbon Content of Unirradiated Portions of the DLC Samples Irradiated with 6.4 MeV Fluorine Ions

Sample No.	Hydrogen $atoms.cm^{-2}$	Carbon $atoms.cm^{-2}$	% H	% C
023/4	3.18E+17	7.65E+17	29.4%	70.6%
024	2.42E+17	5.88E+17	29.2%	70.8%
023/2	2.66E+17	6.18E+17	30.1%	69.9%
016/1	6.20E+17	1.55E+18	28.6%	71.4%

TABLE 45. Variation of Carbon and Hydrogen Content of DLC Films Irradiated with 6.4 MeV Fluorine Ions to Various Fluences

Sample No.	Fluence $ions.cm^{-2}$	Hydrogen $atoms.cm^{-2}$	Carbon $atoms.cm^{-2}$	% H	% C	% H Lost
023/4	3.0E+14	1.81E+17	6.98E+17	20.6%	79.4%	37.6%
024	1.0E+15	8.43E+16	6.29E+17	11.8%	88.2%	67.4%
023/2	3.0E+15	6.00E+16	7.33E+17	7.6%	92.4%	81.0%
016/1	1.0E+16	9.56E+16	1.44E+17	6.4%	93.6%	83.0%

TABLE 46. Hydrogen and Carbon Content of Unirradiated Portions of the DLC Samples Irradiated with 1.0 MeV Gold Ions

Sample No.	Hydrogen $atoms.cm^{-2}$	Carbon $atoms.cm^{-2}$	% H	% C
017	5.85E+17	1.35E+18	30.3%	69.7%
026	3.32E+17	7.42E+17	30.9%	69.1%
021	2.97E+17	6.69E+17	30.7%	69.3%
016/4	5.08E+17	1.14E+18	30.8%	69.2%

TABLE 47. Variation of Carbon and Hydrogen Content of DLC Films Irradiated with 1.0 MeV Gold Ions to Various Fluences

Sample No.	Fluence $_{-2}$ ions.cm	Hydrogen $_{-2}$ atoms.cm	Carbon $_{-2}$ atoms.cm	% H	% C	% H Lost
017	3.0E+14	5.44E+17	1.38E+18	28.3%	71.7%	9.5%
026	1.0E+15	2.30E+17	7.78E+17	22.[illegible]%	7[illegible].2%	33.9%
021	3.0E+15	1.83E+17	7.22E+17	20.2%	79.8%	42.9%
016/1	1.0E+16	2.51E+17	1.06E+18	19.2%	80.8%	46.9%

(b) Resistivity of the DLC film. Plots of the change in resistivity with fluence for one sample bombarded with 6.4 MeV fluorine, and two samples bombarded with 1 MeV gold are shown in Figure 25. The resistivity decreases as the ion fluence increases. The fluorine ion was again more effective than the gold ion in reducing the resistivity.

(c) Effect of Optical Properties.

Figure 26 shows the index of refraction vs wavelength for F implanted DLC. Note the large shift with fluence. Figure 27 shows the extinction coefficient vs wavelength. The main feature seen here is the rise in k, indicating that high energy particles will cause the samples to become less transparent in the visible. Figure 24 shows that the cause of this change of optical properties is a loss of hydrogen from the film. Figure 28 shows that the optical energy gap decreases with decreasing hydrogen content. Thus, Figures 24 and 28 show that implantation decreases the optical gap.

3.4.4 Ballistic Impact and Scratch Studies of Uncoated and Diamondlike Carbon Coated Samples

This section serves to explain testing procedures made on different DLC coated infrared transmitting materials.

The tests were conducted using polished silicon wafers and BK-7 glass substrates. Throughout the testing, we made direct comparison using coated and uncoated material. Two different tests were conducted: sandblasting and scratching with a diamond head scribe.

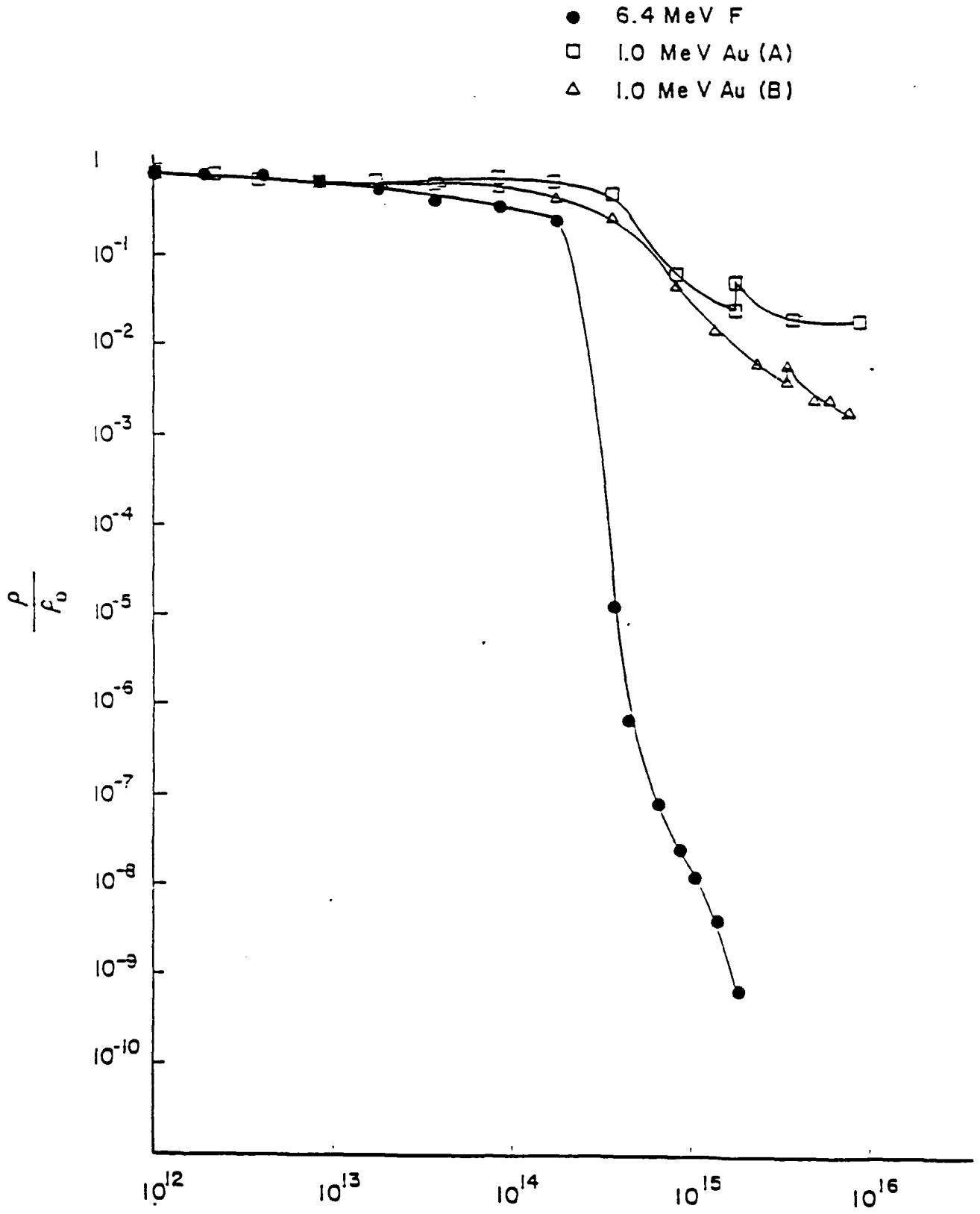

Figure 25 Change in resistivity as a function of fluence of 6.4 MeV fluorine and 1 MeV gold

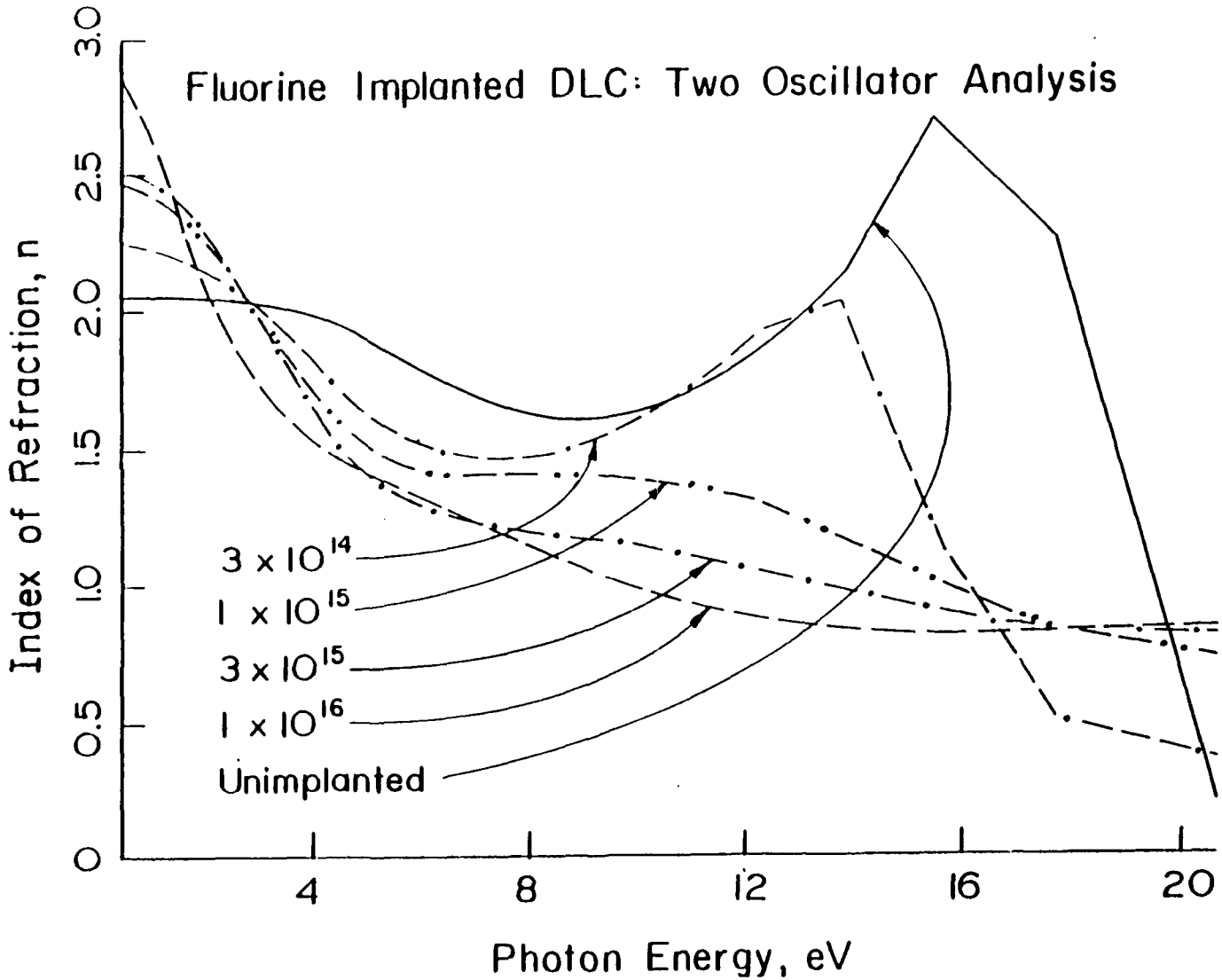

Figure 26 Index of refraction of ion beam deposited DLC after implantation

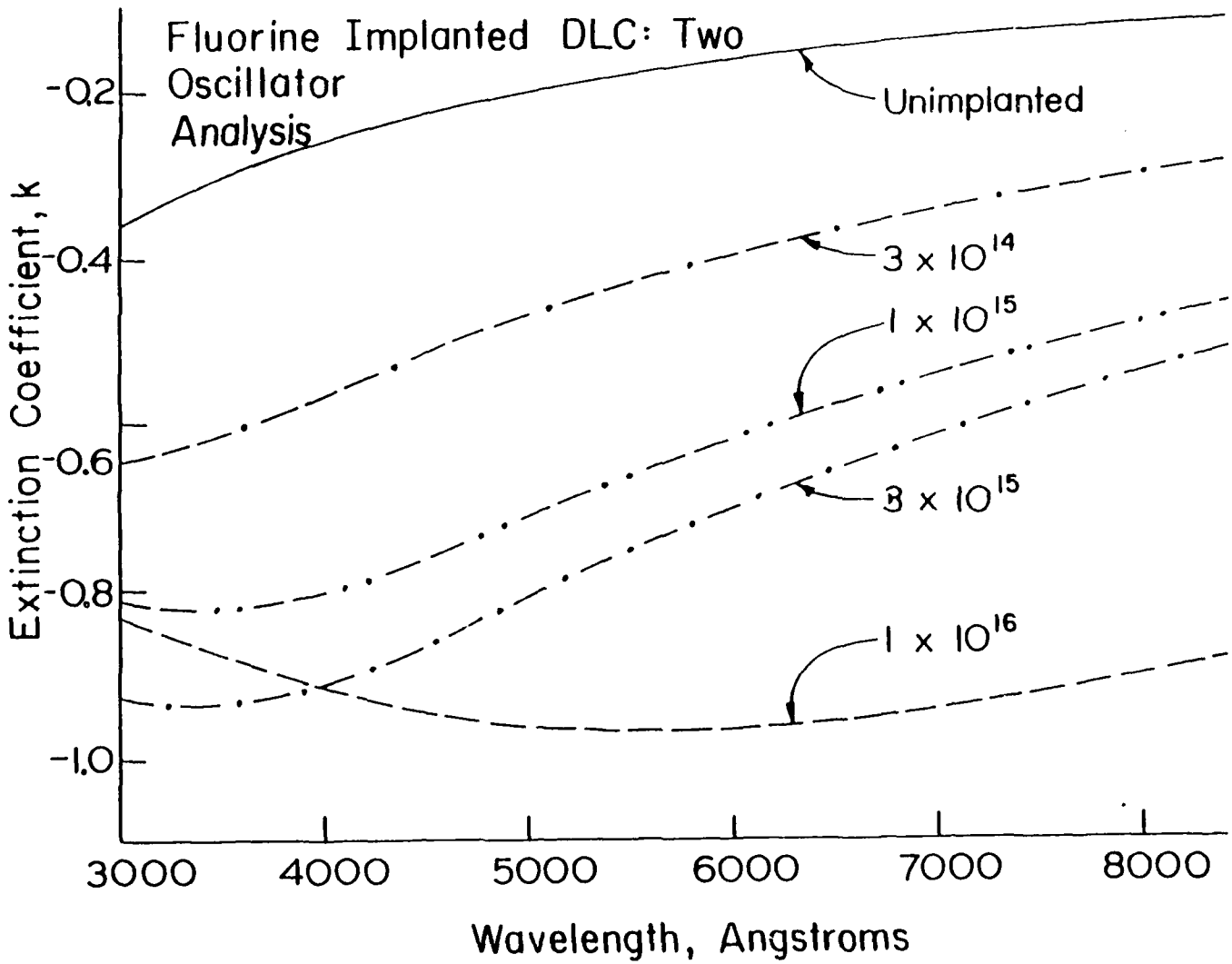

Figure 27 Extinction coefficient of ion beam deposited DLC after F ion implantation

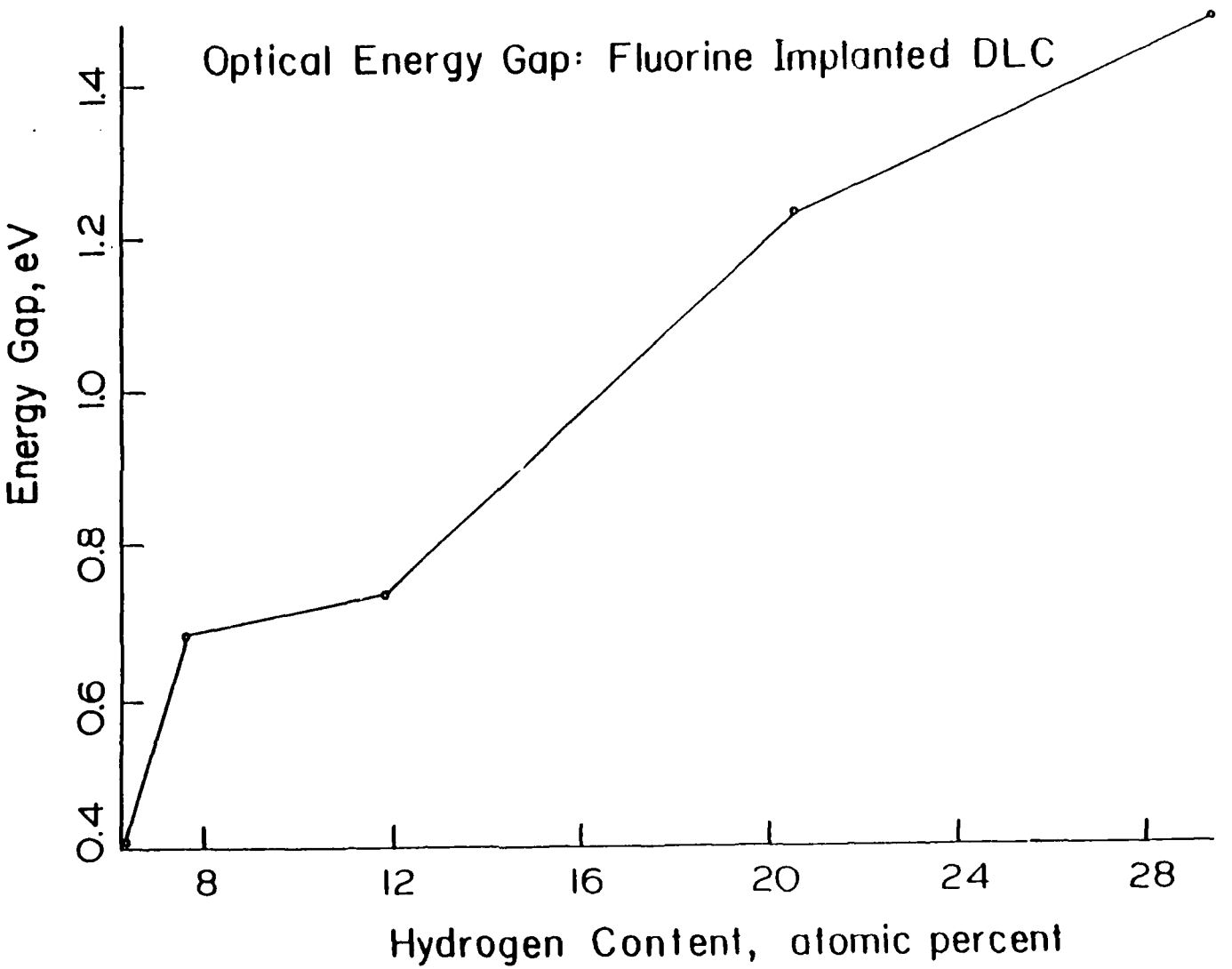

Figure 28 Optical gap vs hydrogen content in ion beam deposited DLC

The sandblasting was done with a small pistol-like "sandblaster" having a source of sand attached, and high pressure (Figure 29). Different grit sizes of sand were used. Sandblasting was done at different angles to the surface and at different distances from the surface, and for different periods of time. Testing was done on materials, with and without DLC films deposited on them, under identical conditions.

TABLE 48. Silicon Substrates, No DLC

Sample No.	Sand Diameter (μm)	Pressure (lbs/in^2)	Angle to Normal (degrees)	Distance (cm)	Time (sec)
1	<74	40	0	4	11
2	149	48	0	5	16
3	74	48	0	4	30
4	<<74	21	0	2	15
5	Scratches with scribe, look below for more detail.				
6	<<74	21	40	2	15
7	250	64	0	4	5

Scratches with a diamond tip scribe were made on the same samples as those used for sandblasting. The scratches were made with different applied forces (Figure 30). From the lightest scratch on the sample to the deepest, we had the following forces:

1- 1.20 newtons
2- 2.27 newtons
3- 2.33 newtons
4- 2.82 newtons

TABLE 49. Silicon Substrates with DLC Approximately 1500 Angstroms Thick

Sample No.	Sand Diameter (μm)	Pressure (lbs/in^2)	Angle to Normal (degrees)	Distance (cm)	Time (sec)
1	74	48	0	5	16
2	149	48	0	5	16

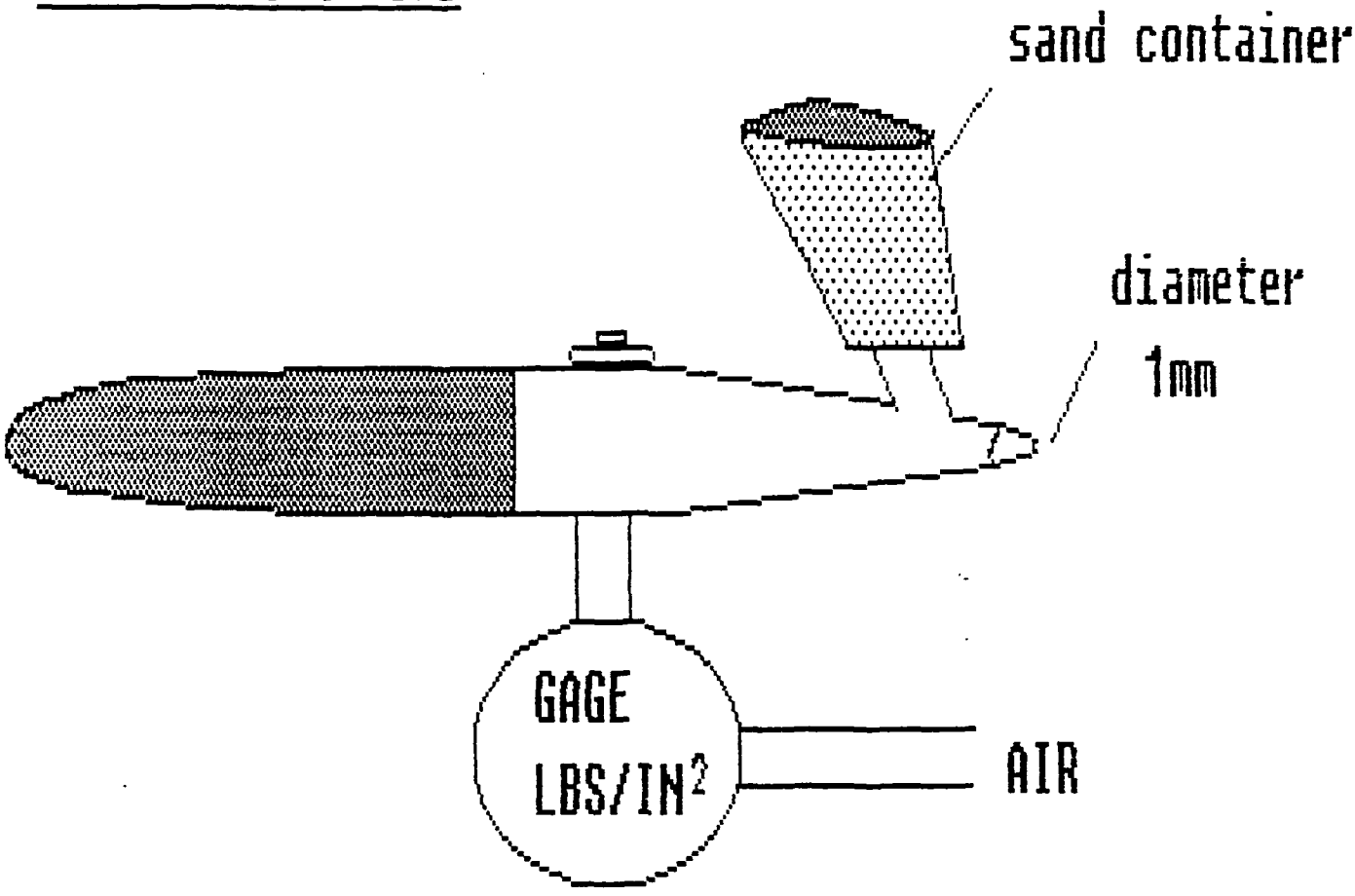

Figure 29 Schematic diagram of sandblasting apparatus

SAMPLE SCRATCHING INSTRUMENT

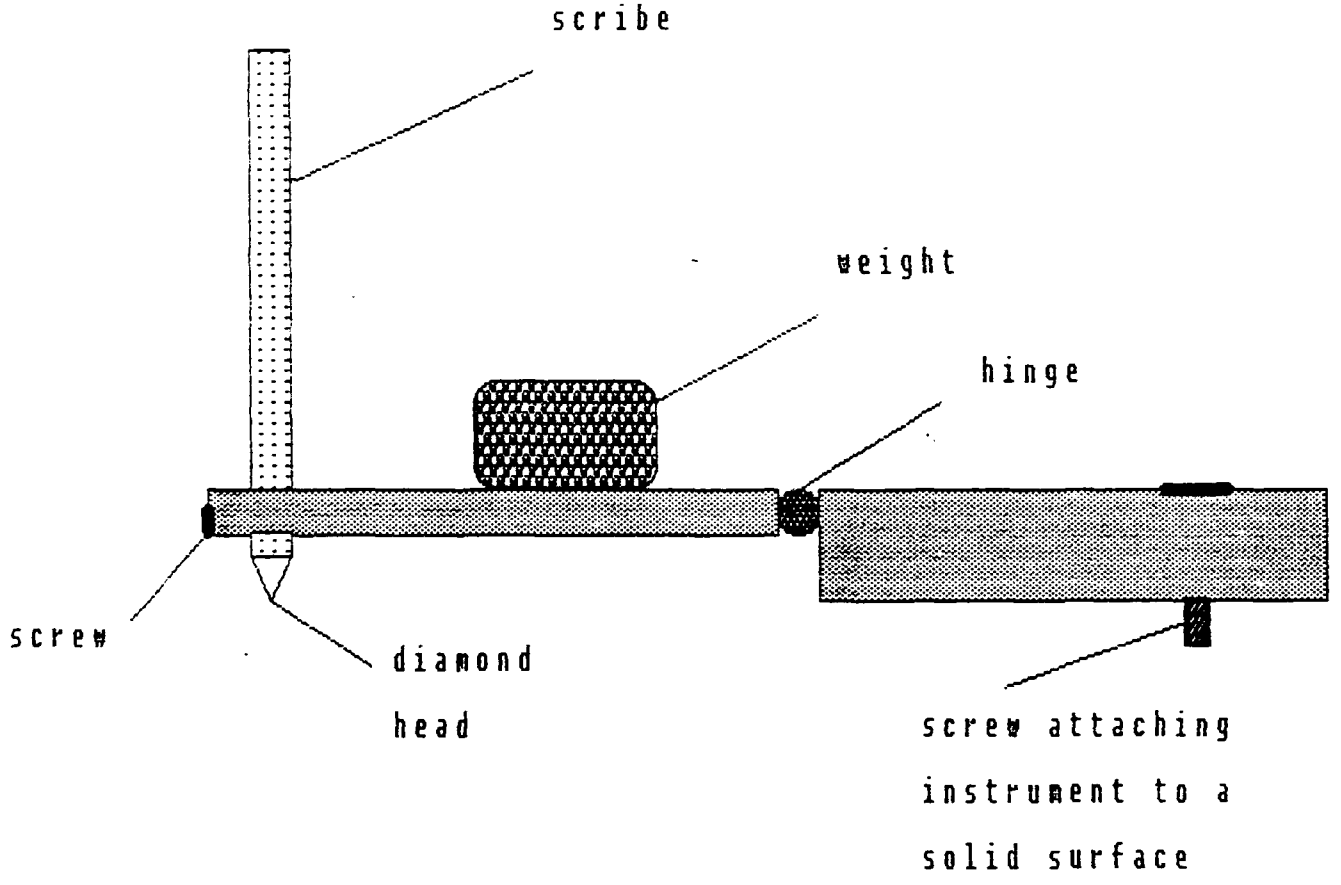

Figure 30 Schematic diagram of scratching apparatus

Pictures were taken in an electron microscope using different gains. The following pictures were taken:

Sample No.	Gain
Without Film:	
2	400
2	3000
3	700
3	10000
5- 2.27 N	3000
5- 2.82 N	7000
With Film:	
1	400
1	3000
2	100
2	400
2	1000

TABLE 50. BK-7 Glass Substrate

Sample No.	Sand Diameter (μm)	Pressure (lbs/in^2)	Angle to Normal (degrees)	Distance (cm)	Time (sec)
1	<<74	30	0	4	20
2	<<74	30	45	4	20
3	<<74	30	0	7.5	20
4	74	30	0	7.5	15
5	74	30	0	4	15

NOTE: No electron microscope pictures were made of BK-7 samples since they were nonconductive. It is important to note that the smaller sand grit affected the surface of the coated and uncoated glass more than did the bigger grit.

The electron microscope pictures were taken at different gains. There was normally a general picture of a sample and an amplified picture of a hole located in the center of the general picture.

It should be noted that the DLC film protects the substrates. This is easily observed by looking at the pictures and comparing coated substrates to uncoated substrates. The coated substrate required a much greater gain for observation of defects to be possible.

3.4.5 Rain Erosion Test

The rain erosion experiment was conducted at the Aeronautical Laboratory's rain erosion test facility at Wright-Patterson Air Force Base. The test samples were DLC films produced by ion-beam deposition on ZnS (CVD Inc., MA). A total of four specimens were used: two with 2000Å DLC coating, one with 4000Å, and one uncoated ZnS control. The test specimens were rotated at 420 mph, and rain droplet impact is randomly distributed over the entire exposure area for a period of 20 minutes. The percent optical transmission of the specimen in the infrared region was measured before and after the test. The surface damage was studied using an optical microscope.

The results demonstrated that the DLC films of 2000Å thickness survived the first 5 minutes of impact. However, at the end of a 20-minute run, about 20% and 0% of DLC film remained, respectively, for 2000Å and 4000Å films. For the control ZnS and the DLC films on ZnS samples, the surface showed micro-cracks, and fractures. However, the total crack area for the control ZnS was found to be more than that with a DLC coating. It is demonstrated that DLC films do protect ZnS substrates upon water impact. Within the experimental uncertainties, the IR transmission did not change before or after the test for these four samples.

3.4.6 Thermal Stability of DLC Film Under Vacuum

The removal of hydrogen in the DLC film upon heating was conducted using DLC films produced by ion-bean deposition on silicon substrates. The DLC films were heated by a high temperature furnace under a vacuum of $\sim 10^{-3}$ torr. These DLC films were heated at 100, 200, 300 and 400°C for one hour each. Proton recoil detection was used to analyze the hydrogen content. The results demonstrated that there was no hydrogen loss in these samples.

3.4.7 NMR Studies

Nuclear magnetic resonance is a valuable tool for studies of local atom bonding interactions in materials. An attempt to do these experiments was made. However, the signal-to-noise level was so low that the experiment could not be completed. To increase the signal-to-noise to a desirable level would have required the production of a hugh amount of samples. Since the deposition chamber was so heavily in use for making samples for other aspects of the contract, these experiments were abandoned.

4.0 DESIGN AND CONSTRUCTION OF A VARIABLE ANGLE OF INCIDENCE SPECTROSCOPIC ELLIPSOMETER

As part of the Phase II SBIR on DLC films, the J. A. Woollam Company (under subcontract to Universal Energy Systems, Inc.) provided a variable angle of incidence spectroscopic ellipsometer (VASE). This represents the state of the art in advanced optical technology. The main uses of VASE are for analysis of complex thin film, surface, and interface materials problems, as well as for the measurement of the optical properties of solids. The latter is done without the need for Kramers-Kronig analysis, and thus accurate data can be obtained over as narrow a spectral range as desired. This is especially useful for optical constant measurement at photon energies where so-called critical point phenomena occur in solids. Exciton transitions and bandgap edges in semiconductors are examples.

Relatively simple applications of ellipsometery include measurements of:

- o The thicknesses of each layer in a multilayer stack, including layers only a single atom thick.
- o Index of refraction and absorption coefficient from 300 to 950 nm.
- o Compositional fractions in a mixed layer. For example, measurement of void fraction in a nominally SiO_2 film.

Ellipsometric measurements have unique features:

- o Measurement in air (or other ambient) as opposed to Auger, and most other surface analysis techniques.
- o Nondestructive depth profiling.
- o Submonolayer sensitivity, as opposed to the sensitivity of Auger depth profiles, which have an inherent width of at least 30 Å and usually 50 to 100Å.

A review of the features of VASE are given in the attached (Appendix) reprint from Solid State Technology (March 1988), which itself makes reference to 17 other books, papers, and reviews for the interested reader.

A schematic of the hardware is shown in Figure 31. The interaction of a light beam with an ambient/solid surface is shown in Figure 32, and Figure 33 through 35 show photographs of the Army ellipsometer as assembled in Lincoln, Nebraska. A lamp and monochrometer provide light over the spectral range from 300 to 950 nm, with a typical bandwidth of 1 nm. (The photograph shows a HeNe laser, which is used occasionally as a light source but mainly for optical alignment.) Light from the monochrometer is collimated, passes through a shutter and polarizer, and impinges the sample under study at a precisely defined angle of incidence to the sample normal. The reflected light is in general elliptically polarized, and the state of polarization is measured by the remainder of the optics and electronics shown in Figure 36. The reflected light passes through the analyzer to the photomultiplier tube and the analog signal is digitized and analysis done in the computer (Wyse 286, shown in the photograph). A commercial ellipsometer base (Gaertner Corp.) is used for setting the angle of incidence. The analyzer housing, motor drive, and digitizing electronics are designed and made by the J. A. Woollam Co.

Data analysis software is the most advanced in the world and is used on the Wyse. Included are: regression analysis for solution of ellipsometric data on structures with up to 5 layers and up to 50 wavelengths, including the Bruggeman effective medium approximation. The program determines n, k ($\varepsilon,\varepsilon_2$) and layer thicknesses. (For an indepth description of both the theory and application of these programs, see Fundamentals and Applications of Ellipsometry, June 1987, Workshop, Lincoln, Nebraska. Copies available from the J. A. Woollam Company on request.)

The program will generate ψ and Δ data for a given assumed layer structure and make three-dimensional plots (to screen and plotter)

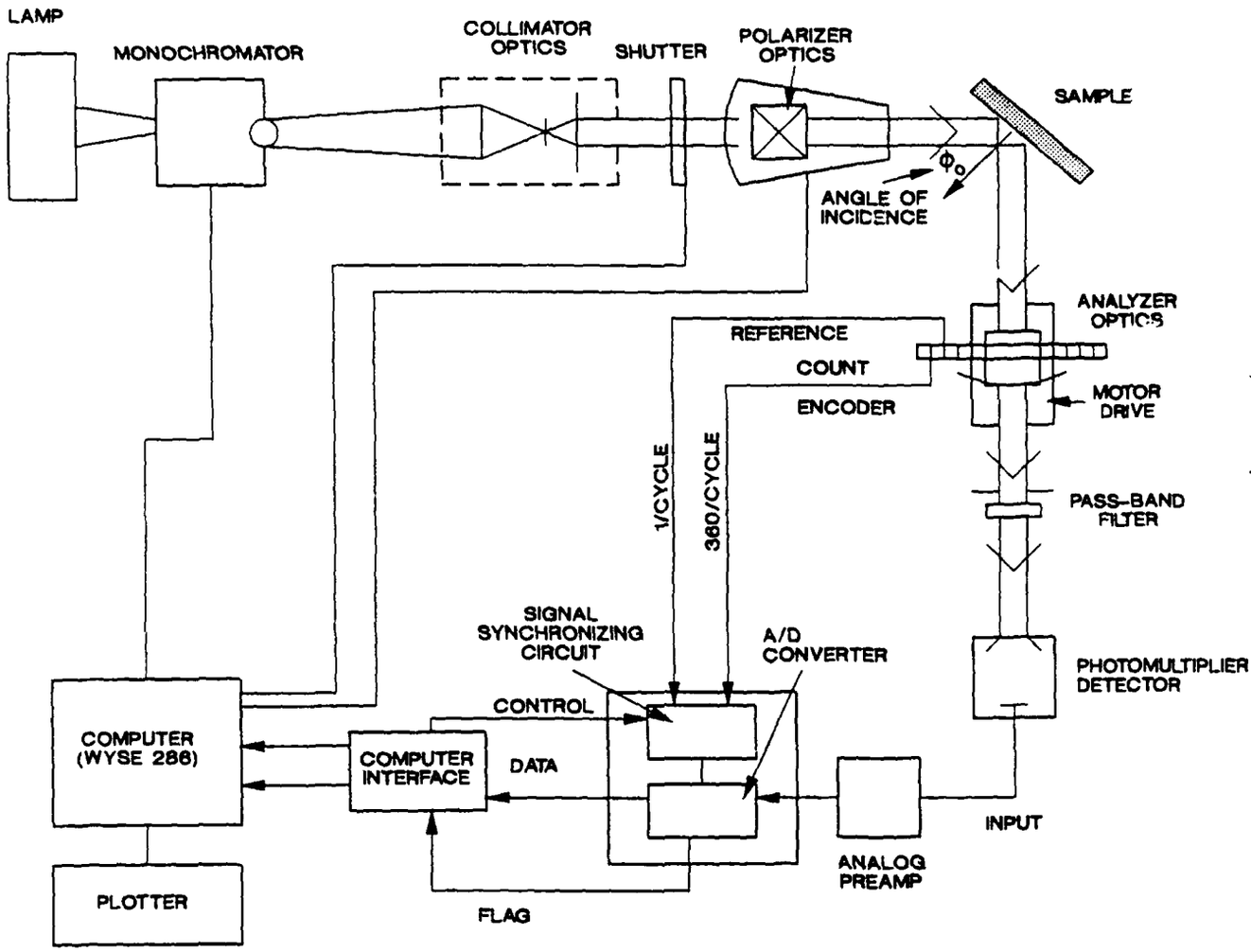

Figure 31. Schematic of variable angle spectroscopic ellipsometer (VASE)

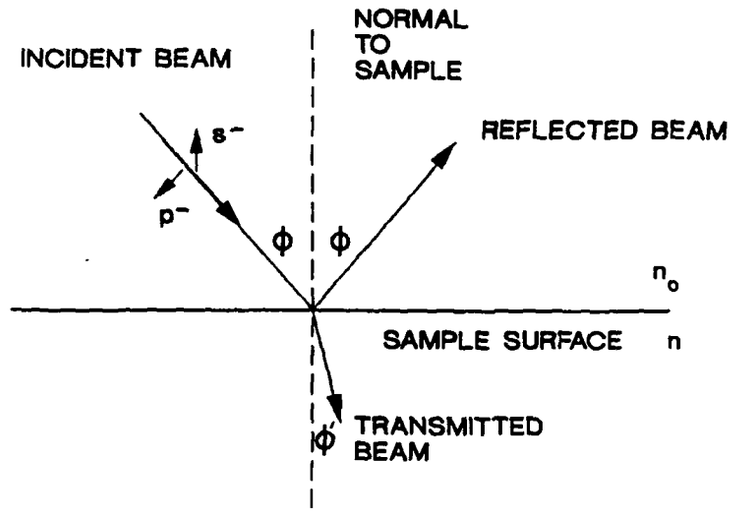

Figure 32 Geometry for optical beam interaction with a sample surface: reflected and refracted light

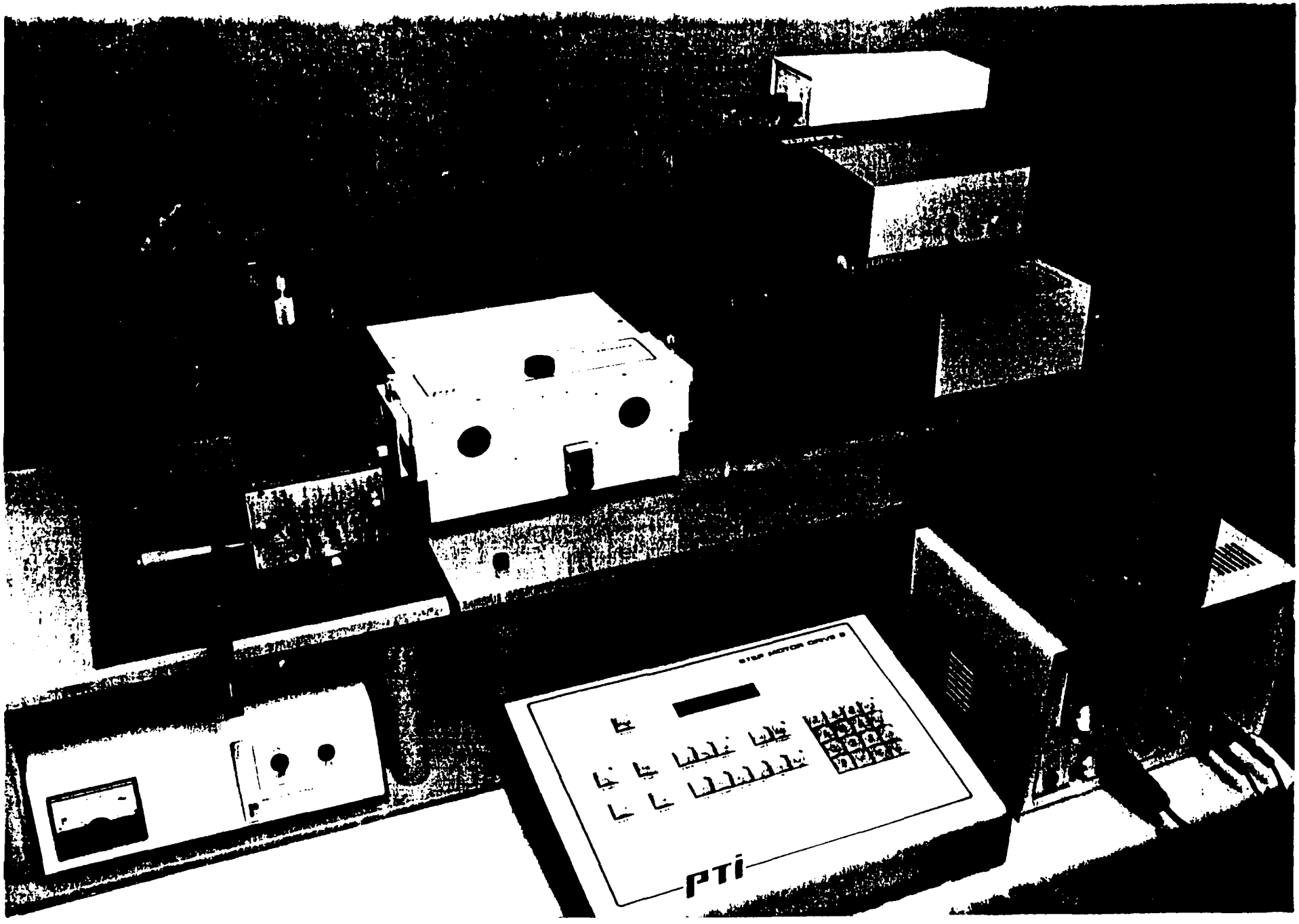

Figure 33 Photograph of the Army ellipsometer

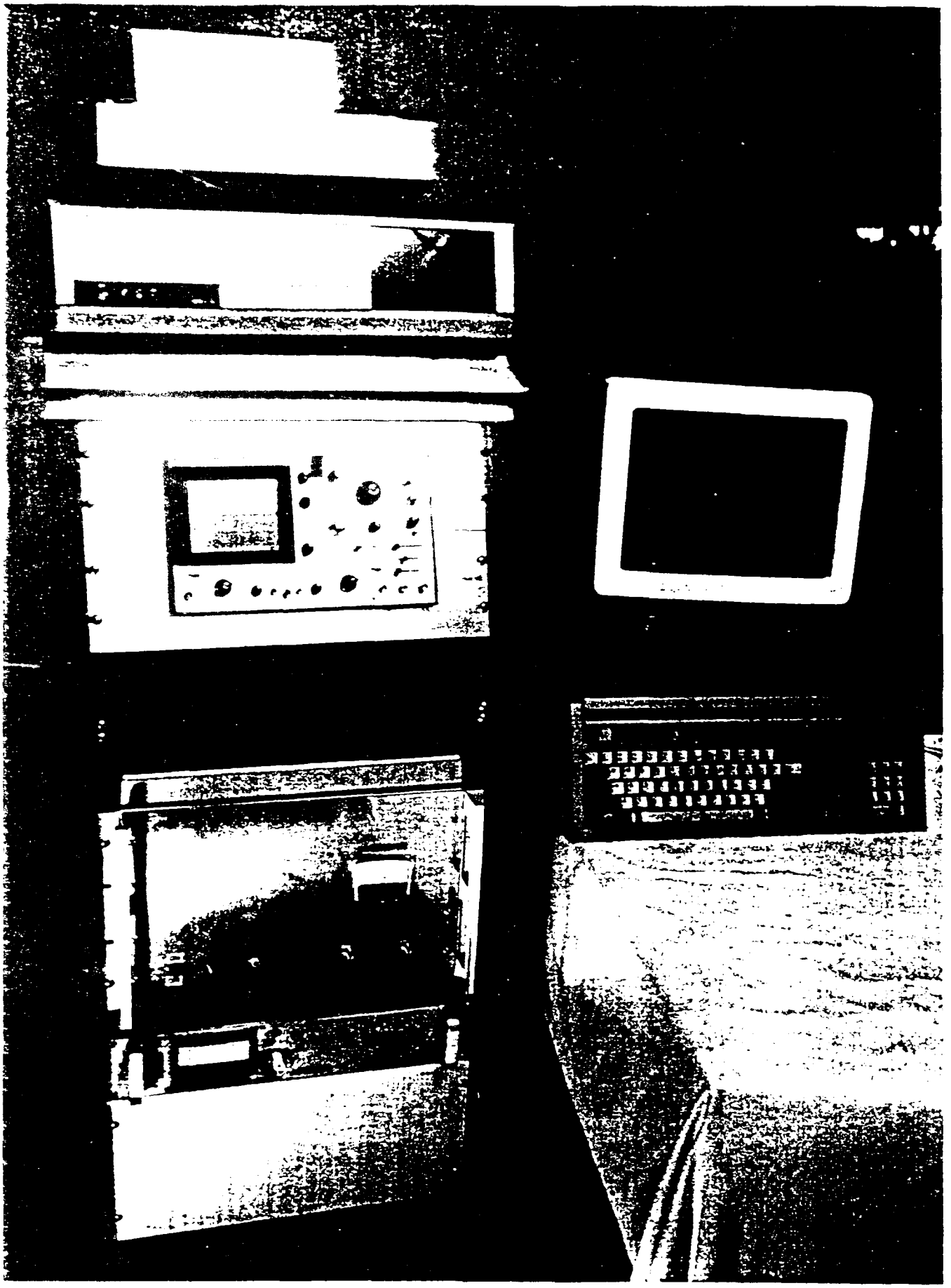

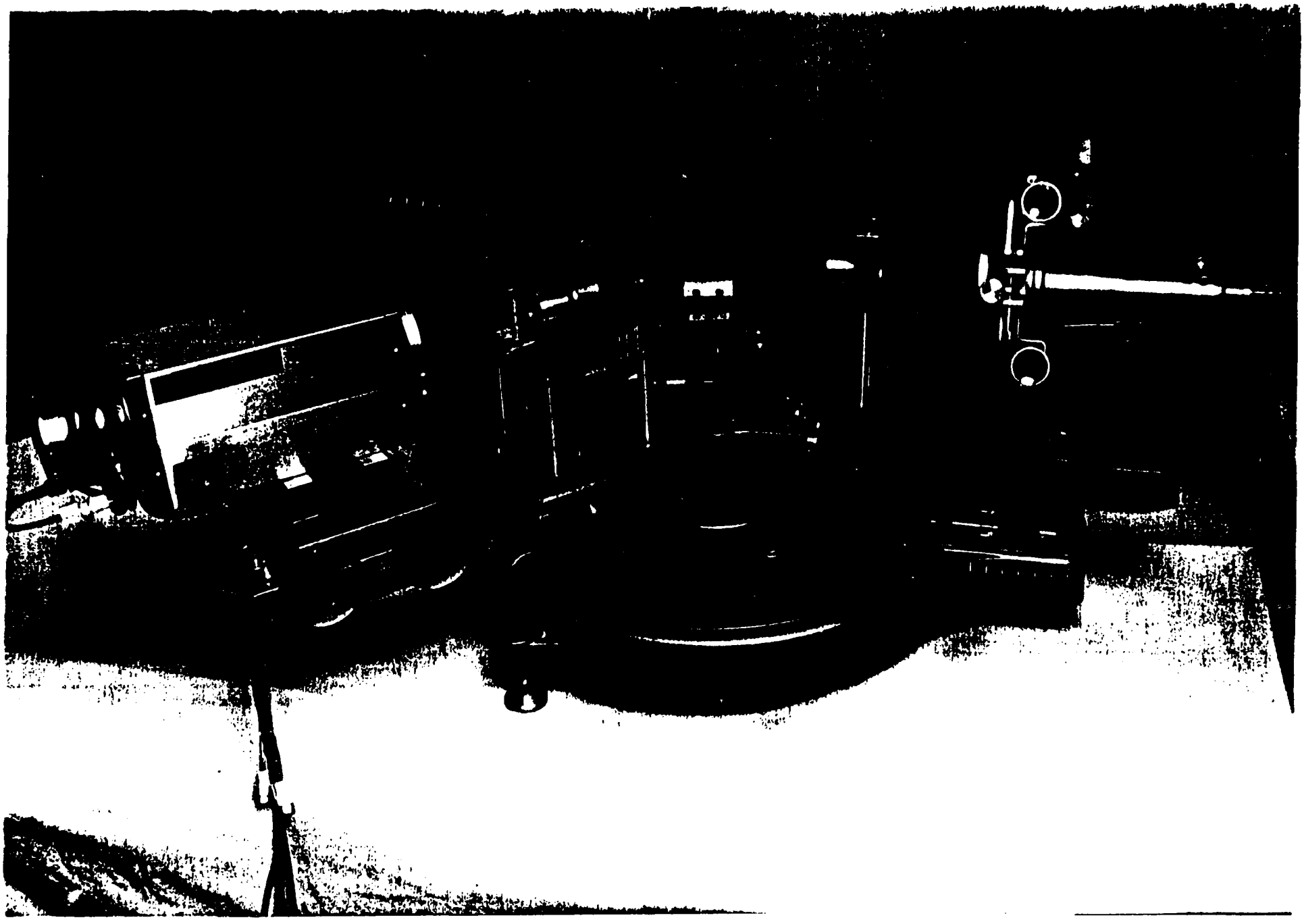

Figure 35. Photograph of the Army ellipsometer taken from the optics region

of ψ or Δ vs wavelength and angle of incidence. For any given three-dimensional plot, a contour plot can be made (uses commercial software adapted to our program). Thus a plot of constant delta near 90 degrees, for example, can be made in the angle of incidence and wavelength plane. This will predict the optimum values of angle and wavelength to use for experiments.

The computer was delivered with a detailed instruction manual including several example applications for both the "generation" mode and the "solution" mode.

5.0 CONCLUSIONS

The results of this contract can be summarized as follows.

The DLC films produced by the ion beam deposition technique are homogeneous, pinhole free and amphorous carbon films, which contain typically 30% H and 70% C. The optimum deposition parameters are determined to be: pure CH_4 gas as the source gas, higher ion energy impact >500 eV and high source pressure. The higher molecular weight cluster ions of polycarbon may be responsible for the DLC films. The possible processes are:

(a) Electron Impact Process

$$CH_4 + e \rightarrow CH_4^+ + 2e \quad (1)$$

$$\rightarrow CH_3^+ + H + 2e \quad (2)$$

(b) Ion-Molecule Reactions

$$CH_4^+ + CH_4 \rightarrow CH_5^+ + CH_3 \quad (3)$$

$$CH_3^+ + CH_4 \rightarrow C_2H_5^+ + H_2 \quad (4)$$

$$C_2H_3^+ + 2H_2 \quad (5)$$

$$C_2H_3^+ + CH_4 \rightarrow C_3H_7^+ + H_2 \quad (6)$$

$$C_3H_5^+ + 2H_2 \quad (7)$$

$$C_4H_7^+, -C_5H_7^+, \text{ etc.} \quad (8)$$

However, the detailed mechanism for DLC formation is still unknown. The addition of H_2 in the ion source increases the hydrogen content in the film.

The substrate cleaning procedure prior to DLC coating was found to play a very important role in adhesion. The standard cleaning semiconductor procedures (i.e., washing with 1.1.1 trichloroethane, acetone and methanol, and drying with nitrogen) can be applied to the substrates of silicon, KG-3, BK-7 and ZnS. The procedure for washing with methanol and drying using a heat gun or dry nitrogen must be used in the substrates of fused silica and HMF. The adhesion of DLC was found to be very good and to vary with particular substrates. The optical properties can be controlled by depositing parameter control, and optical quarter wavelength thickness of DLC could be deposited on the substrates of silicon, lexan, fused silica, KG-3 and BK-7 glass. However, sticking was sometimes a problem for thick films on the substrates of ZnS (>4000Å), ZnSe (>4000Å) and HMF (>1000Å). In general, ion-beam cleaning of the surface was invariably helpful in achieving good adhesion.

The DLC films showed excellent resistance to organic (1.1.1 trichloroethane, acetone, methanol and inorganic acids (sulfuric acid, nitric acid, hydrochloric acid and hydrofluroric acids). Its adhesion to these seven substrates was found to be excellent toward water penetration and extreme thermal cycling. Thus, DLC films can be used as a protective film for abrasion and corrosion resistance on these soft infrared materials. Rain erosion and sand ballistic impact tests on DLC film deposited on ZnS demonstrated that the DLC film protect ZnS to some extent. The thermal stability of DLC films under vacuum was found to be very good. No change in appearance and no loss of hydrogen were found at temperature of 400°C for one hour. The hydrogen content of DLC films can be removed with high energy ion bombardment of Au and F ions. The hydrogen loss increased with increasing of ion fluence and resulted in optical band gap increased.

The ion beam and rf plarma deposition techniques developed in this program have been shown to be useful techniques for producing high quality DLC films. The advantages of these methods are:

(a) The entire process operates under high vacuum resulting in minimal contanimation.

(b) Good adhesion can be achieved by ion-beam cleaning of the substrate surfaces.

(c) Deposition temperatures are very low, a feature which is desirable for optical material coatings.

(d) A scale up process for commercial applications can be achieved by increasing the ion-beam density and area for the case of the ion beam technique, and by direct scale up in size for the rf techniques.

For rf deposition in the Configuration I design, a reasonable set of parameters that result in good films is: 25 watts and 140 μm of 50-50 mixture of methane and argon and a room temperature substrate.

In the Configuration II (30 kHz) design, a reasonable set of deposition conditions is 200 watts and 200 μm of methan and a room temperature stubstrate. At 13.56 MHz, a setting of 200 watts and 100 μm of argon/methan 50-50 mixture with a room temperature substrate yields good films. For all Configuration I and II depositions, there is no true optimal setting. Rather, the user must choose what optical gap, hydrogen concentration, deposition rate is optimum for the user's purposes and use the appropriate parameter settings accordingly. Note also that the best settings for one chamber design probably will not yield the same results in another deposition system; that is, the parameter settings are system dependent. The values given in this final report are in a typical range to try for any new system, however.

6.0 PUBLICATIONS DURING THE CONTRACTING PERIOD

As a result of the work done during this program, eight manuscripts have been submitted and published in refereed journals. Appendix A contains reprints of these articles. The publication information follows.

1. "Diamondlike Carbon for Infrared Optics," B. N. De, S. Orzeszko, J. A. Woollam, D. C. Ingram, and A. J. McCormick, SPIE, August 1988.

2. "Optical properties of Ion-Beam Deposited Ion-Modified Diamondlike (A:C:H) Carbon," S. Orzeszko, J. A. Woollam, D. C. Ingram, and A. W. McCormick, J. Appl. Phys. 64, 2611 (1988).

3. "Ellipsometric Analysis of Thin Film Hermeticity: Application to Diamondlike Carbon," S. Orzeszko, B. N. De, P. G. Snyder, J. A. Woollam, J. J. Pouch and S. A. Altervoitz, J. de Chime Physique 84, 1469 (1987).

4. "Optical-Absorption Edge and Disorder Effects in Hydrogenerated Amorphous 'Diamondlike' Carbon Films," T. Datta, J. A. Woollam, and W. Notchomiprodjo, Physical Review 252 (1987).

5. "Hermeticity of Diamondlike Carbon Thin Film Protective Coatings," S. Orzeszko, B. N. De, J. A. Woollam, J. J. Pouch, and S. A. Altervoitz, Thin Solid Films 288 (1988).

6. "Thin Film Hermeticity: Quantitative Analysis of Diamondlike Carbon Using Variable Angle Spectroscopic Ellipsometery (VASE)," S. Orzeszko, B. N. De, J. A. Woollam, J. J. Pouch, and S. A. Altervoitz, J. Appl. Phys. 283 (1988).

7. "Variable Angle Spectroscopic Ellipsometry", S. A. Altervoitz, J. A. Woollam and P. G. Snyder, Solid State Technology, March 1988.

8. "*The Effect of MeV Ion Irradiation on the Hydrogen Content and* Resistivity of Direct Ion Beam Deposited Diamondlike Carbon," D. C. Ingram and A. W. McCormick, Nuclear Instruments & Methods in Physics Research B34, 68 (1988).

7.0 TECHNICAL PRESENTATIONS AT PROFESSIONAL MEETINGS

Seven presentations were given at professional meetings. Abstracts of those presentations are given in Appendix B. The publication information follows.

1. A. Massengale, J. A. Woollam, and P. G. Snyder, "Ellipsometric Studies of Void Structure and Moisture in Thin Optical and Dielectric Films," Bull. Amr. Phys. Soc. 32, 651 (1987), Paper IQ1.

2. A. Massengale, S. Orzeszko, P. Snyder, J. A. Woollam, J. Pouch, and S. A. Altervoitz, "Moisture Permeation of Diamondlike Carbon Films Studied by Variable Angle Spectroscopic Ellipsometry (VASE)," 18th Biennial Conference on Carbon, July 1987.

3. T. Datta, J. A. Woollam, and W. Notohamiprodjo, "Disorder Effects and Optical Absorption in Diamondlike Carbon Films," 18th Biennial Conference on Carbon, July 1987.

4. J. A. Woollam, P. G. Snyder, and M. C. Rost, "Variable Angle Spectroscopic Ellipsometry (VASE) - A Non-Descructive Characterization Technique for Ultra Thin and Multilayer Materials," 15th International Conference on Metallurgical Coatings (ICMC 88), April 1988.

5. B. N. De, S. Orzeszko, N. J. Ianno, and J. A. Woollam, "Optical Constants and Environmental Stability of Diamondlike Carbon (A-C:H) Deposited on Optical Window Materials," Bulletin of the American Physical Society 33, 635 (1988), Paper M24 5.

6. S. Orzeszko, B. N. De, P. G. Snyder, and J. A. Woollam, "Effects of Moisture on Diamondlike Carbon Protective Coatings: An Ellipsometric Analysis," Bulletin of the American Physical Society 33, 636 (1988), Paper M24 12.

7. J. A. Woollam, S. Orzeszko, B. N. De, J. J. Pouch, and S. A. Altervoitz, "Optical Studies of Diamondlike Carbon and Its Hermeticity," Carbon 88 (European Carbon Conference), September 1988.

8. B. N. De, S. Orzeszko, J. A. Woollam, D. C. Ingram, and A. J. McCormick, "Diamondlike Carbon for Infrared Optics," Society of Photooptical and Instrumentation Engineers (SPIE) August 1988 Meeting.

8.0 PHASE III ACTIVITIES OF DIAMONDLIKE CARBON PROGRAM

The ultimate goal of this program is to apply the DLC coating technology developed during the Phase II program for future military and commercial applications.

Dr. Richard L. C. Wu, principal investigator of this program, gave numerous seminars on diamondlike carbon coatings for the following organizations: (a) CVD, Inc., Woburn, MA; (b) ASD/AEME, Joint Technology Insertion program, Wright-Patterson AFB, OH; (c) Libby Owens Ford Company; (d) Shieffield Measurement Division; (e) LaserMike Division, Techmet Company; (f) AFWAL/MLPJ, Wright-Patterson AFB, OH; (g) ASD/SPME, Wright-Patterson AFB, OH; (h) ASD/VLE, Wright-Patterson AFB, OH; (i) Technology, Inc.; and (j) Epion Corporation.

Dr. John A. Woollam gave diamondlike coating presentations at eight professional society meetings. He also gave lectures at SERI, NASA, AMPEX Corporation, Control Data Corporation, Honeywell Corporation, and CVI Laser Optics.

As a result of the extensive Phase III activities, CVD, Inc., a division of Morton Thiokol, has shown a great interest in adoption and commercialization of this technology. Scientists at CVD, Inc., have closely worked with UES researchers on several critical tests, including rain erosion tests, hardness tests, reflection index, extinction coefficient, and laser adsorption at 10.6 μm (CO_2 laser). In addition, scientists at Wright-Patterson AFB have already participated in the assessment of this coating for potential applications in missile domes.

Table 51 lists the companies which have utilized diamondlike coatings for their specific applications. Several test samples have been coated for the field test. Once the test is proven to be successful, the commercialization of this technology will result. Table 52 lists the potential users which are currently under discussion on applying DLC coatings for various applications.

As a result of work performed under this contract, a small business, J. A. Woollam Company, has been established to commercialize the variable angle of incidence spectroscopic ellipsometer (VASE), which represents the state of the art in advanced optical technology.

TABLE 51. Diamondlike Carbon Coatings Developed by UES Applied to Various Substrates Used by Other Companies During Phase III Activities

COMPANY NAME	SUBSTRATE OF INTEREST	APPLICATION
CVD, Inc. Woburn, MA	ZnS, ZnSe, Cleantran ZnS	Abrasion, corrosion and erosion resistant for IR windows used in DoD missiles
Libbey Owens Ford Company Toledo, OH	Special coated glass	Abrasion, corrosion and resistant for automobile windshields, for solar cells
Sheffield Measurement Division Dayton, OH	Precision measurement	Abrasion, corrosion and erosion resistant for precision instruments
Optical Filter Corporation Natick, MA	ZnS, ZnSe, Germanium optical glass	Antireflection coatings, abrasion, corrosion and erosion resistant for IR windows
LaserMike Division Techmet Company Huber Heights, OH	Optical windows	Environmental protection for He-Ne laser windows
Harshaw/Filtrol Solon, OH	NaCl, KCl, CsI, KBr	Erosion, abrasion and corrosion resistant for optical windows
CVI Laser Optics Albuquerque, NM	Optical components	Environmental protection

TABLE 52. Potential Users Currently Under Negotiation by Applying Diamondlike Carbon Coatings Developed by UES for Various Applications

COMPANY NAME	SUBSTRATE OF INTEREST	APPLICATION
ASD/AEME, Joint Technology Insertion Program Wright-Patterson AFB, OH	ZnS, ZnSe, BK-7 polycarbonates	Abrasion, corrosion and erosion resistant for IR windows used in missiles, aircraft wingtip lights and canopy
AFWAL/FIEA Wright-Patterson AFB, OH	Polycarbonates	Erosion, abrasion and corrosion resistant for aircraft canopy
ASD/SDME, Maverick SPO Wright-Patterson AFB, OH	ZnS, ZnSe	Erosion, abrasion and corrosion resistant for Maverick missiles
ASD/VLE Latirn SPO Wright-Patterson AFB, OH	Optical window materials	Erosion, abrasion and corrosion resistant for optical windows
WR-ALC/MMIRFP Robins AFB, GA	ZnS, BK-7	Erosion, Abrasion and corrosion resistant for Pave Tack IR windows
OOALC/MMWMM Hill AFB, UT	ZnS, ZnSe	Erosion, abrasion and corrosion resistant for missile domes
General Electric Company Utica, NY	Ge	Antireflection
Hughes Aircraft Company Tuscon, AZ	GKN7 glass	Abrasion resistant for GKN7 glass domes

9.0 TENTATIVE MILITARY SPECIFICATION OF DIAMONDLIKE CARBON COATING FOR OPTICAL SYSTEMS

9.1 COATING QUALITY

The coating shall be uniform in quality per MIL-C-48497C, paragraph 3.3.

9.2 COATING DURABILITY

9.2.1 Adherence

Tape test per MIL-M-13508, paragraph 4.4.6.

9.2.2 Hardness

Cheesecloth abrasion test per MIL-M-13508, paragraph 4.4.6.

9.2.3 Temperature

Variations of -80°F and +160°F. per MIL-M-13508, paragraph 4.4.4.

9.2.4 Humidity

Test per MIL-STD-810, Method 507, procedure I.

9.2.5 Maintenance

The coatings shall be cleanable without damage by water, water plus mild detergent, acetone, isopropyl, methyl or ethyl alcohol and methyl ethyl ketone.

REFERENCES

1. J. C. Angus, P. Koidl, and S. Domitz, in: Plasma Deposited Thin Films, J. Mort and F. Jansen, Eds., CRC Press, Baca Raton, FL, 89 (1986).

2. B. Bendow and D. Griscom, "Summary of the Workshop on Diamondlike Carbon Coatings," Albuquerque, NM, Contract MDA 903-81-C-10[illegible] (1982).

3. Amorphous Hydrogenated Carbon Films, Symposia Proceedings, European Materials Research Society, Vol. 17, P. Koidl and P. Oelhafen, Eds., les éditions de physique, Les Ulis Cedex, France.

4. J. A. Woollam, H. Chang, and V. Natavajan, "Diamondlike carbon: A Bibliography of Published Papers and REports," Appl.Phys.Comm.5, 263 (1985).

5. J. Robertson, Advances in Physics, 35(4), 317 (1986).

6. H-C Tsai and D. B. Bogy, J. Vac Sci Technol. A5(6), 3287 (1987)

7. "Diamondlike Carbon Coatings for Optical Systems," UES, 2nd Quarterly Report, November 29, 1986 - February 28, 1987, U.S. Army Contract DAAL04-86-C-00030.

8. M. J. Mirtich, D. Nir, D. Swec, and B. Banks, J. Vac Sci Technol. A4, 2680 (1986).

9. "Semiconductors," Ed. R. A. Smith, 2nd Ed., Cambridge University Press, 1987.

10. "Diamondlike Carbon Coatings for Optical Systems," UES, 4th Quarterly Report, March 1 - May 28, 1987.

11. S. Prawer, R. Kalish, M. Adel, V. Richter, J. Appl. Phys. 61, 4492 (1987).

12. D. C. Ingram and A. W. McCormick, Nuclear Instruments & Methods in Physics Research, B34, 68 (1988).

DISTRIBUTION LIST

No. of Copies	To
	Office of the Under Secretary of Defense for Research and Engineering, The Pentagon, Washington, DC 20301
1	ATTN: Mr. J. Persh
1	Dr. L. Young
1	Mr. K. R. Foster
	Commander, U.S. Army Laboratory Command, 2800 Powder Mill Road, Adelphi, MD 20783-1145
2	ATTN: AMSLC-IM-TL
1	AMSLC-TD
1	AMSLC-TD-A
1	AMSLC-PA
1	AMSLC-TP
	Commander, Defense Technical Information Center, Cameron Station, Building 5, 5010 Duke Street, Alexandria, VA 22304-6145
2	ATTN: DTIC-FDAC
1	National Technical Information Service, 5285 Port Royal Road, Springfield, VA 22161
	Director, Defense Advanced Research Projects Agency, 1400 Wilson Boulevard, Arlington, VA 22209
1	ATTN: Dr. P. Parrish
1	Dr. B. Wilcox
1	Dr. K. Hardmann-Rhyne
	Battelle Columbus Laboratories, Metals and Ceramics Information Center, 505 King Avenue, Columbus, OH 43201
1	ATTN: Mr. W. Duckworth
1	Dr. D. Niesz
	Department of the Army, Office of the Assistant Secretary of the Army (RDA), Washington, DC 20310
1	ATTN: Dr. J. G. Prather, Dep for Sci & Tech
1	Dr. J. R. Sculley, SARD
	Deputy Chief of Staff, Research, Development, and Acquisition, Headquarters, Department of the Army, Washington, DC 20310
1	ATTN: DAMA-ZE, Mr. C. M. Church
	Commander, U.S. Army Research and Development Office, Chief Research and Development, Washington, DC 20315
1	ATTN: Physical and Engineering Sciences Division
	Commander, Army Research Office, P.O. Box 12211, Research Triangle Park, NC 27709-2211
1	ATTN: Information Processing Office
1	Dr. J. Hurt
1	Dr. A. Crowson
1	Dr. R. Reeber
1	Dr. R. Shaw
	Commander, U.S. Army Materiel Command, 5001 Eisenhower Avenue, Alexandria, VA 22333
1	ATTN: AMCQA-EQ, Mr. H. L. Light
1	AMCQA, Mr. S. J. Lorber
	Commander, U.S. Army Electronics Research and Development Command, Fort Monmouth, NJ 07703-5000
1	ATTN: AMDET-ES, Dr. A. Tauber
	Director, Electronics Warfare Laboratory, Fort Monmouth, NJ 07703
1	ATTN: AMDEW-D, Mr. M. Adler
	Commander, U.S. Army Materiel Systems Analysis Activity, Aberdeen Proving Ground, MD 21005
1	ATTN: AMXSY-MP, H. Cohen
	Commander, U.S. Army Night Vision Electro-Optics Laboratory, Fort Belvoir, VA 22060
1	ATTN: DELNV-S, Mr. P. Travesky
1	DELNV-D, Dr. R. Buser
1	DELNV-L, Dr. L. [illegible]ron
	Commander, Harry Diamond Laboratories, 2800 Powder Mill Road, Adelphi, MD 20783
1	ATTN: Technical Information Office
1	SLCHD-RAE
	Director, U.S. Army Research & Technology Labs, Ames Research Center, Moffet Field, CA 94035
1	ATTN: DAVDL-D, Dr. R. Carlson
1	DAVDL-AL-D, Dr. I. C. Statler, MS215-1, Aeromechanics Laboratory

No. of Copies	To
	Commander, U.S. Army Missile Command, Redstone Scientific Information Center, Redstone Arsenal, AL 35898-5241
1	ATTN: AMSMI-RD-CS-R/Doc
1	AMSMI-R, Dr. W. C. McCorkle
	Commander, U.S. Army Aviation Systems Command, P.O. Box 209 St. Louis, MO 63166
1	ATTN: AMSAV-NS, Mr. M. L. Bauccio
1	Technical Library
	Commander, U.S. Army Natick Research, Development, and Engineering Center, Natick, MA 01760
1	ATTN: Technical Library
1	Dr. J. A. Sousa
1	Dr. R. J. Byrne
1	Dr. R. Lewis
	Commander, U.S. Army Satellite Communications Agency, Fort Monmouth, NJ 07703
1	ATTN: Technical Document Center
	Commander, U.S. Army Science and Technology Center Far East Office, APO San Francisco, CA 96328
1	ATTN: Terry L. McAfee
	Commander, U.S. Army Communications and Electronics Command, Fort Monmouth, NJ 07703
1	ATTN: AMSEL-TDD, Mr. T. A. Pfeiffer, Technical Dir.
	Director, Electronic Technology and Devices Lab, Fort Monmouth, NJ 07703
1	ATTN: DELET-D, Dr. C. G. Thornton
	Commander, U.S. Army Tank-Automotive Command, Warren, MI 48397-5000
1	ATTN: Dr. W. Bryzik
1	D. Rose
1	AMSTA-RKA
1	AMSTA-UL, Technical Library
1	AMSTA-R
1	AMSTA-NS, Dr. H. H. Dobbs
	Commander, U.S. Army Armament, Munitions and Chemical Command, Dover, NJ 07801
1	ATTN: Mr. J. Lannon
1	Mr. H. E. Pebly, Jr., PLASTEC, Director
1	Technical Library
1	Dr. T. Davidson
1	Dr. B. Ebihara
	Commander, U.S. Army Armament, Munitions and Chemical Command, Rock Island, IL 61299
1	ATTN: Technical Library
	Commander, Aberdeen Proving Ground, MD 21005
1	ATTN: AMDAR-CLB-PS, Mr. J. Vervier
	U.S. Army Corps of Engineers, Construction Engineering Research Lab, P.O. Box 4005, Champaign, IL 61820
1	ATTN: Dr. Robert Quattrone
	Commander, U.S. Army Belvoir RD&E Center, Fort Belvoir, VA 22060-5606
1	ATTN: STRBE-FS, Mr. W. McGovern, Fuel & Wtr Sup Div
1	AMDME-V, Mr. E. York
1	STRBE-ZTS, Dr. K. H. Steinbach, Office of the Chief Scientist
1	AMDME-ZT, Mr. T. W. Lovelace, Tech Dir
1	Mr. M. Lepera
	Director, U.S. Army Ballistic Research Laboratory, Aberdeen Proving Ground, MD 21005
1	ATTN: SLCBR-BLT, Dr. A. M. Dietrich
1	SLCBR-BLF, Dr. A. Niller
	Commander, Rock Island Arsenal, Rock Island, IL 61299
1	ATTN: SARRI-EN
	Director, U.S. Army Industrial Base Engineering Activity, Rock Island, IL 61299
1	ATTN: AMXIB-MT, Mr. G. B. Ney
	Chemical Research and Development Center, Aberdeen Proving Ground, MD 21010
1	ATTN: AMSMC-CLD(A), Dr. B. Richardson

No. of Copies	To
	Commander, U.S. Army Test and Evaluation Command, Aberdeen Proving Ground, MD 21005
1	ATTN: AMSTE-ME
1	AMSTE-TD, Mr. H. J. Peters
	Commander, U.S. Army Foreign Science and Technology Center, 220 7th Street, N.E., Charlottesville, VA 22901
1	ATTN: Military Tech
1	Mr. J. Crider
1	Ms. P. Durrer
1	Mr. P. Greenbawm
	Chief, Benet Weapons Laboratory, Watervliet, NY 12189
1	ATTN: AMDAR-LCB-TL
1	Dr. G. D'Andrea
1	AMDAR-LCB, Dr. F. Sautter
	Director, Eustis Directorate, U.S. Army Mobility Research and Development Laboratory, Fort Eustis, VA 23604
1	ATTN: SAVDL-E-MOS (AMCCOM)
	Commander, U.S. Army Engineer Waterways Experiment Station, Vicksburg, MS 39180
1	ATTN: Research Center Library
	Project Manager, Munitions Production Base, Modernization and Expansion, Dover, NJ 07801
1	ATTN: AMCPM-PBM-P
	Technical Director, Human Engineering Laboratories, Aberdeen Proving Ground, MD 21005-5001
1	ATTN: SLCHE-D, Dr. J. D. Weisz
	Chief of Naval Research Arlington, VA 22217
1	ATTN: Code 471
1	Dr. A. Diness
1	Dr. R. Pohanka
	Naval Research Laboratory, Washington, DC 20375
1	ATTN: Code 5830
	Headquarters, Naval Air Systems Command, Washington, DC 20360
1	ATTN: Code 5203
	Headquarters, Naval Sea Systems Command, 1941 Jefferson Davis Highway, Arlington, VA 22376
1	ATTN: Code 035
	Headquarters, Naval Electronics Systems Command, Washington, DC 20360
1	ATTN: Code 504
	Commander, Naval Ordnance Station, Louisville, KY 40214
1	ATTN: Code 85
	Commander, Naval Material Industrial Resources Office, Building 537-2, Philadelphia Naval Base, Philadelphia, PA 19112
1	ATTN: Technical Director
	Commander, Naval Weapons Center, China Lake CA 93555
1	ATTN: Mr. F. Markarian
	Commander, U.S. Air Force Wright Aeronautical Labs, Wright-Patterson Air Force Base, OH 45433
1	ATTN: Dr. N. Tallan
1	Dr. H. Graham
1	Dr. R. Ruh
1	Aero Propulsion Labs, Mr. R. Marsh
1	Dr. H. M. Burte
1	AFWAL/MLLP, Mr. D. Forney
1	AFML/MLLM, Mr. H. L. Gegel
1	AFSC/MLLM, Dr. A. Katz
	Commander, Air Force Armament Center, Eglin Air Force Base, 32542
1	ATTN: Technical Library
	National Aeronautics and Space Administration, Lewis Research Center, 21000 Brookpark Road, Cleveland, OH 44135
1	ATTN: J. Accurio, USAMRDL
1	Dr. H. B. Probst, MS 49-1
1	Dr. S. Dutta
1	NASA - Scientific and Technical Information Facility, P.O. Box 8757, Baltimore/Washington International Airport, Maryland 21240

No. of Copies	To
	National Aeronautics and Space Administration, Langley Research Center, Hampton, VA 23665
1	ATTN: Mr. J. Buckley, MS 387
1	Dr. J. Heyman, MS 231
1	Mr. R. L. Long, MS 266
	Commander, White Sands Missile Range, Electronic Warfare Laboratory, OMEW, ERADCOM, White Sands, NM 88002
1	ATTN: Mr. Thomas Reader, AMSEL-WLM-ME
	Department of Energy, Division of Transportation, 20 Massachusetts Avenue, N.W., Washington, DC 20545
1	ATTN: Dr. R. J. Gottschall, ER-131, GTN
1	Mechanical Properties Data Center, Belfour Stulen Inc., 13917 W. Bay Shore Drive, Traverse City, MI 49684
	National Bureau of Standards, Washington, DC 20234
1	ATTN: E. S. Etz, Bldg. 222, Rm A-121
1	D. L. Hunston, Bldg. 224, Rm A-209
1	Dr. D. H. Reneker, Dep. Dir., Ctr for Matl's Sci.
1	Dr. Lyle Schwartz
1	Dr. Stephen Hsu
1	Dr. Allan Draggoo
	U.S. Bureau of Mines, Mineral Resources Technology, 2401 E. Street, N.W., Washington, DC 20241
1	ATTN: Mr. M. A. Schwartz
	National Bureau of Standards, Gaithersburgh, MD 20760
1	ATTN: Dr. S. Wiederhorn
1	Dr. N. Tighe
	National Research Council, National Materials Advisory Board, 2101 Constitution Avenue, Washington, DC 20418
1	ATTN: Dr. K. Zwilsky
1	D. Groves
1	J. Lane
	National Science Foundation, Materials Division, 1800 G Street, N.W., Washington, DC 20006
1	ATTN: Dr. L. Toth
1	Dr. J. Hurt
	AVCO Corporation, Applied Technology Division, Lowell Industrial Park, Lowell, MA 01887
1	ATTN: Dr. T. Vasilos
	Case Western Reserve University, Department of Metallurgy, Cleveland, OH 60605
1	ATTN: Prof. A. H. Heuer
	Defence Research Establishment Pacific, FMO, Victoria, B.C., VOS IBO, Canada
1	ATTN: R. D. Barer
	Ford Motor Company, Turbine Research Department, 20000 Rotunda Drive, Dearborn, MI 48121
1	ATTN: Mr. A. F. McLean
1	Mr. J. A. Mangels
	Ford Motor Company, P.O. Box 2053, Dearborn, MI 48121
1	ATTN: Dr. D. Compton, Vice President Research
	General Electric Company, Research and Development Center, Box 8, Schenectady, NY 12345
1	ATTN: Dr. R. J. Charles
1	Dr. C. D. Greskovich
1	Dr. S. Prochazka
	Georgia Institute of Technology, EES, Atlanta, GA 30332
1	ATTN: Mr. J. D. Walton
	GTE Sylvania, Waltham Research Center, 40 Sylvania Road, Waltham, MA 02154
1	ATTN: Dr. W. H. Rhodes
	Martin Marietta Laboratories, 1450 South Rolling Road, Baltimore, MD 21227
1	ATTN: Dr. J. Venables
	Massachusetts Institute of Technology, Department of Metallurgy and Materials Science, Cambridge, MA 02139
1	ATTN: Prof. R. L. Coble
1	Prof. H. K. Bowen
1	Prof. W. D. Kingery
1	Prof. J. Vander Sande

No. of Copies	To
	Materials Research Laboratories, P.O. Box 50, Ascot Vale, VIC 3032, Australia
1	ATTN: Dr. C. W. Weaver
	Midwest Research Institute, 425 Volker Boulevard, Kansas City, MO 64110
1	ATTN: Mr. G. W. Gross, Head, Physics Station
	Pennsylvania State University, Materials Research Laboratory, Materials Science Department, University Park, PA 16802
1	ATTN: Prof. R. Roy
1	Prof. R. E. Newnham
1	Prof. R. E. Tressler
1	Dr. C. Pantano
1	Mr. C. O. Ruud
	State University of New York at Albany, Department of Physics, Albany, NY 12222
1	ATTN: Prof. W. A. Lanford
	State University of New York at Stony Brook, Department of Materials Science, Long Island, NY 11790
1	ATTN: Prof. F. F. Y. Wang
	Stanford Research International, 333 Ravenswood Avenue, Menlo Park, CA 94025d
1	ATTN: Dr. P. Jorgensen
1	Dr. D. Rowcliffe
	United Technologies Research Center, East Hartford, CT 06108
1	ATTN: Dr. J. Brennan
1	Dr. K. Prewo
	University of California, Lawrence Livermore Laboratory, P.O. Box 808, Livermore, CA 94550
1	ATTN: Mr. R. Landingham
1	Dr. C. F. Cline
1	Dr. J. Birch Holt
	University of Florida, Department of Materials Science and Engineering, Gainevisile, FL 32611
1	ATTN: Dr. L. Hench
	University of Washington, Ceramic Engineering Division, FB-10, Seattle, WA 98195
1	ATTN: Prof. R. Bradt
	Westinghouse Electric Corporation, Research Laboratories, Pittsburgh, PA 15235
1	ATTN: Dr. R. J. Bratton
	Battelle Pacific Northwest Lab, NDT Section, Richland, WA 99353
1	ATTN: Mr. A. Birks, Associate Manager
	Rensselaer Polytechnic Institute, Department of Materials Engineering, Troy, NY 12181
1	ATTN: R. J. Diefendorf
	Oak Ridge National Laboratory, P.O. Box X Oak Ridge, TN 37830
1	ATTN: P. F. Becher
1	V. J. Tennery
1	R. Johnson
	Sandia Laboratories, Albuquerque, NM 87185
1	ATTN: Dr. F. Gerstle, Div 5814
	The John Hopkins University, Department of Civil Engineering/ Materials Science and Engineering, Baltimore, MD 28218
1	ATTN: Dr. R. E. Green, Jr.
1	Director, Office of Science and Technology Policy, Old Executive Office Building, Washington, DC 20223

No. of Copies	To
	Subcommittee on Science, 2319 Rayburn House Office Building, Washington, DC 20515
1	ATTN: Mr. P. C. Maxwell
	Aerospace Corporation, Materials Science Laboratory, 2350 East El Segundo Boulevard, El Segundo, CA 90245
1	ATTN: Dr. L. R. McCreight
	IBM Corporation, Thomas B. Watson Research Center, Yorkstown Heights, NY 10598
1	ATTN: Dr. G. Onoda
	Corning Glass Works, Research and Development Division, Corning, NY 14830
1	ATTN: Dr. W. R. Prindle
	3M Company, New Products Department, 219-01-01, 3M Center, St. Paul, MN 55144
1	ATTN: R. E. Richards
	Technology Strategies, Inc., 10722 Shingle Oak Ct., Burke, VA 22015
1	ATTN: Dr. E. C. Van Reuth
	Rutgers University, Center for Ceramics, Rm A274, P.O. Box 909, Piscataway, NJ 08854
1	ATTN: Prof. J. B. Wachtman, Jr., Director
	Syracuse University, 304 Administration Building, Syracuse, NY 13210
1	ATTN: Dr. V. Weiss
	Lehigh University, Materials Research Center #32, Bethlehem, PA 18015
1	ATTN: Dr. D. M. Smyth
	Alfred University, New York State College of Ceramics, Alfred, NY 14802
1	ATTN: Dr. R. L. Snyder
	Alfred University, Center for Advanced Ceramic Technology, Alfred, NY 14806
1	ATTN: R. M. Spriggs
	University of California, Center for Advanced Materials, D58, Hildebrand Hall, Berkeley, CA 94720
1	ATTN: Prof. G. Somorjai
	Boeing Aerospace Company, 11029 Southeast 291, Auburn, MA 98002
1	ATTN: W. E. Strobelt
	University of California, Materials Science and Mineral Engineering, Heart Mining Building, Rm 284, Berkeley, CA 94720
1	ATTN: Prof. G. Thomas
	Director, U.S. Army Materials Technology Laboratory, Watertown, MA 02172-0001
2	ATTN: SLCMT-TML
1	SLCMT-IMA-V
1	SLCMT-PR
50	SLCMT-EMS, Helen Dauplaise, COR